INFORMATION TO USERS

This material was produced from a microfilm copy of the original document. While the most advanced technological means to photograph and reproduce this document have been used, the quality is heavily dependent upon the quality of the original submitted.

The following explanation of techniques is provided to help you understand markings or patterns which may appear on this reproduction.

1. The sign or "target" for pages apparently lacking from the document photographed is "Missing Page(s)". If it was possible to obtain the missing page(s) or section, they are spliced into the film along with adjacent pages. This may have necessitated cutting thru an image and duplicating adjacent pages to insure you complete continuity.

2. When an image on the film is obliterated with a large round black mark, it is an indication that the photographer suspected that the copy may have moved during exposure and thus cause a blurred image. You will find a good image of the page in the adjacent frame.

3. When a map, drawing or chart, etc., was part of the material being photographed the photographer followed a definite method in "sectioning" the material. It is customary to begin photoing at the upper left hand corner of a large sheet and to continue photoing from left to right in equal sections with a small overlap. If necessary, sectioning is continued again — beginning below the first row and continuing on until complete.

4. The majority of users indicate that the textual content is of greatest value, however, a somewhat higher quality reproduction could be made from "photographs" if essential to the understanding of the dissertation. Silver prints of "photographs" may be ordered at additional charge by writing the Order Department, giving the catalog number, title, author and specific pages you wish reproduced.

5. PLEASE NOTE: Some pages may have indistinct print. Filmed as received.

Xerox University Microfilms

300 North Zeeb Road
Ann Arbor, Michigan 48106

75-20,364

HERMANN, Joachim Josef, 1940-
PHYSICAL MODEL APPROACH TO THE UPTAKE AND RELEASE KINETICS OF OUABAIN AND DIGITOXIN BY HUMAN ERYTHROCYTES.

The University of Michigan, Ph.D., 1975
Chemistry, pharmaceutical

Xerox University Microfilms, Ann Arbor, Michigan 48106

THIS DISSERTATION HAS BEEN MICROFILMED EXACTLY AS RECEIVED.

PHYSICAL MODEL APPROACH TO THE UPTAKE AND RELEASE KINETICS OF OUABAIN AND DIGITOXIN BY HUMAN ERYTHROCYTES

by

Joachim Josef Hermann

A dissertation submitted in partial fulfillment
of the requirements for the degree of
Doctor of Philosophy
(Pharmaceutical Chemistry)
in The University of Michigan
1975

Doctoral Committee:

Professor William I. Higuchi, Chairman
Associate Professor Gordon Flynn
Associate Professor Norman F. H. Ho
Professor John A. Jacquez
Associate Professor Norman Weiner

Meinen lieben Eltern gewidmet

ACKNOWLEDGEMENTS

This author wishes to express his appreciation:

To Professor William I. Higuchi for his inspirational advice, patient guidance and total dedication to this investigation.

To Associate Professor Norman F.H. Ho for his suggestions regarding the mathematical models and his general concern for the successful completion of this project.

To Associate Professor Gordon Flynn, Professor John A. Jacquez and Associate Professor Norman Weiner for their time and effort in providing helpful suggestions.

To my wife, Sandy, for her constant support in all my endeavors and the typing of this manuscript.

In addition, acknowledgement is due to the National Institute of Dental Research for support through NIH Grant DE 00204 and the Smith, Kline and French Laboratories for their Pharmacy Fellowship.

TABLE OF CONTENTS

DEDICATION ii

ACKNOWLEDGEMENTS iii

LIST OF TABLES vi

LIST OF FIGURES viii

NOMENCLATURE xxi

INTRODUCTION 1

LITERATURE REVIEW 3

- General Transport Studies 3
- Physical and Chemical Properties of Human Erythrocytes ... 7
- Cardiac Glycosides 11

STATEMENT OF THE PROBLEM 17

CONSIDERATIONS IN THE APPROACH TO THE INVESTIGATION 18

THEORETICAL CONSIDERATIONS 20

- Model 1 21
- Model 2 24
- Model 3 34
- Model 4 40
- Model 5 44
- Model 6 49

EXPERIMENTAL PROCEDURES AND TECHNIQUES 53

- Cell Suspension Medium 53
- Preparation of Red Blood Cells 53
- Drug Uptake Experiments 54
- Drug Release Experiments 58
- Preparation of Erythrocyte Samples for Scintillation Analysis 59
- Determination of Intercellular Drug Entrapment in the Red Cell Plugs 60
- Calibration of Centrifuge and Hematocrit Tube 61
- Stability of Erythrocyte Suspension with Time 61
- Evaluation of Binding Constants from "Zero Time" Measurements 62
- Equilibrium Dialysis 65
- Purity Determination of Ouabain $-^{3}H$ and Digitoxin $-^{3}H$ 66

Specific Activity Determination of Ouabain -^{3}H and Digitoxin -^{3}H 68

RESULTS OF COMPLEMENTAL STUDIES 70

Intercellular Red Cell Plug Error and Efficiencies 70
Calibration of Centrifuge Tube and Hematocrit Tube 72
Stability of Erythrocyte Suspensions with Time 72
Evaluation of Binding Constants from "Zero Time" Measurements 74
Equilibrium Dialysis 82
Purity Determination of Ouabain -^{3}H and Digitoxin -^{3}H 88
Specific Activity Determination of Ouabain -^{3}H and Digitoxin -^{3}H 88

OUABAIN AND DIGITOXIN TRANSPORT 94

Ouabain Uptake and Release Experiments 94
Summary of Ouabain Transport 119
Digitoxin Uptake and Release Experiments 121
Summary of Digitoxin Transport 154

THE ROLE OF THE PHYSICAL MODEL APPROACH 157

REFERENCES 177

LIST OF TABLES

Table		Page
I.	Results of the analysis for the intercellular red blood cell plug error using PEG – 4,000 – ^{14}C.....	71
II.	Determination of the absolute number of red blood cells in 0.1 ml. RBC plug.....	73
III.	Determination of time dependent stability of pH, hematocrit, number of cells in 0.1 ml. suspension and 0.1 ml.RBC plug.....	75
IV.	Data for the digitoxin – erythrocyte equilibrium binding constant as a function of erythrocyte incubation time.....	77
V.	Data for the digitoxin – FBS equilibrium dialysis experiments.....	84
VI.	Equilibrium dialysis data for the ouabain – FBS interaction.....	85
VII.	Equilibrium dialysis data for the digitoxin – human hemoglobin interaction.....	86
VIII.	Mean values of K or K_{bm} and K_b as determined by different experimental methods.....	87
IX.	Data for the specific activity determination of ouabain – ^{3}H.....	92
X.	Data for the specific activity determination of digitoxin – ^{3}H.....	93
XI.	Summary of transport parameters for the ouabain uptake from media containing different concentrations of ouabain and 0% FBS.....	100
XII.	Summary of transport parameters for the release of cellular ouabain into media containing 0% FBS.....	102
XIII.	Summary of transport parameters for the cellular ouabain uptake from media containing different concentrations of ouabain and 5% FBS.....	106
XIV.	Summary of transport parameters for the cellular release of ouabain into media containing 5% FBS.....	109

Table | Page

XV. Summary of transport parameters for the cellular ouabain uptake from media containing different ouabain concentrations and 15% FBS 113

XVI. Summary of transport parameters for the cellular release of ouabain into media containing 15% FBS 116

XVII. Summary of mean transport parameters for ouabain uptake and release systems containing 0, 5 and 15% FBS 118

XVIII. Summary of transport parameters for the cellular uptake of digitoxin from media containing different digitoxin concentrations and 0% FBS 125

IXX. Summary of transport parameters for the cellular release of digitoxin into media containing 0% FBS 129

XX. Summary of transport parameters for the cellular uptake of digitoxin from media containing different digitoxin concentrations and 5% FBS 134

XXI. Summary of transport parameters for the cellular digitoxin release into media containing 5% FBS 138

XXII. Summary of transport parameters for the cellular digitoxin uptake from media containing different concentrations and 15% FBS 143

XXIII. Summary of transport parameters for the cellular digitoxin release into media containing 15% FBS 148

XXIV. Summary of the mean transport parameters for the digitoxin uptake and release systems containing 0, 5 and 15% FBS 151

XXV. Transport parameters evaluated with equation (75) for the uptake of digitoxin at 30 °C from phosphate buffered saline containing different concentrations of fetal bovine albumin 156

XXVI. Transport parameters used to evaluate ouabain uptake and release with Models 1, 3 and 4 162

XXVII. Transport parameters used to evaluate digitoxin uptake and release data with Models 2 and 6 173

LIST OF FIGURES

Figure		Page
1.	Schematic description of theoretical Model 1.....	22
2.	Schematic description of theoretical Model 2.....	26
3.	Schematic description of theoretical Model 3.....	35
4.	Schematic description of theoretical Model 4.....	41
5.	Schematic description of theoretical Model 5.....	45
6.	Schematic description of theoretical Model 6.....	50
7a.	Chemical structure of ouabain.....	55
7b.	Chemical structure of digitoxin.....	55
8.	Outline of the sequence of procedures for drug uptake experiments.....	56
9.	Photograph of hematocrit tube, centrifuge tube and dialysis chamber.....	57
10.	Amount of digitoxin taken up by 1 ml. RBC versus the concentration of digitoxin in the external phosphate buffered saline at "zero time".....	78
11.	Reversibility check of digitoxin - erythrocyte interaction at "zero time".....	79
12.	"Zero time" data for the ratio of the total digitoxin concentration in the media to the RBC concentration versus FBS levels in the suspension media.....	80
13.	"Zero time" uptake and reversibility of the digitoxin - RBC ghost interaction.....	81
14.	Radiochromatogram scanner recordings for different ouabain $-^{3}H$ samples.....	89
15.	Radiochromatogram scanner recordings for different digitoxin $-^{3}H$ samples.....	90

Figure Page

16. Model 4 plots of the cellular ouabain uptake from media containing different concentrations of ouabain and 0% FBS..... 98

17. Model 4 plots of the cellular ouabain uptake from media containing different concentrations of ouabain and 0% FBS..... 99

18. Model 4 plots of ouabain release into media containing 0% FBS..... 101

19. Equilibrium data of the cell - associated ouabain as a function of the ouabain concentration in the media containing 0% FBS..... 103

20. Model 4 plots of the cellular ouabain uptake from media containing different ouabain concentrations and 5% FBS..... 104

21. Model 4 plots of the cellular ouabain uptake from media containing different ouabain concentrations and 5% FBS..... 105

22. Model 4 plots of ouabain release into media containing 5% FBS..... 107

23. Model 4 plot of ouabain release into medium containing 5% FBS..... 108

24. Equilibrium data of the cell - associated ouabain as a function of the ouabain concentration in media containing 5% FBS..... 110

25. Model 4 plots of the cellular ouabain uptake from media containing different ouabain concentrations and 15% FBS..... 111

26. Model 4 plots of the cellular ouabain uptake from media containing different ouabain concentrations and 15% FBS..... 112

27. Model 4 plots of ouabain release into media containing 15% FBS..... 114

28. Model 4 plots of ouabain release into media containing 15% FBS..... 115

Figure Page

29. Equilibrium data of the cell - associated ouabain as a funtion of the ouabain concentration in the media containing 15% FBS..... 117

30. Model 6 plots of cellular digitoxin uptake from media containing different concentrations of digitoxin and 0% FBS..... 124

31. Model 6 plot of cellular digitoxin release into medium containing 0% FBS..... 126

32. Model 6 plot of cellular digitoxin release into medium containing 0% FBS..... 127

33. Model 6 plot of cellular digitoxin release into medium containing 0% FBS..... 128

34. Equilibrium data of the total cell - associated digitoxin as a function of the unbound digitoxin concentration in media containing 0% FBS..... 130

35. Equilibrium data of the cellular digitoxin bound to Langmuir sites as a function of the unbound digitoxin concentration in media with 0% FBS..... 131

36. Model 6 plots of cellular digitoxin uptake from media containing different concentrations of digitoxin and 5% FBS..... 132

37. Model 6 plots of cellular digitoxin uptake from media containing different concentrations of digitoxin and 5% FBS..... 133

38. Model 6 plot of cellular digitoxin release into medium containing 5% FBS..... 135

39. Model 6 plot of cellular digitoxin release into medium containing 5% FBS..... 136

40. Model 6 plot of cellular digitoxin release into medium containing 5% FBS..... 137

41. Equilibrium data of the total cell - associated digitoxin as a function of the unbound digitoxin in the media containing 5% FBS..... 139

42. Equilibrium data of the cellular digitoxin bound to Langmuir sites as a function of the unbound digitoxin in media containing 5% FBS..... 140

Figure Page

43. Model 6 plots of the cellular digitoxin uptake from media containing different concentrations of digitoxin and 15% FBS..... 141

44. Model 6 plots of the cellular digitoxin uptake from media containing different concentrations of digitoxin and 15% FBS..... 142

45. Model 6 plot of cellular digitoxin release into media containing 15% FBS..... 144

46. Model 6 plot of cellular digitoxin release into media containing 15% FBS..... 145

47. Model 6 plot of cellular digitoxin release into media containing 15% FBS..... 146

48. Model 6 plot of cellular digitoxin release into media containing 15% FBS..... 147

49. Equilibrium data of the total cell - associated digitoxin as a function of the unbound digitoxin concentration in the media containing 15% FBS..... 149

50. Equilibrium data of the cellular digitoxin bound to Langmuir sites as a function of the unbound digitoxin in media containing 15% FBS..... 150

51. Cellular ouabain uptake data analyzed with Models 1, 3 and 4..... 160

52. Cellular ouabain release data analyzed with Models 1, 3 and 4..... 161

53. Plot of $(C/C_c - C)$ versus the ouabain concentration in the media for the equilibrium ouabain uptake data..... 163

54. Plot of (C/C_m) versus the ouabain concentration in the media for the equilibrium ouabain uptake data..... 164

55. Model 4 plot of ouabain uptake data evaluated with different values of k_r..... 166

56. Model 4 plot of ouabain release data evaluated with different values of k_f..... 167

57. Cellular digitoxin uptake data analyzed with Models 2 and 6..... 171

58. Cellular digitoxin release data analyzed with Models 2 and 6..... 172

NOMENCLATURE

A_c = Surface area per cell, 155×10^{-8} cm.^{2}/RBC

C = Free drug concentration in the suspension medium

C* = Serum bound drug concentration in the suspension medium

C_c = Total drug concentration associated with cells

C_D = Concentrations of drug in the donor side of the dialysis chamber

C_f = Unbound drug concentration in the cell interior

C_i = Total concentration of drug inside the cells

C_m = Concentration of drug that is bound to cell - associated Langmuir sites

C_R = Concentration of drug in the receiver side of the dialysis chamber

C_s = Concentration of drug that is bound to the plasma membrane and linearly related to C

C_T = Total drug concentration in the suspension medium

DPM = Disintegrations per minute

FBS = Fetal bovine serum

H = Volume occupied by cells in 1 ml. of cell suspension

K = Intrinsic partition coefficient, defined by equation (8)

K_b = Digitoxin - fetal bovine serum equilibrium binding constant

K_{bm} = Intrinsic plasma membrane - drug equilibrium binding constant, defined by equation (14)

$K_{bm,ex}$ = Experimental plasma membrane - drug equilibrium binding constant, defined by equation (34)

K_{bh} = Digitoxin - human hemoglobin equilibrium binding constant

K_{bo} = Ouabain - fetal bovine serum equilibrium binding constant

K_{eff} = Effective partition coefficient, defined by equation (37)

K_{ex} = Experimental partition coefficient, defined by equation (32)

K_I = Drug - erythrocyte equilibrium dissociation constant

k = Overall Langmuir rate constant, ml.RBC/mole

k_f = Langmuir adsorption rate constant, cm./sec.

k_r = Langmuir desorption rate constant, moles/$cm.^2$ sec.

N = Number of erythrocytes in 1 ml.RBC, 1.15×10^{10} RBC/ml.RBC

P = Intrinsic permeability coefficient, cm./sec.

P_{eff} = Effective permeability coefficient, defined by equation (36)

Q = Maximum amount of drug that can bind to cell - associated Langmuir sites per cell

R_f = Rate of cellular Langmuir adsorption

R_r = Rate of cellular Langmuir desorption

T = Total amount of drug in 1 ml. of cell suspension

t = Time, min.

$t_{\frac{1}{2}}$ = Half-life to equilibrium, min.

θ = Fraction of cellular Langmuir sites occupied by drug molecules

S = Fraction of serum (or hemoglobin) in the medium

V = Volume of medium in 1 ml. of cell suspension

V_c = Volume of cell, 87×10^{-12} $cm.^3$/RBC

KEY TO OTHER SYMBOLS USED IN THE TEXT

The symbols (a, a', b, b', c, c' etc.) used to define algebraic expressions for a particular model are defined explicitly in each model and are not interchangeable between models.

INTRODUCTION

Much attention has been directed in recent years by scientists of various disciplines to achieve a better understanding of the mechanism of drug transport across membranes. At one extreme, *in vitro* studies utilizing model biological membranes such as monolayers, lipid bilayers, interfacial films of oil-water emulsion droplets and gelatin-oil coascervates have been carried out on the basis that principles which regulate the transport of real and complex systems may be elucidated from these simple systems (1 - 4). At the other extreme, there have been numerous *in situ* investigations of drug transport across the gastric, intestinal, rectal, buccal and cutaneous walls of animals and man (5 - 9). Furthermore, transport studies have been conducted using a variety of suspension cultures as well as human and animal erythrocyte suspensions. These cell suspension sytems, combined with the proper use of physicochemical theories and well designed experiments, are most useful in that they may provide a method that allows for the quantification of parameters that play an important role in drug activity behavior. Ultimately, it is the hope that the cell suspension system approach may answer questions such as cellular drug delivery and bioavailability at the site of action, it may be utilized for the design of proper dosage regimens or it may aid in the appraisal of advantageous modification of the drug itself.

Numerous physical and chemical models have been proposed to account for different transport mechanisms. Some of these models, such as those postulated for the active transport of certain ions (10) and the carrier-facilitated diffusion of many sugars across the erythrocyte membrane (11) may have some truth to them, but are still purely

hypothetical and the lack of knowledge of the precise mechanism for these systems makes their critical evaluation impossible. Very recently, some most promising physical models for the diffusional transport of drugs across cell membranes have been described and experimentally substantiated (12) which, in turn, have provided the impetus for this study.

In the present investigation, an attempt has been made to develop suitable methodology for a cell suspension transport study using human erythrocytes as the experimental model. Although the red cell is one of the simplest in nature, it was selected for this investigation because of its physiological significance, its ready availability, its robust nature which allows for high speed centrifugation without serious damage, its small but rather homogeneous cell volume, its relative stability in various artificial suspension media as well as the fact that it possesses the commom fundamental cellular feature of regulating the uptake and release of substances.

The main objective of this study has been (a) to develop the human erythrocyte suspension system such that it would allow for the quantitative analysis of cellular uptake and release of the cardiac glycosides ouabain and digitoxin by physicochemical techniques and (b) to derive mechanistically instructive physical models which are capable of explaining the kinetic data as well as provide a quantitative assessment of some significant transport parameters of these drugs possessing distinct characteristics such as plasma membrane and serum binding.

The major contribution of this investigation to drug transport studies has been the derivation and successful evaluation of physical models which are believed to be mechanistically unique.

LITERATURE REVIEW

General Transport Studies

The amount of work published on transport studies involving cell suspension systems is voluminous. Basically, these studies fall into one of three categories. They are concerned with either (1) active transport, (2) carrier-facilitated diffusion or (3) simple diffusion. Many of these studies are of a qualitative nature with few attempts made to explain the results in a quantitative manner.

(1) Active Transport - The highly selective nature of the erythrocyte membrane towards sodium and potassium has been of great interest to cell physiologists for many years. The movement of these ions against a concentration gradient has led to the stipulation that the transport must be of an active nature involving chemical energy. Some indications have been obtained that show that the energy for the transfer of sodium and potassium across the membrane is provided by the hydrolysis of ATP. Several models have been proposed to explain in molecular terms the active transport phenomenon and have been summarized by Caldwell (10).

(2) Carrier Facilitated Diffusion - Transport studies with several monosaccharides revealed that the rate of uptake was not dependent on the concentration difference (11,13). A carrier mechanism was postulated to account for the passage of these sugars across the erythrocyte membrane. The carrier was assumed to be in the lipid region of the membrane and to react with the sugar at one surface in order to form a carrier complex. This sugar complex was then assumed to diffuse across the membrane in the direction of its concentration gradient and liberate the sugar molecule into the cell interior. Although experimental agreement was found with the mathematical model for this carrier-facilitated diffusion, it should

still be stressed that the carrier-facilitated diffusion models remain hypothetical.

(3) Simple Diffusion - The hemolytic action of fatty acids was investigated by Bodansky (14) and related to permeability and lipid solubility. It was shown that the rate of diffusion of the acids increased with increasing size of the non-polar groups and for a given fatty acid, within a limited range of concentrations, the rate of diffusion was determined by the concentration. In this early study the author recognized that the hemolysis technique which he used to study the rate of transport of molecules may not have been ideal since the changes produced in the erythrocyte membrane up to the point of complete hemolysis could give erroneous results.

The relative rate of penetration of the lower saturated monocarboxylic acids into erythrocytes were investigated by Green (15). A rapid mixing chamber apparatus was developed and used in conjunction with a spectrophotometer to measure the relative rates of penetration of the acids. The measurement of penetration depended upon the experimental observation that oxyhemoglobin dissociates to a new equilibrium with an increase in the hydrogen ion concentration inside the cell. The C_1 to C_5 acids appeared to penetrate in the order of their relative solubility in oil. The author concluded that molecular size of the C_6 to C_8 acids may be the limiting factor in the rate of penetration and that these higher molecular weight acids of the homologous series may represent a balance of the opposing forces, increasing molecular volume which tends to retard penetration on the one hand and increased solubility in lipid regions which, on the other hand, tends to increase the penetration rate.

Holder and Hayes (16) studied the diffusion characteristics into erythrocytes of eight sulfonamides including five carbonic anhydrase

inhibitors and three anti-bacterial drugs. The penetration rates of these drugs were measured both from whole plasma and from buffered saline media. All drugs appeared to diffuse passively along the concentration gradient into the cells. The rate-limiting step in the passage of these drugs was considered to be the plasma membrane. The aqueous diffusion layer was of little significance in affecting the overall rates of penetration. The authors concluded that the two most important characteristics which influenced the drug uptake rates are plasma - drug binding and lipid solubility, but failed to factor out these effects in their physical model.

Some general physical models for the diffusional transport of drugs across membranes of cells in culture suspensions were described by Ho et al. (17). These models, with modifications to account for particular characteristics of the diffusing solute molecules, such as membrane - and serum - drug binding, have been proven to be most successful in connection with several systems (12).

The uptake of cholesterol by Burkitt lymphoma cells in culture suspension was investigated by Turi et al. (18). The experimental data were evaluated by a physical model involving the rapid equilibration of the solute in the cell interior after permeation through the plasma membrane. Excellent agreement was found between the experimental data and the predictions by the model. Effective permeability and partition coefficients were calculated and found to be a function of the fetal bovine serum level used. The results were consistent with the mechanism in which only the unbound solute in the external medium participates in the transport process.

The same authors studied the kinetics of uptake and release of

desmosterol, cholesterol and β -sitosterol by Burkitt lymphoma cells (19). All three sterols were found to bind to the fetal bovine serum that was present in the external medium. Effective permeability and partition coefficients of the sterols were found to be inversely proportional to the serum concentration. The experimental data was in good agreement with the model for the passive transport of the unbound sterol molecules across the rate-determining plasma membrane.

The transport properties of three cardiac glycosides were determined with Burkitt lymphoma cells by Turi et al. (20). Ouabain exhibited no binding to either the plasma membrane or the fetal bovine serum in the external medium, digoxin bound to the plasma membrane while digitoxin was found to bind to both plasma membrane as well as the fetal bovine serum. The experimental data from uptake and release experiments correlated well with the respective physical models for the diffusional transport of the free drug in the external medium.

The kinetics of adenosine uptake into erythrocytes were investigated by Roos and Pfleger (21). At relatively high adenosine concentrations in the incubation medium, the rate of drug uptake was observed to be directly dependent on the concentration of the drug, but at low concentrations of adenosine, the uptake rate was higher than predicted from simple diffusion and appeared to be similar to a saturable enzymatic reaction. Based on these observations, the investigators proposed a model in which the uptake of adenosine by erythrocytes is the sum of Michaelis-Menten kinetics and the law of diffusion. Which of the two uptake mechanisms predominated depended upon the substrate concentration. Evidence for the validity for this physical model was obtained by comparing the uptake of inosine, adenosine, N^6 - methyladenosine and N^6 - dimethyladenosine. These four purine derivatives possess different octanol/water partition coefficients as a

consequence of the different groups at the C - 6 position of the purine molecule. In the presence of dipyrimadole which inhibited the uptake due to Michaelis-Menten kinetics, the uptake by diffusion correlated well with the partition coefficients of the four derivatives.

Sha'afi et al. (22) investigated the water entry into human erythrocytes under an osmotic pressure gradient using a rapid reaction stop - flow apparatus. The red cell volume changes were determined from 90^{o} scattered light. The permeability coefficient for water was measured as 5.3×10^{-3} cm./sec., whereas the thickness of the unstirred layer around the red cell was estimated as 5.5 μ for their particular experimental conditions.

Physical and Chemical Properties of Human Erythrocytes

Human red cells are the final result of haemopoiesis. After the mitotic division of primitive, undifferentiated cells the nucleus is lost from the normoblast as the reticulocyte is formed. At this stage, the cell still possesses mitochondria, an endoplasmic reticulum and an active aerobic metabolic pathway. Upon maturation of the cells, the aerobic metabolic pathway as well as mitochondria are lost. It is at this stage that the cells are released from the bone marrow into the blood circulatory system. Thus, the human red cells, possessing neither nucleus nor mitochondria, are the end result of a series of changes in structure in the hemopoeitic tissue from a primitive cell to a highly differentiated one (23).

Once in the blood stream, human erythrocytes are biconcave discs and their approximate dimensions are: volume 87 μ^3, surface area 155 μ^2, and outer and inner diameter 8.5 μ and 2.5 μ, respectively (24). This intricate structure is advantageous to the cell as it allows for some

swelling without significantly changing the surface area of the cell.

The hemoglobin-free red cell ghost has a mass of 11 to 12 x 10^{-13} gm. and a membrane density of 1.15 gm./cm^3 (25). The thickness of the erythrocyte plasma membrane was estimated to be 75 Å using electron microscopy techniques (26) and the equivalent pore radius for human red cells was reported to be 4.2 Å (27).

The red cell contains approximately 65% water and 35% solids. Of the solids, the hemoglobin comprises about 32 of the 35% solids; most of the remaining 3% forms the stroma of the red cell which consists largely of protein, phospholipid and cholesterol. Inorganic ions in the erythrocyte include potassium, chloride, bicarbonate and phosphate; of these, potassium is present in the largest amount, being comparable quantitatively to the sodium of the plasma (28).

The model for the plasma membrane structure is still subject to much speculation. The most commonly accepted model today is that proposed by Danielli and Davson (29) which was further modified by Robertson (30). In this model it is accepted that the backbone structure of the unit membrane is a bimolecular lipid leaflet arranged with hydrophobic tails opposing each other end to end on the inside and the polar heads on the outside covered with layers of protein. More recently, several new models for the ultrastructure of biological membranes have been proposed.

The first challenge to the concept of the unit membrane was raised by Sjostrand (31), who studied mitochondrial membranes and smooth - surfaced membranes of mouse kidney cells using high resulution electron microscopy technique. Perfectly cross-sectioned membranes showed a definite bridging at relatively uniform intervals between the outer and inner membrane. These observations led the author to the following innovative

membrane model: membranes are made up from many globular subunits. These globular subunits would exist of lipids in the form of small micelles with the hydrocarbon end of the lipids extended into the inner side of the micelles. The polar surfaces of the micelles are coated with proteins to prevent the fusion of the lipid micelles. Furthermore, protein molecules, especially those present within the septa, were to stabilize the globular lipid structure.

Based on much of the information gathered from recent membrane studies, Green and Perdue (32) produced what they believed to be a more biochemically acceptable model for the ultra structure of membranes. Each membrane is assumed to be comprised of a specific lipoprotein repeating unit. These repeating units, consisting of a basepiece essential for the maintenance of the membrane structure and a detachable sector, are characteristic in structure and size for any particular membrane but may vary considerably in chemical composition and enzymatic function.

Other, more complicated membrane models have been proposed in recent years and the reader is referred to an excellent review article by Hendler (33). The overall view at the present time concerning the ultrastructure of membranes seems to be represented best by the lipid bilayer continuum with local areas either permanently modified or possessing the potential for transient modification in order to accomplish certain specific functions.

The chemical composition of the erythrocyte membrane has been largely determined from erythrocyte ghosts. The chemical analysis of such ghosts has shown that the membrane is predominantly a mixture of proteins, phospholipids and carbohydrates. The total phospholipid content was found to be equivalent to 4.1 to 4.7 x 10^{-12} mg./ μ^2 of cell surface or about 40%

of the total membrane mass and to consist mainly of a mixture of lecithin, sphingomylin and cephalin (34-36). A total fatty acid and cholesterol composition of 105 and 81 μ g x 10^{-14}/ μ^2 of red cell membrane, respectively, was reported for the erythrocyte ghosts (37,38). To date, proteins of the red cell ghosts have been the least well characterized of the membrane components; and this may well be due to the difficulty of first getting rid of hemoglobin. It has been shown, however, that proteins constitute approximately 52% of the plasma membrane mass and that nine or ten principle polypeptides comprise about 80% of the total protein mass. A possible arrangement for the major erythrocyte membrane proteins was proposed by Steck (39), where the membrane glycoproteins are assumed to penetrate into or through the lipoidal region of the membrane, with all their carbohydrates exposed to the extracellular space. The remaining proteins are predicted to be less tightly bound by specific protein association at the plasma membrane interface.

Electrophoretic mobility studies of human red cells (40) indicate that the plasma membrane possesses a negative surface charge at the physiological pH and that single cells in saline medium, Rouleaux columns and single cells in plasma all migrate with the same velocity in an electrical field of fixed strength which indicates that protein or other plasma components are not essential in order to maintain the surface charge. The relationship between the electrophoretic mobility of erythrocytes and pH shows that the mobility has a maximum at pH 9.4 and falls with decreasing pH to reach zero mobility at about pH 2. Various kinds of maltreatment of erythrocytes such as successive washing with saline or freezing and thawing to produce red cell ghosts indicated little effect on the electrophoretic mobility (41), thus suggesting that the surface

charge is tightly bound to the plasma membrane.

A major advance in the investigations of the electrophoretic mobility of erythrocytes was achieved when the nature of the surface charge was established unequivocally as due to the carboxyl group of sialic acid (42). Treating erythrocytes with neuraminidase resulted in a marked reduction of the mobility at pH 6.4 and the isoionic point increased from about 2 to approximately 5. For human erythrocytes, the number of sialic acid molecules present on the plasma membrane was estimated to be 24×10^6.

Cardiac Glycosides

Cardiac glycosides have a long and interesting history. Physicians were praising the medicinal properties of whole leaf preparations from Digitalis purpurea as early as the 16th century. Since that time, there has been a gradual increase in the use of digitalis like substances and today the cardiac glycosides are referred to as venerable and irreplaceable drugs. Obtained mainly from certain plants, these compounds are characterized by their high specific and powerful action which they exert upon the cardiac muscle. In the proper dosage, many of them are very valuable in the treatment of congestive heart failure due to heart disease or other causes. These drugs stimulate the heart to a greater contractile activity and restore its original tonicity.

Some of the most widely used cardiac glycosides are ouabain, digoxin, digitoxin, lanatoside C and strophanthin. From a therapeutic point of view, the differences in action of any of these glycosides are purely quantitative and not qualitative, i.e., they vary only in the rate, intensity and duration of their action but not in their manner. The nature of action of these compounds at the molecular level is yet to be specifically elucidated. However, what is known is that only very small quanti-

ties are required to obtain the desired therapeutic effects from these drugs. For example, for ouabain the initial dose is 0.3 to 0.5 mg. followed at 30 min. intervals by 0.1 mg. until the desired effect is obtained or a total of 1.0 mg. is reached; whereas for digitoxin the initial dose is 0.6 mg. followed by .4 mg. every six hours until the therapeutic effect is obtained (43).

The binding properties of cardiac glycosides to serum proteins have been studied with the primary aim being the establishment of possible connections between the serum - glycoside binding magnitude and the duration of the therapeutic effects of these glycosides as well as the speed with which the full effect of the dose of any of them is achieved.

Farah (44) studied the binding properties of various cardiac glycosides with sera and serum albumins of different species using dialysis methods. Digitoxin, foliandrin and digilanid were shown to combine with serum proteins while both g- and k-strophanthin did not.

Using salt precipitation and dialysis methods, Spratt and Okita (45) demonstrated that digitoxin binds to serum proteins. The results of their study agreed qualitatively but not quantitatively with those of previous workers who found that digitoxin binding by serum proteins is correlated with the albumin content of protein fractions.

Lukas and Peterson (46) assayed digitoxin in plasma, urine and stool of patients maintained on this drug. The analysis, using equilibrium dialysis, revealed that 97% of the digitoxin in human plasma is reversibly bound to protein and that the binding is almost entirely attributable to an interaction of the glycoside with plasma albumin. Thus, only 3% of the plasma digitoxin exists in a freely diffusable unbound state. The total concentration of digitoxin in the red cells was

estimated to be 2% of that in the plasma.

The therapeutic effect and duration of action of the glycosides are, in fact, closely related to their protein binding characteristics. Digitoxin, which extensively binds to serum proteins, is relatively slow acting, reaching its full effect in about 6 hours but the duration of action is much greater than those of ouabain or digoxin. The half-life of digitoxin in man is approximately 106 hours (47) and 30 days are required for the complete elimination of a single dose. A single injection of ouabain, a drug which does not bind to serum proteins, produces its full effect within 2 hours but the duration of action of this drug, having a biological half-life of 22 hours (47), is much shorter. Digoxin is intermediate in both the development of its full effect as well as the duration of its action.

More recently, the cardiac glycosides have received much attention by physiologists for reasons other than their therapeutic usefulness. In 1953, Schatzmann (48) demonstrated that the active transport of sodium and potassium in red blood cells was prevented in the presence of low concentrations of the cardiac glycoside strophanthin k. Since then, a great deal of work has been done to reveal the effects that various cardiac glycosides have on the transport of sodium, potassium and certain other ions in a great variety of tissues. It was believed that such studies could, at least in principle, yield information regarding the mechanism of active transport. The earlier studies on the action of cardiac glycosides on ion transport have been reviewed by Glynn (49).

By incubating human red blood cells in media containing tritiated ouabain and by measuring the sodium and potassium fluxes, Hoffman (50) showed that the uptake of ouabain by the red cells with time was associated

with a parallel decrease in the sodium - potassium pump activity. Complete inhibition of the pump was observed when approximately 200 ouabain molecules were bound to each cell. Thus, the author concluded that the glycoside interacted very specifically with sites that are associated with the sodium pump mechanism.

The possible cellular localization of the cardiac glycoside receptor sites were investigated by Smith et al. (51). For this purpose, ouabain and digoxin were coupled to several macromolecules. These high molecular weight conjugates were expected to enter the intact myocardial or red blood cell at very low rates. Consequently, any pharmacologic activity observed could be attributed to the interaction of the conjugate with a cell surface receptor. The effects of these conjugates were studied in several glycoside - sensitive systems including the contractile response of isolated cardiac muscle, the active rubidium (Rb^+) uptake by erythrocytes, the enzymatic activity of isolated myocardial microsomal (Na^+ and K^+) - activated ATPase and the enzymatic activity of solubilized erythrocyte (Na^+ and K^+) - activated ATPase. With the solubilized red cell system, the biological activity observed with these conjugates was comparable to that exhibited by the free cardiac glycosides thereby ensuring that the chemical reaction used to couple the macromolecules to the glycosides did not inactivate the drugs. In the other systems, the macromolecular-glycoside conjugates were 100- to 1,000 - fold less active than the free glycosides, and the small amount of activity measured was attributed to persistent contamination of the conjugates with free cardiac glycosides. The conclusions drawn by the authors were that, if the receptors for the cardiac glycosides are associated with the plasma membrane, then "they may lie deep within it".

Gardner and Conlon (52)[1] studied the effect of sodium and potassium on ouabain binding by human erythrocytes. Human red cells were incubated for various lengths of time in media with differing cation composition and containing a wide range of ouabain - ^{3}H concentrations. The authors found a nonlinear relationship between ouabain binding and the ouabain concentration in the external medium and reported that the cellular ouabain binding, in fact, followed a Langmuir isotherm. From the saturation plateau of the Langmuir isotherm it was estimated that there were approximately 1,000 ouabain binding sites per human erythrocyte. Furthermore, by hemolysing red cells that had been incubated long enough in the presence of tritiated ouabain to reach complete cellular saturation followed by high speed centrifugation of the lysed red cell suspension, the investigators were able to demonstrate that 98% of the total cellular radioactivity was associated with the plasma membrane, i.e., essentially all the cellular ouabain was bound to the red cell membrane and only an insignificant amount had permeated into the cell interior. Replacing some of the sodium in the suspension medium with potassium or choline resulted in a reduction of both the rate of ouabain uptake by the erythrocytes and the cellular saturation value. These results led to the proposal of a model which postulated that the erythrocyte membrane contains a finite number of receptors, each composed of a glycoside - binding site and a cation - binding site. When sodium occupies the cation - binding site, the affinity of the glycoside - binding site for ouabain is increased; while, when potassium or choline occupies the cation - binding site, the affinity of the glycoside - binding site for ouabain is decreased.

---

1. This investigator became aware of this publication only after more than half of this study was completed.

Finally, it is shown in the study that the ouabain - binding site also has an affinity for digitoxin and its aglycone digitoxigenin as well as for digoxin but not for other structurally similar steroids such as progesterone, testosterone, cortisone, hydrocortisone and aldosterone.

The uptake of digoxin by human erythrocytes was studied by Gardner et al. (53). The findings of these investigators were that the accumulation of digoxin by intact human red cells is a result of two processes: binding of digoxin to the plasma membrane and uptake of digoxin across the membrane into the cell interior. The binding of the drug to the erythrocyte membrane occurred as a saturable function of the extra cellular concentration with approximately 1,000 digoxin receptor sites per cell and was reversible though at an apparently much slower rate than uptake. The binding was also dependent upon the cation composition of the suspension medium and it was inhibited by other glycosides such as ouabain, digitoxin and digitoxigenin. In addition to the saturable binding of digoxin to the membrane, a linear component of digoxin accumulation was observed and this component was assumed to represent uptake of digoxin across the erythrocyte membrane into the cell.

STATEMENT OF THE PROBLEM

Although many transport studies have been carried out utilizing cell suspension systems and numerous models proposed for various transport mechanisms, it is nevertheless obvious from the previous section that there is an existing need for suitable methodology which can further assess the phenomenon of drug transport in cell suspension systems both quantitatively and mechanistically.

The purpose of this investigation is to fill some of the existing voids by thoroughly examining the importance and relationships between the various factors involved in cellular drug transport. To achieve this aim, the following objectives were considered to be essential:

(1) The derivation of mechanistically instructive physical models which are mathematically and experimentally accessible.

(2) The development of an experimental cell suspension transport system that could be readily tested in a quantitative manner by physicochemical techniques.

As will be shown, the approach to the problem in the above described manner was not only elucidative with respect to the ouabain - and digitoxin - erythrocyte transport mechanism but also allowed for the factorization and quantification of such transport related parameters as drug - plasma membrane adsorption and desorption rate constants, drug - erythrocyte binding and drug - serum binding.

CONSIDERATIONS IN THE APPROACH TO THE INVESTIGATION

The purpose of a research project to a large measure, determines the approach to the problem. Thus, the development of meaningful methodology for the establishment of the mechanistic understanding and the quantitative assessment of the cellular drug transport phenomenon requires that two important qualifications be considered in the approach: the conception of physical models and the design of experiments.

The purpose of the physical model is to provide a theoretical frame of reference for the transport process. It must be based on mechanistically sound physical concepts and it should encompass all the significantly relevant parameters involved in the transport of drug molecules by cells. Ideally, the model will also provide guidelines to the design of experiments, but more importantly, it must allow for rigorous experimental testing by physicochemical techniques. Only when these criteria have been met and when the model is well capable of explaining the kinetic data for both drug uptake and drug release experiments does the model achieve its heuristic purpose, for only then can it serve in the interpretation of experimental data to obtain quantitative estimates of transport related parameters and only then will it lead to definite conclusions regarding the drug transport mechanism itself.

The design of suitable experiments for the transport study was largely dictated and directly related to the physical models to be examined. The basic experiments consisted of collecting kinetic data for the uptake and release of the cardiac glycosides ouabain and digitoxin by human erythrocytes under various experimental conditions. It was felt that by changing the drug concentration in the transport systems over a wide range and by altering the composition of the suspension medium, the

physical models would be subjected to the most severe scrutiny and, in turn, this approach would allow for the elimination of an unsuitable model. The basic transport studies were further supplemented by experiments that would appraise and quantify such transport related factors as the binding of the drugs to serum components, the plasma membrane and the cell interior.

In order to eliminate any possible experimental uncertainties in these systems, the establishment of reliable and reproducible baseline experiments was considered to be of major importance. In this regard, considerable effort was directed towards the maintenance of a constant cell concentration and cell volume throughout a given experiment, the integrity of cells during the experiments as well as the effect of cell storage on the transport properties. Furthermore, sampling techniques for the red blood cell had to be developed which included the evaluation of entrapment of extracellular radioactivity in the erythrocyte samples and a novel, more expeditious method for the preparation of erythrocytes for scintillation analysis was necessary. The possibility of biodegradation of the cardiac glycosides in the presence of erythrocytes, which could lead to erroneous interpretations of the experimental results, made it imperative that the radioactive drugs be extracted from both the suspension medium as well as the intact erythrocytes in order to analyze their purities and stabilities. Finally, the specific activity of the tritiated glycosides had to be determined in order to allow for the conversion of the measured radioactivity in samples to the chemically conventional molar unit.

THEORETICAL CONSIDERATIONS

Six physical models are presented in the following section that are most appropriate for the experimental systems in this study. They represent various sets of possible physical processes that occur during drug uptake by cells from the suspension medium.

Model 1. Diffusion of the drug into and/or through the plasma membrane followed by rapid linear binding of the drug within the membrane and/or the cell interior. No binding of the drug molecules to components in the suspension medium.

Model 2. Instantaneous and reversible linear binding of the drug to the plasma membrane and serum components in the suspension medium. Diffusion of the free drug into and/or through the plasma membrane followed by rapid equilibration in the plasma membrane and/or in the cell interior.

Model 3. Diffusion of the drug molecules into or through the plasma membrane followed by rapid binding onto Langmuir sites beyond the rate-determining barrier. No significant binding of drug molecules to components in the suspension medium.

Model 4. Slow Langmuir binding of drug molecules to the plasma membrane. No binding of drug molecules to components in the suspension medium.

Model 5. Instantaneous and reversible binding of the drug to the plasma membrane and components of the suspension medium followed by slow Langmuir binding of the free drug molecules to the plasma membrane.

Model 6. Instantaneous, reversible and linear binding of the drug to serum components present in the external medium. Rapid per-

meation and equilibration of the free drug molecules in the cell interior followed by slow binding of the free drug molecules to Langmuir sites located on the plasma membrane.

Other models representing more complex physical situations are certainly possible. However, the present discussion will be restricted to these six models.

Model 1

The following simple passive transport model for the quasi-steady state rate of uptake of non-ionized molecules by a cell in suspension was used by Turi (12) to analyze the data of ouabain transport into Burkitt lymphoma cells

$$\frac{dC_i}{dt} = \frac{A_c P}{V_c} \left(C - \frac{C_i}{K} \right) \qquad \text{(Eq. 1)}$$

where P is the intrinsic permeability coefficient of the plasma membrane, A_c is the surface area of the cell, V_c is the cell volume, C is the drug concentration of the external medium, C_i is the total drug concentration inside the cell and K is the intrinsic partition coefficient. This model is shown in Figure 1.

Mass balance for the drug requires that

$$T = V C + H C_i \qquad \text{(Eq. 2)}$$

where T is the total amount of drug in one ml. of cell suspension, and V and H are the volume of medium and the volume of the cells in one ml. of suspension, respectively.

The above mass balance equation is applicable only to suspensions in which the cell volume distribution is narrow, as is the case with human red blood cells. Otherwise, the cell volume distribution should be taken into account for systems containing cells of non-uniform cell volumes.

Solving equation (2) for C and substituting into equation (1) yields

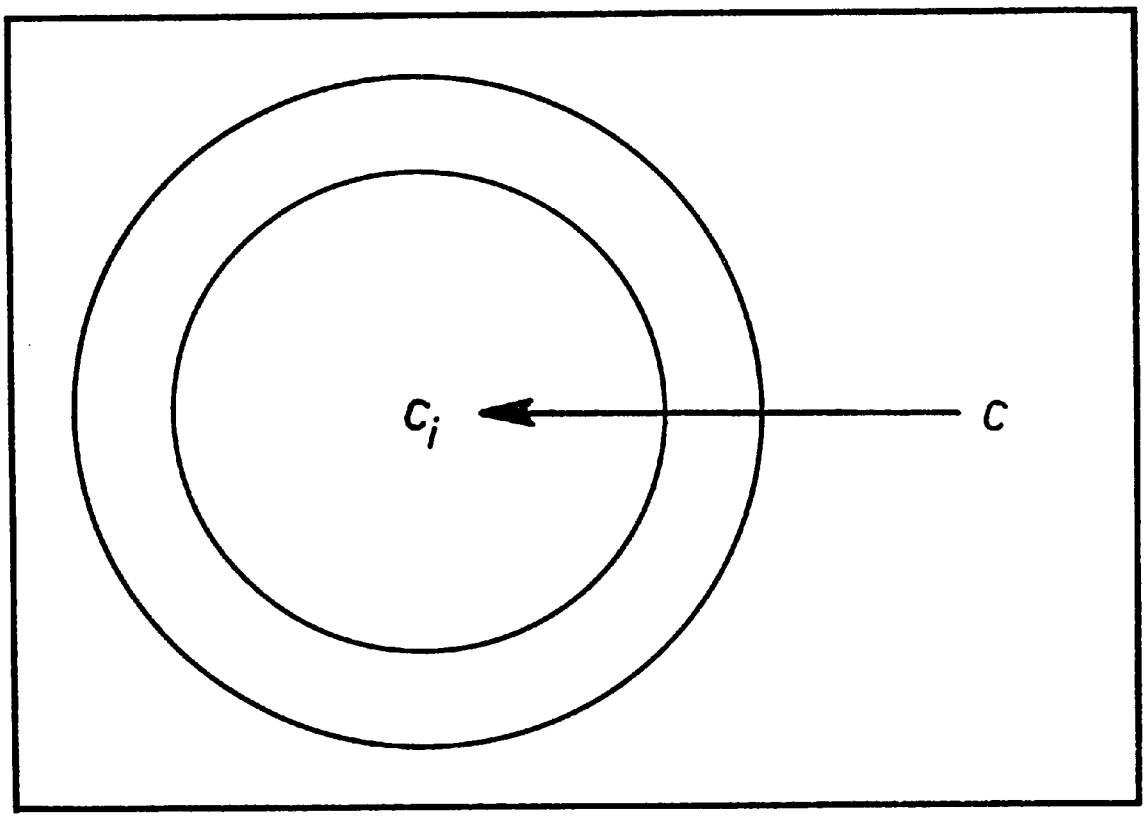


Figure 1. Schematic description of Model 1. Simple diffusion of the drug through the plasma membrane into the cell interior. C and C_i represent the drug concentrations of the suspension medium and the cell interior, respectively.

$$\frac{dC_i}{dt} = \frac{A_c P}{V_c} (a - b C_i) \qquad \text{(Eq. 3)}$$

where a=(T/V) and b=(H /V) + (1/K).

Integrating equation (3) renders the solution for Model 1

$$\ln (1 - \frac{b C_i}{a}) = - \frac{A_c b P t}{V_c} \qquad \text{(Eq. 4)}$$

Rearrangement of equation (4) leads to the uptake function ($U.F._1$) for Model 1

$$U.F._1 = (- \frac{V_c}{60 b A_c}) \ln (1 - \frac{b C_i}{a}) = P t \qquad \text{(Eq. 5)}$$

where the factor 60 is required in order to determine the permeability coefficient, P, in units of cm./sec. from the slope of the $U.F._1$ versus time in min. plot.

The exponential form of equation (5) gives the total cellular concentration at any time

$$C_i = \frac{a}{b} [1 - \exp (- \frac{60 A_c b P t}{V_c})] \qquad \text{(Eq. 6)}$$

The intrinsic permeability coefficient can be evaluated from experimental data with equations (5 or 6) provided K is known and it can also be obtained from initial kinetic data. For initial rates, equation (4) reduces to

$$C_i = \frac{a A_c P t}{V_c} \qquad \text{(Eq. 7)}$$

Therefore, the intrinsic permeability coefficient, P, can be obtained from the initial slope of the C_i versus time in sec. plot.

The intrinsic partition coefficient is determined from equilibrium conditions, i.e., when $(dC_i/dt)_{t=\infty} = 0$ and is defined as

$$K = C_i/C \qquad (t = \infty) \qquad \text{(Eq. 8)}$$

An expression for the half-life to equilibrium for this model can be found in this manner. With the condition that $C_i = \frac{1}{2} C_{i(\infty)}$ when $t = t_{\frac{1}{2}}$, equation (6) can be written as

$$\frac{1}{2} C_{i(\infty)} = \frac{a}{b} \left(1 - \exp \frac{- 60 A_c b P t_{\frac{1}{2}}}{V_c} \right) \qquad \text{(Eq. 9)}$$

whereas in the limit, when $t \to \infty$, equation (6) reduces to

$$C_{i(\infty)} = \frac{a}{b} \qquad \text{(Eq. 10)}$$

Combining equations (9 and 10) renders the expression for the half-life to equilibrium as

$$t_{\frac{1}{2}} = \frac{(\ln 2) V_c}{b A_c P} \qquad \text{(Eq. 11)}$$

Thus, the intrinsic permeability coefficient can also be estimated from the half-life to equilibrium provided the intrinsic partition coefficient is known.

In the above physical model, the rate-determining barrier for the passive diffusion of molecules into the cell is attributed to the plasma membrane. Drug molecules that permeate the plasma membrane are assumed to instantaneously distribute themselves in the cell interior. The effect of the aqueous diffusion layer in the drug uptake is taken to be negligible. Furthermore, this model assumes that adsorption of drug molecules to the cell membrane as well as to serum components present in the external medium is not significant.

Model 2

This model assumes that the drug molecules bind instantaneously, linearly and reversibly both to the cell plasma membrane and to the serum present in the suspension medium. The unbound drug molecules and the mem-

brane bound drug molecules are able to permeate the plasma membrane while the serum bound species do not. A schematic diagram of this model is shown in Figure 2.

The present model represents a combination of two models previously derived by Turi (12). The mathematical treatment of this new model requires that plasma membrane and serum binding effects be considered in equation (1) in the following manner.

The distribution of drug in this system is given by the mass balance relationship.

$$T = V\,C + V\,C^{*} + H\,C_c \qquad \text{(Eq. 12)}$$

where C^{*} is the serum bound drug concentration in the medium and C_c is the total cellular drug concentration. The above mass balance equation, as in Model 1, requires that the cell volume distribution be narrow.

The total drug concentration in the cells, C_c, is given by

$$C_c = C_i + C_s \qquad \text{(Eq. 13)}$$

where C_s is the concentration of drug that is instantaneously and reversibly bound to the plasma membrane. This membrane bound drug concentration is assumed to be linearly related to the concentration of unbound drug in the external medium. Thus,

$$C_s = K_{bm}\,C \qquad \text{(Eq. 14)}$$

where K_{bm} is the intrinsic plasma membrane equilibrium binding constant.

The interaction between the free drug and serum components in the medium can be expressed by the equilibrium reaction:

$$\text{Drug} + \text{Serum} \underset{}{\overset{K_b}{\rightleftharpoons}} \text{Drug} \cdot \text{Serum}$$

Assuming that the number of binding sites of the serum components is very large with respect to the free drug molecules in the external medium, the

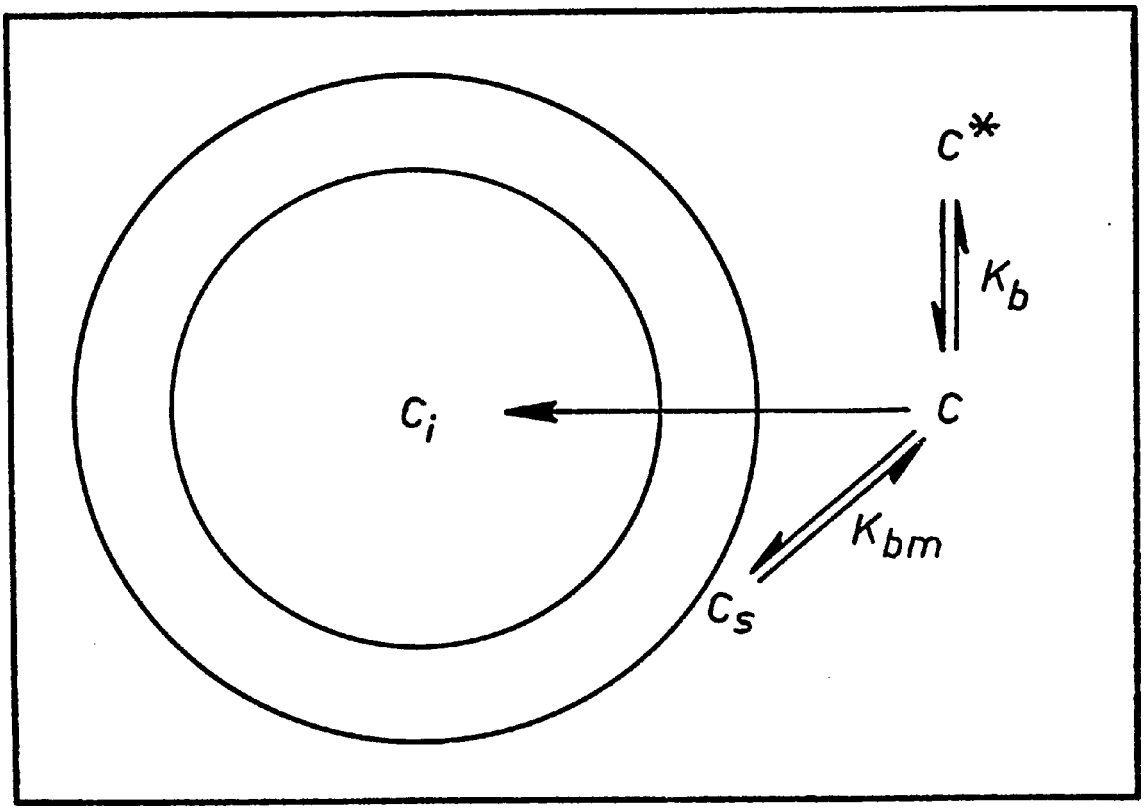


Figure 2. Schematic description of Model 2. The free drug in the suspension medium is in equilibrium with serum - bound and plasma membrane - bound drug. The membrane is permeable only to unbound drug molecules. The C and C* are the free and serum - bound drug concentrations in the medium, whereas C_i and C_s represent the drug concentrations inside the cell and on the cell surface, respectively. The K_b and K_{bm} are the equilibrium binding constants.

serum - drug equilibrium binding constant, K_b, is given by

$$K_b = C^*/SC \qquad \text{(Eq. 15)}$$

where S is the volume fraction of serum in the medium. After rearranging equation (15), the serum bound drug concentration is

$$C^* = K_b\ S\ C \qquad \text{(Eq. 15a)}$$

Substituting equation (15a) into equation (12) gives

$$T = V\ (\ 1 + K_b\ S\ )\ C + H\ C_c \qquad \text{(Eq. 16)}$$

With the use of equation (14), equation (16) can be written as

$$T = \frac{V\ (\ 1 + K_b\ S\ )}{K_{bm}}\ C_s + H\ C_c \qquad \text{(Eq. 17)}$$

and, upon rearrangement, the cell surface concentration is

$$C_s = \frac{T\ K_{bm}}{V\ (\ 1 + K_b\ S\ )} - \frac{H\ K_{bm}}{V\ (\ 1 + K_b\ S\ )}\ C_c \qquad \text{(Eq. 17a)}$$

The fact that, in this model, the free drug binds reversibly to the plasma membrane makes it impossible to experimentally distinguish the intracellular drug concentration, C_i, from the total concentration associated with the cell. For this reason, it is best to express the terms dC_i/dt and $(C - C_i/K)$ in equation (1) in terms of the total cellular drug concentration, C_c, which is experimentally accessible.

The term dC_i/dt in equation (1) can be modified using equation (13) to give

$$\frac{dC_i}{dt} = \frac{d}{dt}\ (\ C_c - C_s\ ) \qquad \text{(Eq. 18)}$$

Substituting the expression for the cell surface concentration (Eq. 17a) into equation (18) and differentiating with respect to time yields

$$\frac{dC_i}{dt} = \left(1 + \frac{H\, K_{bm}}{V\,(1 + K_b\, S)} \right) \frac{dC_c}{dt} \qquad \text{(Eq. 19)}$$

The term $(C - C_i/K)$ in equation (1) can be changed with equations (13, 16 and 17a) to give

$$(C - C_i/K) = \frac{T\left(1 + \frac{K_{bm}}{K}\right)}{V\,(1 + K_b S)} - \left[\frac{H\left(1 + \frac{K_{bm}}{K}\right)}{V\,(1 + K_b S)} + \frac{1}{K} \right] C_c \qquad \text{(Eq. 20)}$$

Substituting the expressions obtained for dC_i/dt and $(C - C_i/K)$, (equations 19 and 20 respectively), into equation (1) gives the differertial equation for Model 2

$$\left[1 + \frac{H\, K_{bm}}{V(1 + K_b S)}\right] \frac{dC_c}{dt} = \frac{A_c\, P}{V_c} \left[\frac{T\left(1 + \frac{K_{bm}}{K}\right)}{V(1 + K_b S)} - \left[\frac{H\,\left(1 + \frac{K_{bm}}{K}\right)}{V(1 + K_b\, S)} + \frac{1}{K} \right] C_c \right] \qquad \text{(Eq. 21)}$$

For simplicity, letting

$$a = \frac{H}{V\,(1 + K_b\, S)}$$

$$b = \frac{T\left(1 + \frac{K_{bm}}{K}\right)}{V\,(1 + K_b S)}$$

and

$$c = \frac{H\left(1 + \frac{K_{bm}}{K}\right)}{V\,(1 + K_b S)} + \frac{1}{K}$$

equation (21) becomes

$$\frac{dC_c}{dt} = \frac{A_c\, P}{V_c(1 + a\, K_{bm})} (b - c\, C_c) \qquad \text{(Eq. 22)}$$

The integration of equation (22) leads to the linear uptake function ($U.F._2$) for Model 2

$$U.F._2 = \frac{V_c\,(1 + a\, K_{bm})}{60\, c\, A_c} \ln \left(\frac{b - c\, C_{c(o)}}{b - c\, C_c} \right) = P\, t \qquad \text{(Eq. 23)}$$

where $C_{c(o)}$ is the total cellular concentration at zero time which, in effect, is equal to the initial surface concentration. The factor 60 is necessary for determining the permeability coefficient, P, in units of cm./sec. from the plot of U.F.$_2$ *versus* time in min. Before the uptake function can be plotted, the magnitudes of K_{bm}, K_b and K must be found. The determination of these phenomenological constants will be discussed later.

The exponential form of equation (23) gives the total cell concentration at any time:

$$C_c = \frac{b}{c} - \frac{b - c\,C_{c(o)}}{c} \exp\left[- \frac{60\,c\,A_c\,P\,t}{V_c(1 + a\,K_{bm})} \right] \qquad \text{(Eq. 24)}$$

Equations (23 and 24) are important because they allow for the estimation of the intrinsic permeability coefficient from kinetic data. It is predicted that a plot of U.F.$_2$ *versus* time for systems containing different serum concentrations will give an identical positive slope, the magnitude of which is equal to the intrinsic permeability coefficient.

An expression for the half-life to equilibrium for the drug uptake process can be obtained in this manner. Differentiating equation (22) leads to the following differential equation

$$\frac{d^2C_c}{dt^2} = \left[- \frac{A_c\,c\,P}{V_c(1 + a\,K_{bm})} \right] \frac{dC_c}{dt} \qquad \text{(Eq. 25)}$$

which has the general solution

$$C_c = u_1 + u_2 \exp\left[- \frac{c\,A_c\,P}{V_c(1 + a\,K_{bm})} \right] \qquad \text{(Eq. 26)}$$

The integration constants u_1 and u_2 can be evaluated with the following boundary conditions: When $t = \infty$, then $C_c = C_{c(\infty)}$ and $u_1 = C_{c(\infty)}$; when $t = 0$, then $C_c = C_{c(o)}$ and $u_2 = (C_{c(o)} - C_{c(\infty)})$. Substituting the

values obtained for u_1 and u_2 into equation (26) and with the condition that $C_c = \frac{1}{2}(C_{c(o)} + C_{c(\infty)})$ when $t = t_{\frac{1}{2}}$, one can write the half-life to equilibrium as

$$t_{\frac{1}{2}} = \frac{(\ln 2)\, V_c\, (1 + a K_{bm})}{c\, A_c\, P} \qquad \text{(Eq. 27)}$$

Equation (27) shows that the intrinsic permeability coefficient is inversely proportional to the half-life in the drug uptake process.

The experimental partition coefficient, K_{ex}, is an apparent partition or distribution coefficient. It can be evaluated from equilibrium conditions, i.e. when $(dC_c/dt)_{t=\infty} = 0$ and is defined as

$$K_{ex} = C_c / C_T \qquad (t = \infty) \qquad \text{(Eq. 28)}$$

where C_T, the total drug concentration of the medium, is

$$C_T = C + C^* \qquad \text{(Eq. 29)}$$

Utilizing equations (13 and 29), equation (28) becomes

$$K_{ex} = \frac{C_i + C_s}{C + C^*} \qquad (t = \infty) \qquad \text{(Eq. 30)}$$

and with equations (14 and 15a)

$$K_{ex} = \frac{C_i + K_{bm} C}{(1 + K_b S)\, C} \qquad (t = \infty) \qquad \text{(Eq. 31)}$$

Using the basic definition of $K = C_i/C$ when $t = \infty$,

$$K_{ex} = \frac{K + K_{bm}}{1 + K_b S} \qquad (t = \infty) \qquad \text{(Eq. 32)}$$

Then, by rearranging equation (32), one obtains the intrinsic partition coefficient for the system in which the drug binds both to the plasma membrane and the serum that is present in the medium, i.e.

$$K = K_{ex}\, (1 + K_b S) - K_{bm} \qquad (t = \infty) \qquad \text{(Eq. 32a)}$$

The linear form of equation (32a) is

$$\frac{1}{K_{ex}} = \frac{K_b}{K + K_{bm}} (S) + \frac{1}{K + K_{bm}} \qquad (t = \infty) \qquad \text{(Eq. 32b)}$$

A plot of $1/K_{ex}$ versus (S) permits the direct evaluation of K_b, which is equal to the ratio of the slope to the intercept. Also, once the intrinsic partition coefficient, K, or the membrane binding constant, K_{bm}, is known for a particular drug-cell suspension system, it is possible to calculate one or the other of the constants from the intercept. Generally, it is easier to obtain K_{bm} from the experimental data, as will be seen. The estimation of serum binding and plasma membrane binding constants by the application of equation (32b) is of particular interest with systems in which the rate of drug uptake into the cells is too rapid to allow for reliable sampling at initial times of the drug uptake experiment. Furthermore, the K_b found by the analysis of the kinetic data can be corroborated by dialysis studies.

A relationship between the intrinsic plasma membrane binding constant, K_{bm}, which is defined in equation (14) in terms of the free drug concentration in the medium, and the experimental plasma membrane binding constant, $K_{bm,ex}$, when there is serum binding in the medium can be deduced from

$$C_s = K_{bm,ex} C_T \qquad \text{(Eq. 33)}$$

Substituting equations (14, 15a and 29) into equation (33) yields

$$K_{bm} = K_{bm,ex} (1 + K_b S) \qquad \text{(Eq. 34)}$$

The intrinsic plasma binding constant, K_{bm}, and the serum binding constant K_b, can also be evaluated from initial transport data in this manner. Combining equations (14, 15a and 29) leads to

$$\frac{C_T}{C_s} = \frac{K_b}{K_{bm}} (S) + \frac{1}{K_{bm}} \qquad (t = 0) \qquad \text{(Eq. 35)}$$

With the use of equation (35) the equilibrium binding constants can be evaluated from a plot of (C_T/C_s) *versus* (S). It follows that the K_{bm} can be calculated from the intercept and K_b is equal to the slope divided by the intercept. It is important to note that equation (35) is applicable only to initial transport data, i.e., when the drug has only adsorbed to the plasma membrane and not yet permeated into the cell interior. Therefore, the evaluation of the binding constants by this method is useful with systems in which the drug permeates the cell membrane at a relatively slow rate ($P < 10^{-6}$ cm./sec.) thereby allowing either experimental sampling equivalent to "zero time" or extrapolation of experimental data with reasonable accuracy to zero time[1].

The intrinsic plasma membrane binding constant, K_{bm}, can also be evaluated from initial transport data by means of equation (14). The slope of a plot of C_s *versus* C is equal to K_{bm}. The determination of K_{bm} by the use of equation (14) requires that the suspension medium contain no serum. Otherwise, the same experimental conditions are required as those ascribed to equation (35).

In the derivation of the uptake function, described by equation (23), the effect of serum-drug binding has been factored out thereby allowing the computation of the intrinsic permeability coefficient from the slope of the $U.F._2$ *versus* time plot. The uptake function can also be derived for this model in terms of effective or experimental parameters as shown below.

---

1. The analysis by centrifugation used in this study has a sampling time of approximately two minutes. More expeditious sampling techniques would allow for the evaluation of binding constants of more rapidly permeating drugs by means of equation (35).

The effective permeability coefficient, P_{eff}, and the effective partition coefficient, K_{eff}, can be defined as[1]

$$P_{eff} = \frac{P}{1 + K_b S} \qquad \text{(Eq. 36)}$$

and

$$K_{eff} = \frac{K}{1 + K_b S} \qquad \text{(Eq. 37)}$$

The rearrangement of equation (21) gives

$$\left[1+ \frac{H K_{bm}}{V(1+K_b S)}\right] \frac{dC_c}{dt} = \frac{A_c P}{V_c(1+K_b S)} \left[\frac{T(1+\frac{K_{bm}}{K})}{V} - \left[\frac{H(1+\frac{K_{bm}}{K})}{V} + \frac{1+K_b S}{K} \right] C_c \right] \qquad \text{(Eq. 21a)}$$

and with equations (36 and 37)

$$\left[1+\frac{H K_{bm} K_{eff}}{V K}\right] \frac{dC_c}{dt} = \frac{A_c P_{eff}}{V_c} \left[\frac{T(1 + \frac{K_{bm}}{K})}{V} - \left[\frac{H (1 + \frac{K_{bm}}{K})}{V} + \frac{1}{K_{eff}} \right] C_c \right] \qquad \text{(Eq. 38)}$$

Then by letting

$$a' = \frac{H K_{eff}}{V K}$$

$$b' = \frac{T (1 + \frac{K_{bm}}{K})}{V}$$

and

$$c' = \frac{H (1 + \frac{K_{bm}}{K})}{V} + \frac{1}{K_{eff}}$$

one can write equation (38) as

---

1. The effective parameters, P_{eff} and K_{eff}, are defined in a manner that is consistent with previously published data (18). It should be noted that, according to equations (34 and 37), $K_{eff} = K_{ex} - K_{bm,ex}$.

$$\frac{dC_c}{dt} = \frac{A_c P_{eff}}{V_c(1 + a' K_{bm})} (b' - c' C_c) \qquad \text{(Eq. 39)}$$

The integration of equation (39) gives the following linear uptake function ($U.F._2'$) for Model 2

$$U.F._2' = \frac{V_c (1 + a' K_{bm})}{60 c' A_c} \ln \left[\frac{b' - c' C_{c(o)}}{b' - c' C_c} \right] = P_{eff} t \qquad \text{(Eq. 40)}$$

in which all parameters have previously been defined.

The uptake function ($U.F._2'$) described by equation (40) is mathematically equivalent to the uptake function of ($U.F._2$) defined by equation (23). The difference lies in that the slope of a plot of $U.F._2'$ versus time, according to equation (36), is a function of the serum concentration in the external medium and is equal to the effective or experimental permeability coefficient, P_{eff}, whereas, in equation (23), the slope is equal to the intrinsic permeability coefficient, P, which is independent of the serum concentration since the effect of serum-drug binding has been factored out.

Model 3

In this model the rate-limiting step of the drug uptake process is attributed to the slow diffusion of the drug into or through the plasma membrane followed by rapid binding of the drug molecules to Langmuir sites that are located within the plasma membrane and/or in the cell interior. Any association of the drug with serum components in the suspension medium and the effect of the aqueous diffusion layer on the drug uptake is considered to be insignificant. A schematic representation of this model is given in Figure 3.

The rate of total drug uptake by cells for this model can be expressed as

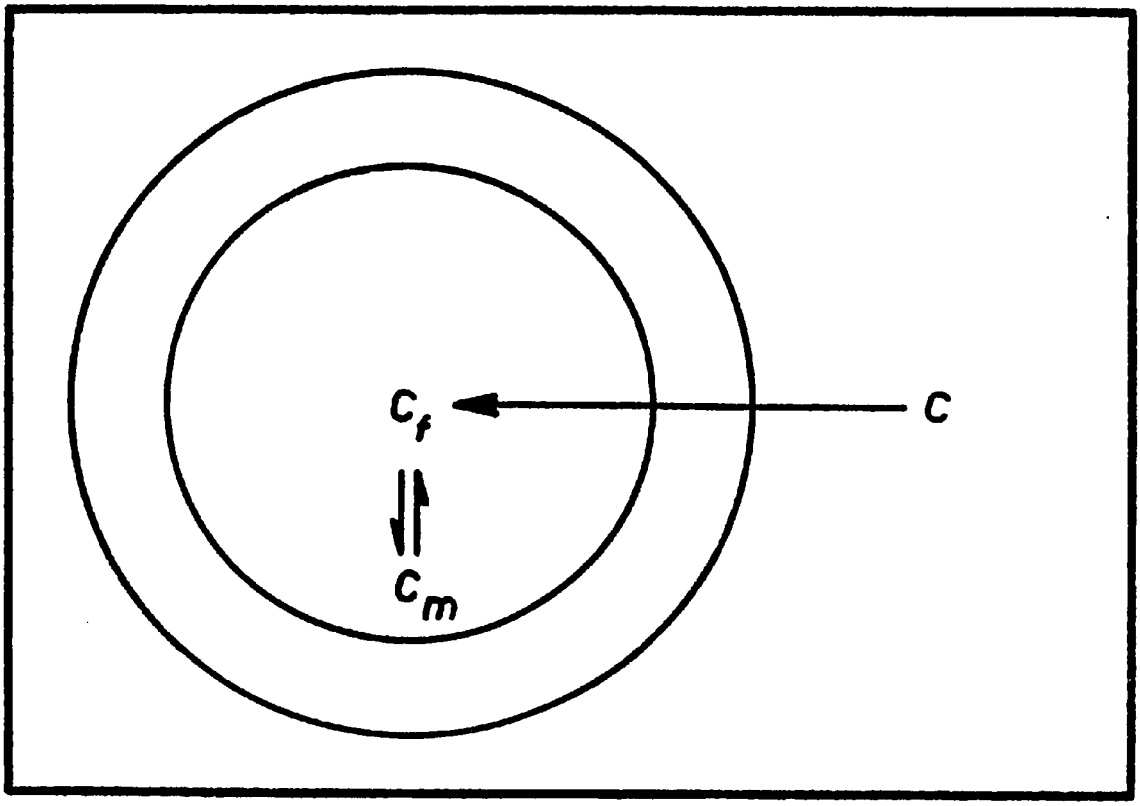


Figure 3. Schematic description of Model 3. Simple diffusion into the cell membrane and/or cell interior followed by rapid adsorption to Langmuir sites. The C is the drug concentration in the medium. The C_f and C_m represent the unbound cellular drug concentration and the cellular drug concentration bound to Langmuir sites, respectively.

$$\frac{dC_c}{dt} = N A_c P (C - C_f) \qquad \text{(Eq. 41)}$$

where C_f is the concentration of the free drug in the cells and N is the number of cells in a one ml. plug of erythrocytes.[1]

The total drug concentration associated with cells, C_c, is given by

$$C_c = C_m + C_f \qquad \text{(Eq. 42)}$$

where C_m represents the cellular concentration of drug that is adsorbed to Langmuir sites.

The cellular concentrations, C_m and C_f, are related by the Langmuir equation, i.e.,

$$C_m = \frac{Q N k C_f}{1 + k C_f} \qquad \text{(Eq. 43)}$$

where Q represents the maximum amount of drug that is taken up by each cell and k is the ratio of the adsorption to the desorption rate constant. Mass balance for the drug requires that

$$T = V C + H C_m + H C_f \qquad \text{(Eq. 44)}$$

Combining equations (42 and 44) and rearrangement gives an expression for the drug concentration in the medium as

$$C = \frac{T}{V} - \frac{H}{V} C_c \qquad \text{(Eq. 45)}$$

Substituting equation (43) into equation (42) yields a quadratic equation the solution of which is

$$C_f = \frac{- (1 + Q N k - k C_c) \pm [(Q N k + 1 - k C_c)^2 + 4 k C_c]^{\frac{1}{2}}}{2 k} \qquad \text{(Eq. 46)}$$

---

1. Based on a mean cell volume of 87×10^{-12} cm.^{3} for human erythrocytes, N = 1.15×10^{10} RBC/ml. of RBC.

The differential equation for Model 3 can now be obtained by substituting equations (45 and 46) into equation (41)

$$\frac{dC_c}{dt} = N A_c P \left[\frac{T}{V} - \frac{H}{V} C_c - \frac{kC_c - QNk - 1 \pm [(1+ QNk - kC_c)^2 + 4kC_c]^{\frac{1}{2}}}{2k} \right] \qquad \text{(Eq. 47)}$$

Then, by letting

$$a = \frac{N A_c P}{2k}$$

$$b = 1 + Q N k + \frac{2 k T}{V}$$

$$c = - \left(\frac{2 k H}{V} + k \right)$$

$$d = 1 + 2 Q N k + Q^2 N^2 k^2$$

$$e = 2 k - 2 Q N k^2$$

and

$$f = k^2$$

equation (47) can more conveniently be written in the form

$$\frac{dC_c}{dt} = a [b + c C_c \pm (d + e C_c + f C_c^2)^{\frac{1}{2}}] \qquad \text{(Eq. 48)}$$

Since there appears to be no simple analytical solution to equation (48), the differential equation is best analyzed using the numerical Runge - Kutta method (54).

For initial rates, equation (47) simplifies to

$$\frac{dC_c}{dt} = \frac{N A_c T}{V} P \qquad \text{(Eq. 49)}$$

Thus, the permeability coefficient, P, can be estimated from the initial slope of the C_c <u>versus</u> time in sec. plot.

The maximum amount of drug that can bind to each cell can be found from equilibrium data of uptake experiments. When steady-state

conditions prevail, i.e. when $(dC_c/dt)_{t=\infty} = 0$, then $C_{(\infty)} = C_{f(\infty)}$ and equation (42) can be written as

$$C_m = C_c - C \qquad (t=\infty) \qquad \text{(Eq. 50)}$$

Equation (43), upon rearrangement and with the use of equation (50) can now be written in the linear form

$$\frac{C}{C_c - C} = \frac{1}{Q\,N}\,C + \frac{1}{k\,Q\,N} \qquad (t=\infty) \qquad \text{(Eq. 51)}$$

A plot of $(C/C_c - C)$ <u>versus</u> C should give a straight line the slope of which allows for the evaluation of the maximum amount of drug that can bind to each cell, Q. The overall rate constant for the drug binding process can also be estimated from the above mentioned plot. The ratio of the slope to the intercept is identical to the Langmuir rate constant.

With the assumption that $C_m >> C_f$, the derivation of this model can be modified in this manner:

Considering the above assumption in equations (42 and 44) and with the use of equation (43), the differential equation (41) for this model can be written as

$$\frac{dC_m}{dt} = 60\,N\,A_c\,P\left(\frac{T}{V} - \frac{H}{V}\,C_m - \frac{C_m}{Q\,N\,k - k\,C_m}\right) \qquad \text{(Eq. 52)}$$

where the factor 60 is required to estimate the permeability coefficient, P, in units of cm./sec. from the C_m <u>versus</u> time in min. plot.

Then, by letting

$$a' = \frac{60\,N^2\,A_c\,Q\,T\,k\,P}{V}$$

$$b' = -\,60NA_cP\left(\frac{H\,Q\,N\,k}{V} + \frac{T\,k}{V} + 1\right)$$

$$c' = \frac{60\,N\,A_c\,P\,H\,k}{V}$$

$$d' = Q\ N\ k$$

and

$$e' = k$$

equation (52) can be expressed in the form

$$\frac{dC_m}{dt} = \frac{a' + b'\ C_m + c'\ C_m^{\,2}}{d' - e'\ C_m} \qquad \text{(Eq. 53)}$$

Integrating equation (53) renders the following new solution for this model

$$\left[\frac{d'}{(-q)^{\frac{1}{2}}} + \frac{b'\ e'}{2c'(-q)^{\frac{1}{2}}}\right] \ln\left[\frac{\dfrac{2c'C_m + b' - (-q)^{\frac{1}{2}}}{2c'C_m + b' + (-q)^{\frac{1}{2}}}}{\dfrac{2c'C_{m(o)} + b' - (-q)^{\frac{1}{2}}}{2c'C_{m(o)} + b' + (-q)^{\frac{1}{2}}}}\right] - \frac{e'}{2c'} \ln\left[\frac{a' + b'C_m + c'C_m^{\,2}}{a' + b'C_{m(o)} + c'C_{m(o)}^{\,2}}\right] = t \qquad \text{(Eq. 54)}$$

where $q = 4\ a'c' - b'^2$ and $C_{m(o)}$ is the cellular drug concentration at zero time.

For initial rates, equation (52) reduces to

$$\frac{dC_m}{dt} = \frac{60\ N\ A_c\ T\ P}{V} \qquad \text{(Eq. 55)}$$

and the permeability coefficient, P, in units of cm./sec. can be estimated from the initial slope of the C_m *versus* time in min. plot.

According to equation (41), steady - state conditions for the cellular drug uptake prevail when $C = C_f$. At equilibrium then, equation (43) can be written in the linear form as

$$\frac{C}{C_m} = \frac{1}{Q\ N}\ C + \frac{1}{Q\ N\ k} \qquad (t = \infty) \qquad \text{(Eq. 56)}$$

The maximum amount of drug that can bind to each cell, Q, for this modified Model 3 can be estimated from the slope of the plot C/C_m *versus* C and the overall Langmuir rate constant, k, can be calculated from the

slope and the intercept of the same plot.

Model 4

This model assumes that the drug uptake by cells is the direct result of adsorption of the drug to the plasma membrane. The rate - limiting step of the drug uptake process is attributed to the slow, reversible binding of the drug molecules to Langmuir binding sites located in the plasma membrane. The actual rate of binding is expressed in terms of the kinetic parameters of the Langmuir equation itself. The binding of the drug to serum components and the effect of the aqueous difusion layer on the drug uptake process are taken to be negligible. This model is shown in Figure 4.

The rate of drug adsorption, R_f, is given by

$$R_f = N A_c k_f C (1 - \theta) \qquad \text{(Eq. 57)}$$

where k_f is the Langmuir adsorption rate constant and θ is the fraction of the membrane sites per cell that is occupied by the drug molecules.

The rate of drug desorption, R_r, can be written as

$$R_r = N A_c k_r \theta \qquad \text{(Eq. 58)}$$

The overall rate of drug uptake can now be expressed by

$$\frac{dC_m}{dt} = 60 N A_c [k_f C (1 - \theta) - k_r \theta] \qquad \text{(Eq. 59)}$$

where the factor 60 is required to determine the rate constants k_f and k_r in units of cm./sec. and moles/cm.^{2} sec., respectively, from the C_m *versus* time in min. plots.

The cell concentration is given by

$$C_m = Q N \theta \qquad \text{(Eq. 60)}$$

The mass balance relationship for this system is

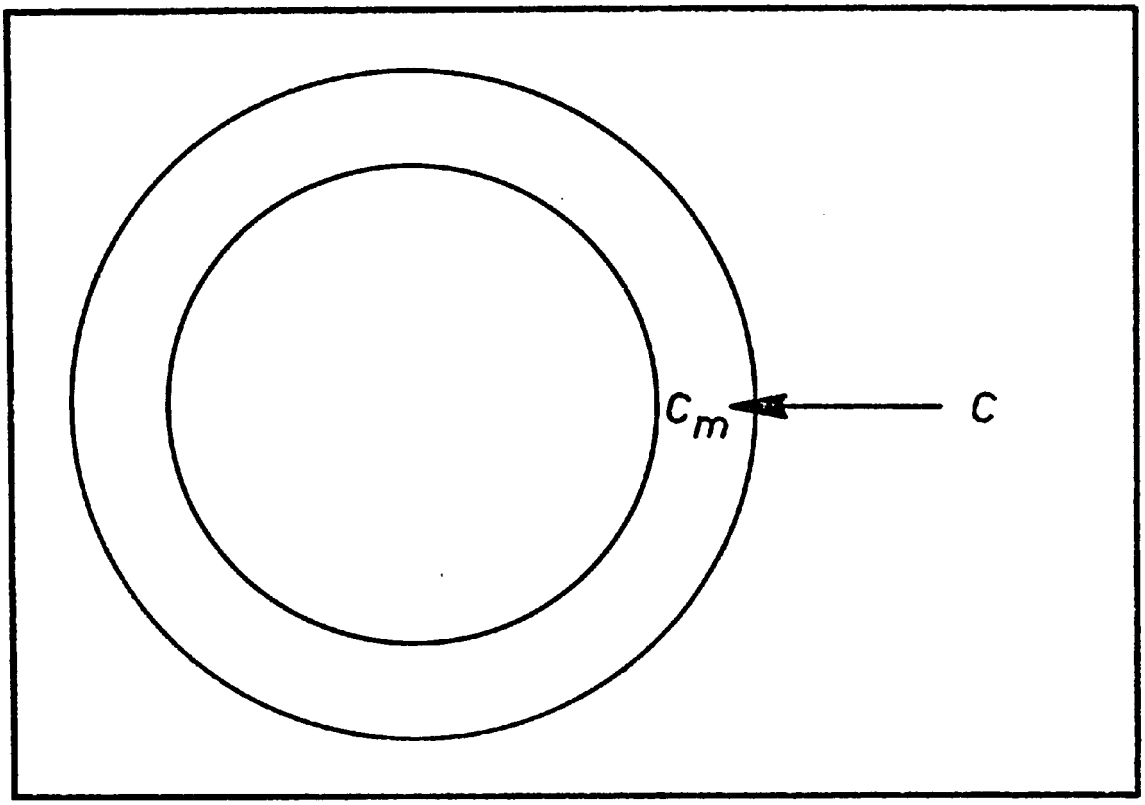


Figure 4. Schematic description of Model 4. Cellular drug uptake resulting from adsorption of drug to membrane associated Langmuir sites. The C is the drug concentration of the medium and C_m represents the cellular drug concentration bound to Langmuir sites.

$$T = V\ C + H\ C_m \qquad \text{(Eq. 61)}$$

Solving equations (60 and 61) for Θ and C, respectively, and substituting into equation (59) yields the differential equation for Model 4

$$\frac{dC_m}{dt} = 60\ N\ A_c \left[\frac{k_f T}{V} - \left(\frac{k_f H}{V} + \frac{k_f T}{VQN} + \frac{k_r}{QN} \right) C_m + \frac{k_f H}{VQN} C_m^2 \right] \qquad \text{(Eq. 62)}$$

Then, by letting

$$a = \frac{60\ N\ A_c\ k_f\ T}{V}$$

$$b = -\ 60\ N\ A_c \left(\frac{k_f H}{V} + \frac{k_f T}{VQN} + \frac{k_r}{QN} \right)$$

and

$$c = \frac{60\ k_f\ H\ A_c}{V\ Q}$$

it is convenient to write equation (62) in the form

$$\frac{dC_m}{dt} = a + b\ C_m + c\ C_m^2 \qquad \text{(Eq. 63)}$$

Integrating equation (63) renders the following solution for this model

$$C_m = \frac{(-q)^{\frac{1}{2}} - b + \left[b + (-q)^{\frac{1}{2}} \right] \left[\frac{2\ c\ C_{m(o)} + b - (-q)^{\frac{1}{2}}}{2\ c\ C_{m(o)} + b + (-q)^{\frac{1}{2}}} \right] \exp\ (-q)^{\frac{1}{2}}\ t}{2\ c \left[1 - \frac{2\ c\ C_{m(o)} + b - (-q)^{\frac{1}{2}}}{2\ c\ C_{m(o)} + b + (-q)^{\frac{1}{2}}}\ \exp\ (-q)^{\frac{1}{2}}\ t \right]}$$

(Eq. 64)

where $q = 4\ a\ c - b^2$ and $C_{m(o)}$ is the cellular drug concentration at zero time.

Equation (64) can be used to evaluate the magnitudes of the adsorption and desorption rate constants, k_f and k_r, from drug uptake and drug release data by obtaining the best fit of the theory with the kinetic data. For the theoretical analysis of drug uptake data with

equation (64), the value of $C_{m(o)}$ is set equal to zero.

For initial rates of drug uptake, equation (59) reduces to

$$\frac{dC_m}{dt} = \frac{60\ N\ A_c\ k_f\ T}{V} \qquad \text{(Eq. 65)}$$

Thus, the adsorption rate constant, k_f, can be estimated from the initial slope of the C_m *versus* time in min. plots. It should be noted that the adsorption rate constant is identical to the intrinsic permeability coefficient in Models (1, 2 and 3).

For initial rates of drug release from cells with completely saturated binding sites, equation (59) simplifies to

$$\frac{dC_m}{dt} = 60\ N\ A_c\ k_r \qquad \text{(Eq. 66)}$$

Therefore, the desorption rate constant, k_r, can be evaluated with release data from the initial slope of the C_m *versus* time in min. plots.

The Langmuir isotherm equation for this model is

$$C_m = \frac{k_f\ Q\ N\ C}{k_r + k_f\ C} \qquad \text{(Eq. 67)}$$

Equation (67) in its linear form has been described in Model 3 with equation (56).

The maximum amount of drug that can be taken up by each cell, Q, can either be calculated from the slope of the $(C/C_m)_{t=\infty}$ *versus* $C_{(\infty)}$ plot with equation (56) or it can directly be estimated from the saturation value of the Langmuir isotherm, i.e. the plateau of the $C_{m(\infty)}$ *versus* $C_{(\infty)}$ plot.

The magnitude of the dissociation constant for the drug - erythrocyte complex, K_I, can be computed from the Langmuir rate constants. The ratio of k_r to k_f is equal to the dissociation constant of the drug -

erythrocyte complex.

Model 5

This model analyzes the situation where the free drug in the suspension medium is assumed to bind instantaneously, linearly and reversibly to "hard" binding sites located on the cell membrane and to serum components in the suspension medium. The slow drug uptake by the cells that follows the initial surface binding is attributed to the direct, reversible binding of the unbound drug molecules in the suspension medium to "soft" Langmuir binding sites on the plasma membrane. The actual rate of drug binding to the "soft" Langmuir sites is, analogously to Model 4, ascribed to the kinetic parameters of the Langmuir equation. The effect of the aqueous diffusion layer on the drug uptake process is assumed to be negligible. This model is schematically shown in Figure 5.

The mathematical treatment of this model requires modification of equation (59) in order to account for the additional instantaneous, linear and reversible binding of the drug to the plasma membrane and the effect of the drug - serum binding.

The total drug concentration associated with the cells in this model can be expressed by

$$C_c = C_m + C_s \qquad \text{(Eq. 68)}$$

Then, by applying the same deductive reasoning as in Model 2 (equations 12 through 19) but with the use of equation (68) rather than equation (13), the term dC_m/dt in equation (59) can be expressed as

$$\frac{dC_m}{dt} = \left(1 + \frac{H K_{bm}}{V (1 + K_b S)} \right) \frac{dC_c}{dt} \qquad \text{(Eq. 69)}$$

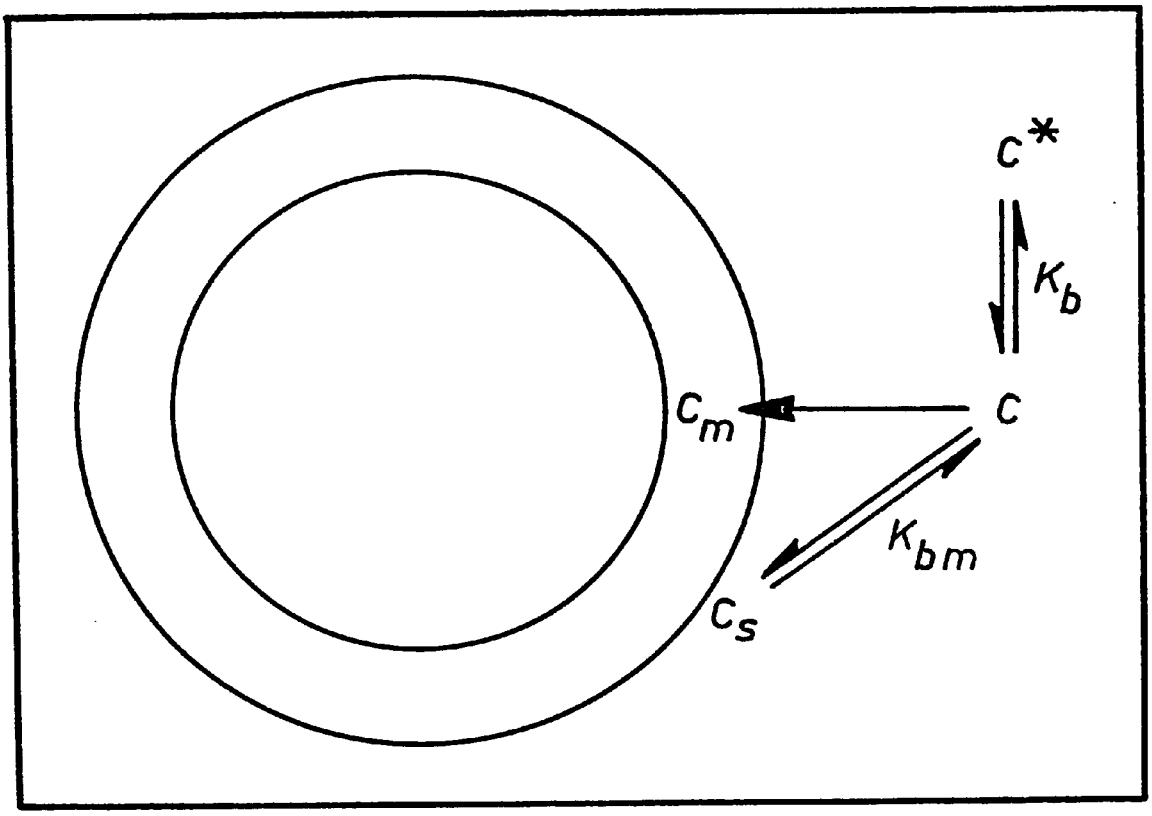


Figure 5. Schematic description of Model 5. The unbound drug in the medium is in rapid equilibrium with the serum - bound and plasma membrane - bound drug. The slow drug uptake by cells is the result of adsorption of free drug molecules in the medium to Langmuir sites associated with the membrane. The C and C* are the concentrations of the free and serum - bound drug in the medium. The C_s and C_m represent the membrane - bound and Langmuir site - bound cellular drug concentrations, respectively. The K_b and K_{bm} are equilibrium binding constants.

In order to account for the drug - serum binding and the total cell concentration, C_c, the term $[k_f C (1 - \Theta) - k_r \Theta]$ in equation (59) can be modified in the following manner.

An expression for the free drug concentration in the medium is obtained by combining equations (14, 15 and 29)

$$C = \frac{C_T}{1 + K_b S} \qquad \text{(Eq. 70)}$$

Mass balance for the distribution of the drug in this system is given by equation (12).

Substituting equations (14, 60 and 70) into equation (68) yields an expression for the total cell concentration as

$$C_c = Q N \Theta + \frac{K_{bm} C_T}{1 + K_b S} \qquad \text{(Eq. 71)}$$

Then, with equations (12, 70 and 71)

$$[k_f C(1 - \Theta) - k_r \Theta] = \left[\frac{k_f T}{V(1+ K_b S)} + \frac{k_f K_{bm} T^2}{V^2 QN(1+ K_b S)^2} + \frac{k_r K_{bm} T}{VQN(1+ K_b S)} \right]$$

$$- \left[\frac{k_f H}{V(1+ K_b S)} + \frac{k_f T}{VQN(1+ K_b S)} + \frac{2k_f K_{bm} HT}{V^2 QN(1+ K_b S)^2} + \frac{k_r}{QN} \right.$$

$$\left. + \frac{k_r K_{bm} H}{QNV(1+ K_b S)} \right] C_c + \left[\frac{k_f H}{QNV(1+ K_b S)} + \frac{k_f K_{bm} H^2}{QNV^2(1+ K_b S)^2} \right] C_c^2$$

Substituting equations (69 and 72) into equation (59) renders the differential equation for Model 5

$$\left[1+\frac{HK_{bm}}{V(1+K_bS)}\right]\frac{dC_c}{dt} = 60\,NA_c\left[\left[\frac{k_fT}{V(1+K_bS)}+\frac{k_fK_{bm}T^2}{V^2QN(1+K_bS)^2}+\frac{k_rK_{bm}T}{VQN(1+K_bS)}\right]\right.$$

$$-\left[\frac{k_fH}{V(1+K_bS)}+\frac{k_fT}{VQN(1+K_bS)}+\frac{2k_fK_{bm}HT}{V^2QN(1+K_bS)^2}+\frac{k_r}{QN}\right.$$

$$\left.\left.+\frac{k_rK_{bm}H}{VQN(1+K_bS)}\right]C_c+\left[\frac{k_fH}{VQN(1+K_bS)}+\frac{k_fK_{bm}H^2}{V^2QN(1+K_bS)^2}\right]C_c^2\right]$$

(Eq. 73)

Then, by letting

$$a = \frac{60\,N\,A_c\,V}{V(1+K_bS)+H\,K_{bm}}\left[\frac{k_fT}{V}+\frac{k_fK_{bm}T^2}{V^2QN(1+K_bS)}+\frac{k_rK_{bm}T}{VQN}\right]$$

$$b = \frac{-60\,N\,A_c\,V}{V(1+K_bS)+H\,K_{bm}}\left[\frac{k_fH}{V}+\frac{k_fT}{VQN}+\frac{2k_fK_{bm}TH}{V^2QN(1+K_bS)}+\frac{k_r(1+K_bS)}{QN}+\frac{k_rK_{bm}H}{VQN}\right]$$

and

$$c = \frac{60\,N\,A_c\,V}{V(1+K_bS)+H\,K_{bm}}\left[\frac{k_fH}{VQN}+\frac{k_fK_{bm}H^2}{V^2QN(1+K_bS)}\right]$$

equation (73) can conveniently be written as

$$\frac{dC_c}{dt} = a + b\,C_c + c\,C_c^2 \qquad \text{(Eq. 74)}$$

Integrating equation (74) yields the solution for Model 5

$$C_c = \frac{(-q)^{\frac{1}{2}} - b + \left[b + (-q)^{\frac{1}{2}}\right]\left[\frac{2\,c\,C_{c(o)}+b-(-q)^{\frac{1}{2}}}{2\,c\,C_{c(o)}+b+(-q)^{\frac{1}{2}}}\right]\exp\,(-q)^{\frac{1}{2}}\,t}{2\,c\left[1-\frac{2\,c\,C_{c(o)}+b-(-q)^{\frac{1}{2}}}{2\,c\,C_{c(o)}+b+(-q)^{\frac{1}{2}}}\exp\,(-q)^{\frac{1}{2}}\,t\right]}$$

(Eq. 75)

where $q = 4\,a\,c - b^2$.

Equation (75) is used to evaluate the magnitudes of the adsorption and desorption rate constants, k_f and k_r, from drug uptake and release studies by obtaining the best fit of the model with the kinetic data.

In order to properly calculate the value of the maximum amount of drug that can be taken up by each cell, Q, for this model with equation (56) it is necessary that the equilibrium cell concentration due to the binding of the drug to Langmuir sites, C_m, be separated from the total concentration associated with cells, C_c. Furthermore, equation (56) requires that the equilibrium concentration of the external medium is expressed in terms of the free drug concentration.

Combining equations (14, 68 and 70) renders the relationship which allows for the computation of the cellular drug concentration, C_m, from the total cell concentration, C_c, as

$$C_m = C_c - \frac{K_{bm}\, C_T}{1 + K_b S} \qquad \text{(Eq. 76)}$$

whereas the free drug concentration in the external medium can be calculated with equation (70).

Therefore, by the use of equations (70 and 76), the value of the maximum amount of drug that can bind to plasma membranes associated Langmuir sites per cell can, according to equation (56), be estimated from a plot of C_m versus C or its magnitude can directly be assessed from the plateau of the Langmuir isotherm.

The drug - serum and drug - plasma membrane equilibrium binding constants, K_b and K_{bm}, can be evaluated from initial drug uptake data with equation (35) described in Model 2.

Model 6

This last model considers the situation in which free drug molecules in the suspension medium are assumed to instantaneously permeate the plasma membrane followed by the establishment of rapid equilibrium between the intracellular and extracellular drug concentration. Furthermore, the free drug in the suspension medium is assumed to linearly and reversibly bind to serum components present in the extracellular phase. The slow cellular drug uptake that follows the rapid equilibration of the drug in the cell interior is attributed to the direct and reversible binding of free extracellular drug molecules to Langmuir sites present in the plasma membrane. The kinetic parameters of the Langmuir equation, comparably to Models 4 and 5, are assumed to govern the rate of the slow drug uptake. This model is diagrammed in Figure 6.

Except for some differences in terminology, the derivation of this model is mathematically identical to that of Model 5. In the present model, the total cell associated drug concentration, C_c, is given by

$$C_c = C_m + C_i \qquad \text{(Eq. 77)}$$

where C_i has the same meaning as in Models 1 and 2 with the only exception being that in the present model this cellular drug concentration is the result of rapid diffusion and equilibration of the drug in the cell interior.

This rapidly equilibrating cell concentration, C_i, is assumed to be directly proportional to the free drug concentration in the external medium, i.e.

$$C_i = K\,C \qquad \text{(Eq. 8)}$$

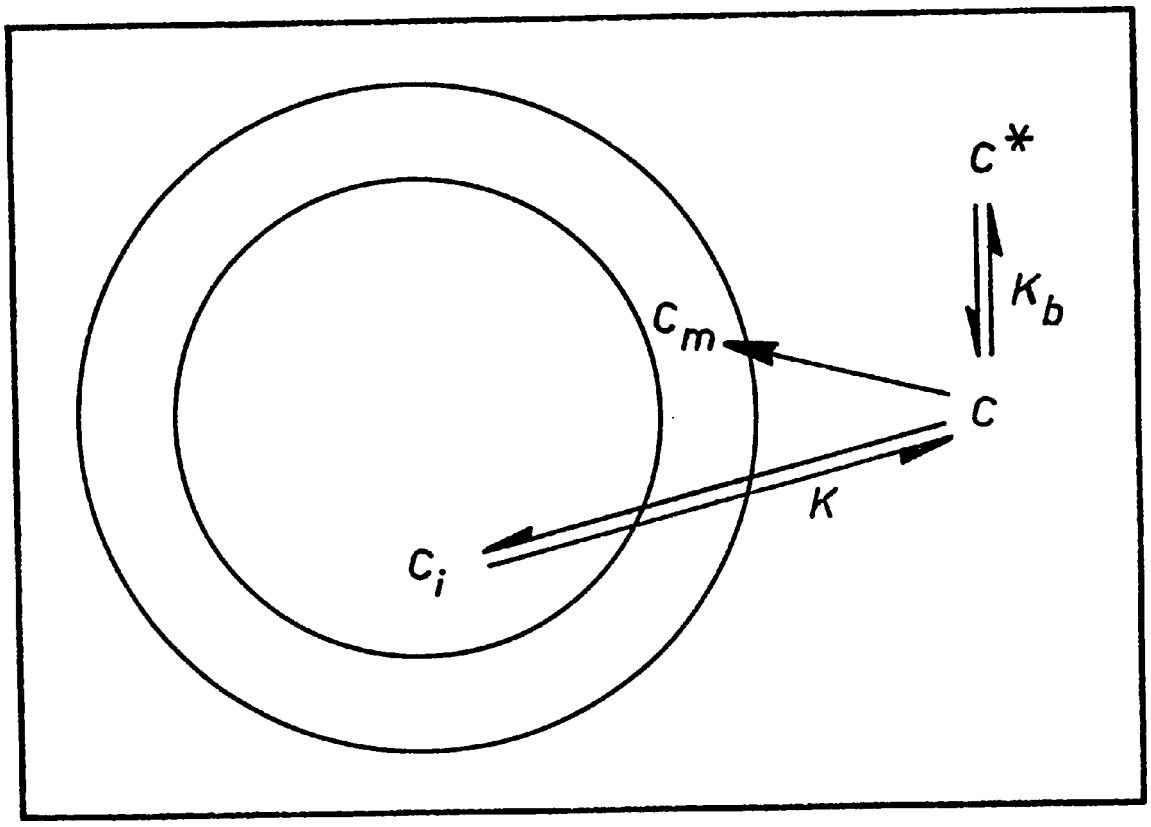


Figure 6. Schematic description of Model 6. The free drug in the medium rapidly permeates the plasma membrane to establish equilibrium between the cell interior drug concentration and the free drug concentration. The free drug also binds to serum in the medium. The slow cellular drug uptake is attributed to adsorption of free drug molecules to cell membrane associated Langmuir sites. The C and C* represent the free and serum - bound drug concentrations of the medium, whereas C_i is the concentration of drug in the cell interior and C_m is the cellular drug concentration bound to Langmuir sites. The K and K_b are the intrinsic partition coefficient and the serum binding equilibrium constant, respectively.

which, in fact, is the definition for the intrinsic partition coefficient in Model 1.

Since equation (8) is mathematically equivalent to equation (14), the derivation of this model precisely follows that of Model 5 except that the surface concentration, C_s, and the plasma membrane binding constant, K_{bm}, must be replaced in all expressions of Model 5 by the cellular drug concentration, C_i, and the partition coefficient, K, respectively.

The solution to Model 6 is then given by equation (75) with the algebraic expressions for the present model being

$$a = \frac{60\ N\ A_c\ V}{V(1+K_bS)+HK}\left[\frac{k_fT}{V}+\frac{k_fKT^2}{V^2QN(1+K_bS)}+\frac{k_rKT}{VQN}\right]$$

$$b = \frac{-\ 60\ N\ A_c\ V}{V(1+K_bS)+HK}\left[\frac{k_fH}{V}+\frac{k_fT}{VQN}+\frac{2k_fKHT}{V^2QN(1+K_bS)}+\frac{k_r(1+K_bS)}{QN}+\frac{k_rKH}{VQN}\right]$$

and

$$c = \frac{60\ N\ A_c\ V}{V(1+K_bS)+HK}\left[\frac{k_fH}{VQN}+\frac{k_fKH^2}{V^2QN(1+K_bS)}\right]$$

The intrinsic partition coefficient, K, can be evaluated from initial drug uptake data with equation (8) provided there is no serum present in the suspension medium.

Furthermore, combining equations (8, 15 and 29) yields the following linear relationship

$$\frac{C_T}{C_i} = \frac{K_b}{K}(S) + \frac{1}{K} \qquad (t = 0) \qquad \text{(Eq. 78)}$$

which, experimentally analogous to equation (35), allows for the

evaluation of the intrinsic partition coefficient, K, and the serum binding constant, K_b, from "zero time" drug uptake data in the presence of different fetal bovine serum levels.

Substituting equations (8 and 67) into equation (72) renders the following expression for the total cell - associated drug concentration as a function of the unbound drug concentration in the suspension medium

$$C_c = \frac{k_f Q N C}{k_r + k_f C} + K C \qquad \text{(Eq. 79)}$$

Finally, it should be noted that although Models 5 and 6 are mathematically indistinguishable, their respective transport mechanisms differ. Any differentiation between these two models requires that suitable experiments, supplementary to transport studies, be carried out which can establish whether the linear drug uptake component by cells is the result of instantaneous, linear and reversible adsorption of drug molecules to the plasma membrane, as proposed in Model 5, or whether this linear component can be attributed to rapid diffusion of the drug into the cell interior, as postulated in Model 6.

Until it was experimentally resolved whether or not the instantaneous cellular drug uptake was the result of plasma membrane binding or rapid diffusion of the drug into the cell interior, the equilibrium binding constants K_{bm} and K were used interchangeably and the process was generally referred to as the instantaneous drug - erythrocyte interaction.

EXPERIMENTAL PROCEDURES AND TECHNIQUES

Cell Suspension Medium

A phosphate buffered saline solution prepared from 0.150 M NaCl and 0.01 M phosphate[1] at pH 7.4 was used as the basic component of the medium (16). The osmotic pressure of this solution was 300 milliosmoles/kg. Various amounts of fetal bovine serum[2] (FBS), ranging from 0 to 50% on a volume basis, were added to the above buffer to complete the suspension medium. No change in the pH was observed upon the addition of fetal bovine serum to the phosphate buffered saline. However, a slight decrease in the osmotic pressure (to 297 milliosmoles/kg.) was noted at 50% fetal bovine serum concentration. Neomycin sulfate[3] (0.5mg./ml.) was added to the medium in most experiments in order to reduce the possibility of bacterial contamination of the cell suspension system.

Preparation of Red Cells

Whole citrated blood was obtained, generally 8 to 20 hours after being drawn, from the Department of Hematology, University of Michigan Hospital, and immediately prepared for experimental use. The donors' hematological case history was not known.

Blood samples, most often pooled from various donors, were centrifuged at 800 x g for 10 minutes. After centrifugation, the plasma and buffy coat, consisting mainly of leucocytes and platelets, were discarded. The remaining packed erythrocytes were resuspended and washed three times in approximately eight volumes of phosphate buffered saline. A final washing was carried out with the medium in which the cells were

---

1. 1.14×10^{-3}M $NaH_2PO_4 \cdot H_2O$ and 8.86×10^{-3}M Na_2HPO_4.
2. KAM Laboratories, St. Joseph, Mo. 64506. Lot No. 4061.
3. SIGMA Chemical Corp., St. Louis, Mo. 63178. USP-grade.

to be subsequently used. All experiments were started immediately after the final wash.

Drug Uptake Experiments

Transport studies of ouabain - ^{3}H [1] and digitoxin - ^{3}H [2] into erythrocytes were conducted using media containing 0, 5 and 15 per cent fetal bovine serum levels. The chemical structure of ouabain and digitoxin is shown in Figure 7a and 7b, respectively. The temperature in all experiments was 30 ^{o}C. Red blood cells from ten donors were pooled for each uptake experiment. A schematic description of the sequence of procedures used for the drug uptake studies is given in Figure 8.

Differing aliquots of the labelled drugs in their respective solvents were transferred into a 125 ml. Erlenmeyer flask. After evaporation of the solvent, 50 ml. of medium was pipetted into the flask which was agitated in a horizontal motion by means of a Burrell shaker. At zero time, 3 to 4 ml. of a concentrated red cell suspension were introduced into the flask. The hematocrit of the resulting cell suspensions ranged between 5 and 7 per cent. Next, 2 ml. samples of the cell suspension were withdrawn from the reaction flask at various times and placed into a centrifuge tube. The centrifuge tube, the narrow stem of which was calibrated to contain 0.1 ml., is shown in Figure 9. The samples were immediately centrifuged at 5,000 x g for 10 minutes. The compacted cellular sediment was always in excess of the 0.1 ml. calibration mark. A 0.1 ml. sample of the supernatant was withdrawn with an automatic pipet[3] and transferred into a scintillation vial for later assay. The pipet tip was first rinsed with 0.5 ml. of water and then

---

1. New England Nuclear, Boston, Mass. 02118. NET - 211, Lot No. 772-055.
2. New England Nuclear, Boston, Mass. 02118. NET - 216, Lot No. 747-007.
3. Sargent-Welch Sci. Co., Skokie, Ill. 60076. Eppendorf Microliter Pipet.

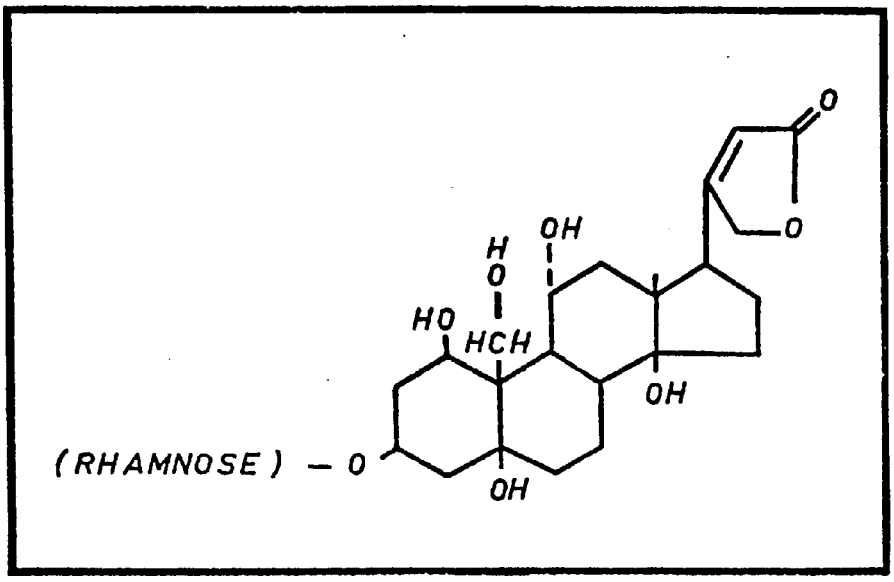


Figure 7a. Chemical structure of ouabain. The ouabain used in this study had a general tritium label and a specific activity of 10.2 Ci/mM. The molecular weight of ouabain is 584.7.

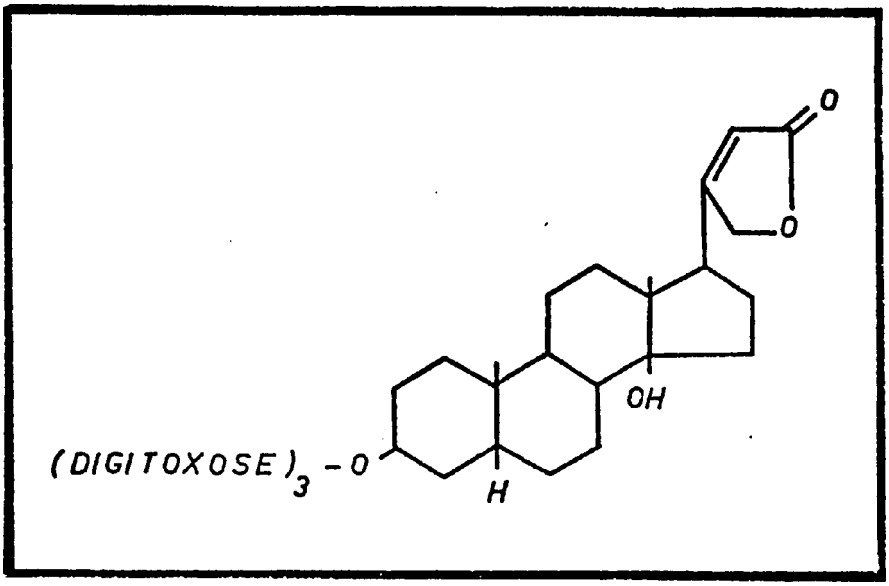


Figure 7b. Chemical structure of digitoxin. The digitoxin used in this study had a general tritium label and a specific activity of 15.7 Ci/mM. The molecular weight of digitoxin is 764.9.

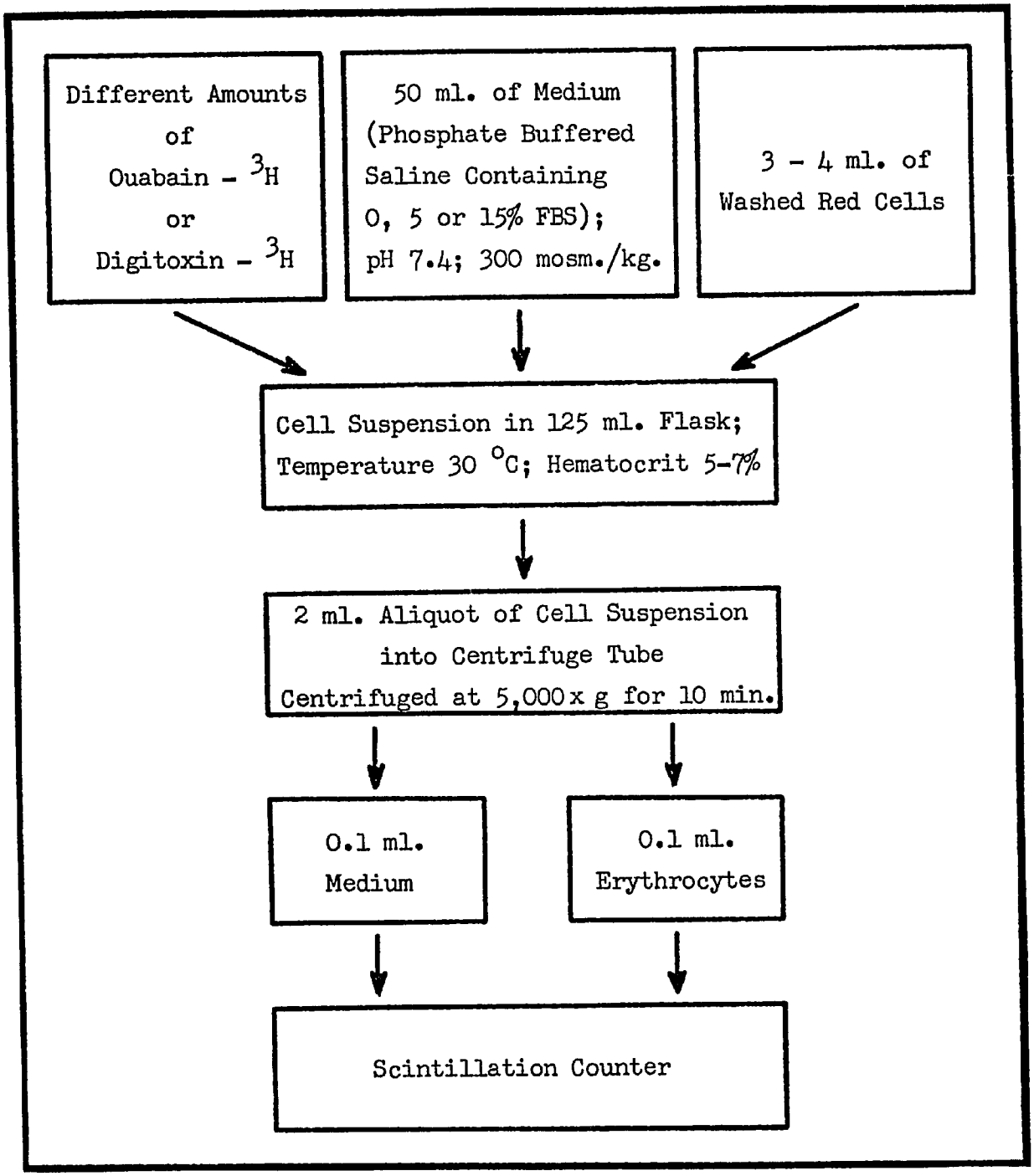


Figure 8. Outline of the sequence of procedures for drug uptake experiments.

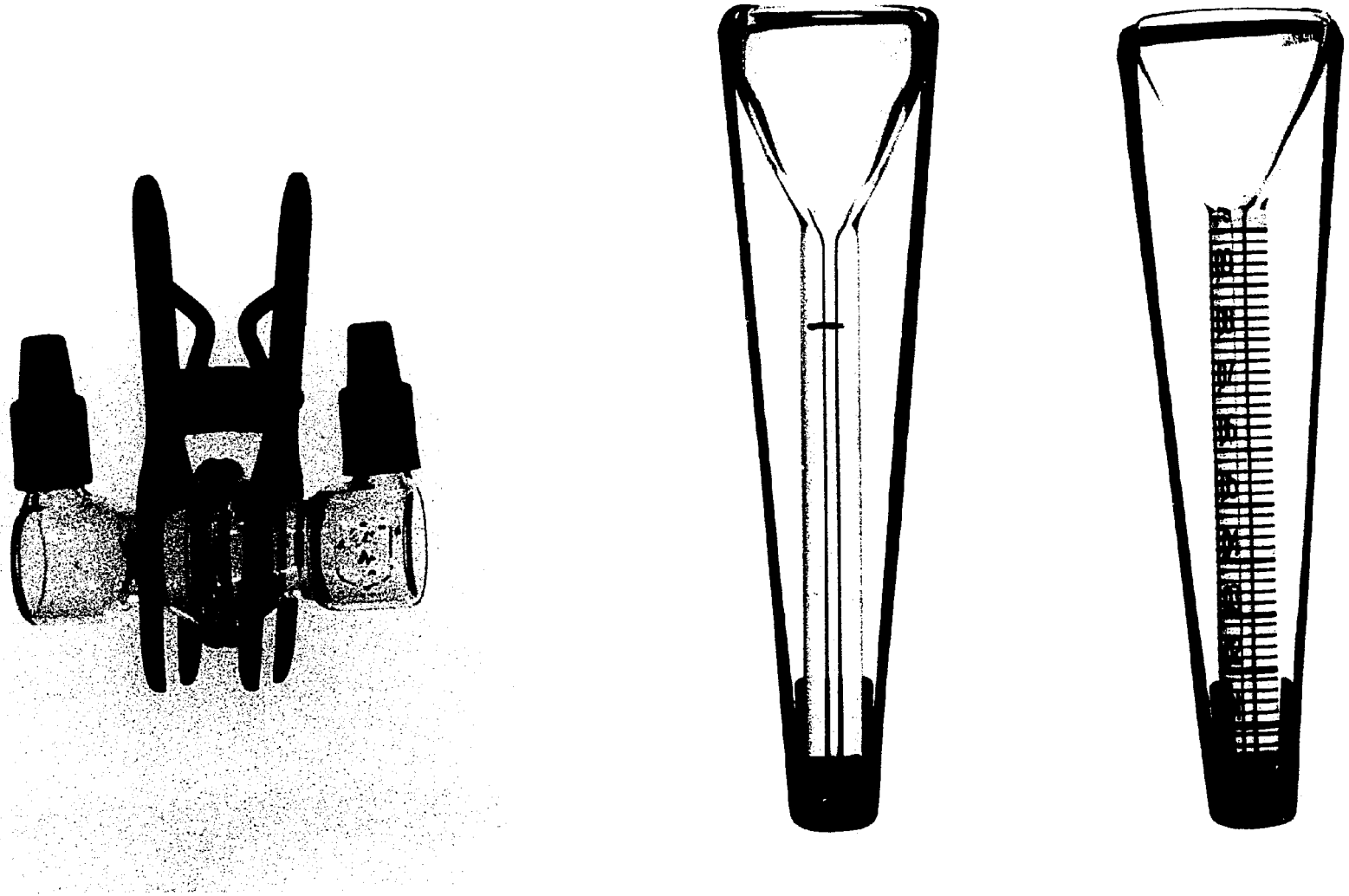


Figure 9. Photograph of the hematocrit tube on the right, centrifuge tube in the middle and dialysis chamber on the left. Actual dimensions 1.2 times magnified.

flushed with 10 ml. of Aquasol[1] (a combination tissue solubilizer and scintillation cocktail) to improve the experimental precision and accuracy. (Digitoxin was found to reversibly bind to the plastic pipet tips.) The remaining medium and red cell sediment in excess of the 0.1 ml. calibration mark were aspirated off and discarded. The bulb and stem above the calibration mark were then washed three times with buffered saline to remove any drug adhering to the glass walls. The remaining 0.1 ml. red cell plug was flushed out into a scintillation vial with 1 ml. of water and stored in the freezer for future assay. Thus, the depletion of drug from the medium as well as the total cellular drug uptake were followed simultaneously.

Four 0.1 ml. samples of the cell suspension were withdrawn from the reaction flask and transferred into scintillation vials at various times to permit the computation of drug mass balance for the entire duration of the experiment. In this case, the pipet tips were flushed with 1 ml. of water both to improve accuracy and to enhance hemolysis of the red cells. The vials were also stored in the freezer.

The hematocrit of the cell suspension was determined at the beginning and at the end of an experiment. A 1 ml. aliquot of the cell suspension was removed from the incubation flask and placed into a hematocrit tube which was immediately centrifuged at 5,000 x g for 10 minutes. The value of the hematocrit was read directly from the stem which was calibrated in units of 0.002 ml.. A hematocrit tube is shown in Figure 9.

Release Experiments

The procedure utilized to study the release kinetics of ouabain and digitoxin from erythrocytes was as follows. Approximately 5 ml. of

---

1. New England Nuclear, Boston, Mass. 02118. NEF - 934.

red cells were incubated in 15 ml. of media containing different concentrations of either of the two tritiated glycosides and 0, 5 and 15 per cent fetal bovine serum. The cells were incubated from 1 to 10 hours. With an incubation time of 10 hours and with relatively high drug concentrations, the transport process had reached steady-state conditions, whereas with shorter incubation periods and lower drug concentrations the drug uptake had not yet reached equilibrium.

At the end of the incubation period a 0.1 ml. sample of erythrocytes and of medium was collected, as previously described, for later assay. The remaining erythrocyte suspension was centrifuged at 800 x g for 10 minutes. Subsequently, the supernatant was discarded and 4 ml. of the preincubated cells were collected with a glass syringe. At zero time, the 4 ml. of erythrocytes were introduced into a 125 ml. Erlenmeyer flask containing 50 ml. of medium. The FBS level in the media was 0, 5 or 15 per cent and, except for two specific release studies, did not contain any drug.

The remaining course of the release experiments was followed analogously to the procedure outlined for uptake studies.

Preparation of Erythrocyte Samples for Scintillation Analysis

The red-colored hemoglobin in erythrocytes produces very high quenching effects making it essentially impossible to analyze the radioactivity in erythrocytes that have merely been hemolysed and digested in a scintillation cocktail. The method used, to date, for erythrocyte liquid scintillation analysis is based solely on the extraction of the radioactive compound from the cells using either Bray's solution (55) or 10% perchloric acid. This method is cumbersome and it is impossible to completely recover all the cell-associated radioactivity. For this

reason, a novel and more complete procedure was developed.

The samples containing red cells were removed from the freezer and allowed to thaw. Subsequently, 0.1 ml. of 1M HCl and 0.1 ml. of 30% H_2O_2 were added to each vial. Making sure that the caps on the scintillation vials were tightly sealed, the samples were then digested and decolorized at 70 °C for 8 hours after which time, 10 ml. of Aquasol was added to each vial. The resulting scintillation liquid was a clear and nearly colorless solution. After storing all vials in the dark for at least a 24 hour period, the samples were assayed using a Beckman liquid scintillation spectrometer[1]. The efficiency of each sample was checked by adding 0.02 ml. of tritiated water[2] of known specific activity.

Determination of Intercellular Drug Entrapment in the Red Cell Plug

The amount of medium trapped in the 0.1 ml. red cell plug after centrifugation was analyzed using radioactive polyethylene glycol[3] (PEG - 4,000 - ^{14}C). This compound was reported to be nonabsorbable by tissue (57).

One ml. samples of washed cells from different donors were injected into vials containing PEG - 4,000 - ^{14}C in 12 ml. of phosphate buffered saline. After shaking the vials vigorously for 15 sec., a 2 ml. sample from each vial was transferred into a centrifuge tube and immediately centrifuged at 5,000 x g for 10 minutes. Next, 0.1 ml. of the supernatant and the corresponding 0.1 ml. red cell plug were collected in separate vials, prepared for scintillation assay and counted as previously described. The efficiencies of the samples containing super-

---

1. Beckman Instruments, Fullerton, Cal. 92634. Model LS-200.
2. New England Nuclear, Boston, Mass. 02118. NES-003.
3. New England Nuclear, Boston, Mass. 02118. NEC-473.

natant or digested red cells were checked by the addition of a known amount of toluene - ^{14}C [1].

Calibration of Centrifuge Tube and Hematocrit Tube

Four separate red cell suspensions were prepared by mixing 1 ml. of erythrocytes from different donors with 15 ml. of phosphate buffered saline. Two ml. suspension aliquots from each of these suspensions were then transferred into two standard type centrifuge tubes and two hematocrit tubes. Both types of tubes were calibrated to contain 0.1 ml. of erythrocytes. After centrifugation at 5,000 x g for 10 minutes, the 0.1 ml. red cell plugs were collected and each suspended in one liter of saline (0.9% NaCl). The number of cells in these suspensions were subsequently counted using a Coulter counter[2]. In order to account for errors due to coincidence counting and dead-time, aliquots of these cell suspensions were diluted into saline in the ratios of 1:2.5, 1:5, 1:10, 1:25, 1:50 and 1: 100. With the suspensions of the highest dilution, it was expected that errors due to coincidence counting and dead-time were at a minimum thereby allowing for the estimation of the absolute number of cells in the original red cell plugs.

In all cell countings, an equal suspension volume (0.5 ml.) was analyzed with a 70 micron orifice tube. Coulter counter threshold and current settings were 10 and 7, respectively.

Stability of Erythrocyte Suspension with Time

Experiments were conducted entirely simulative to uptake studies except that no radioactive drug was used. These experiments were carried out with media containing 0% and 30% FBS concentrations. The following

---

1. New England Nuclear, Boston, Mass. 02118. NES-006.
2. Coulter Industrial Sales Co., Chicago, Ill. Model A.

variables were tested throughout a 12 hour period at 4 hour intervals:

1. the pH of the cell suspension
2. the hematocrit of the cell suspension
3. the number of cells in 0.1 ml. of cell suspension
4. the number of cells per 0.1 ml. red cell plug

The pH of the cell suspension was measured with the aid of a pH meter.

The hematocrit of the cell suspension was determined by placing 1 ml. of the suspension into a hematocrit tube followed by centrifugation at 5,000 x g for 10 minutes. The value of the hematocrit was read directly from the calibrated stem of the hematocrit tube.

The number of erythrocytes in 0.1 ml. of cell suspension and in 0.1 ml. of the red cell plug was estimated by first diluting these volumes with phosphate buffered saline to one liter. The number of erythrocytes in these suspensions were then counted with a Coulter counter. No adjustments were made for coincidence and dead-time error.

Evaluation of Binding Constants from "Zero Time" Measurements

Preliminary uptake studies with digitoxin revealed that a fraction of this drug is instantaneously taken up by erythrocytes and that the instantaneously accumulated amount of drug in the erythrocytes is directly proportional to the concentration of the external medium. This rapid uptake of digitoxin by erythrocytes also appeared to be a function of the fetal bovine serum level in the suspension medium, thereby strongly suggesting that digitoxin interacts with the serum. Ouabain, on the other hand, did not exhibit any of these characteristics.

In the following section, the procedures are described that were used to quantify the rapid digitoxin -erythrocyte interaction as well as the digitoxin - serum binding effect from "zero time" measurements.

(a) Evaluation of K_{bm} (Models 2 and 5, equation 14) or K (Model 6, equation 8): Aliquots (12 ml.) of phosphate buffered saline containing different concentrations of tritiated digitoxin, but no fetal bovine serum, were placed into separate vials and maintained at 30 °C. Neomycin sulfate (0.5 mg./ml.) was added to some of the 12 ml. buffered saline samples in order to examine its influence on the magnitude of K_{bm} or K. A 1 ml. aliquot of red cells, each from a different donor, was introduced into the vials and the suspension vigorously shaken for 15 sec. Four 2 ml. suspension samples were then transferred from each vial into separate centrifuge tubes and centrifuged at 5,000 x g for 10 minutes. Then, 0.1 ml. of the supernatants and the corresponding 0.1 ml. RBC plugs were collected and assayed.

(b) Reversibility of Instantaneous Digitoxin - Erythrocyte Interaction (equation 14 or 8): A vial, containing 4 ml. of phosphate buffered saline and digitoxin -^{3}H but no fetal bovine serum, was kept at 30 °C. At zero time, a 1 ml. sample of erythrocytes was added and the suspension vigorously shaken for 15 sec. Subsequently, a 1 ml. sample of the suspension was placed into a centrifuge tube. The remaining cell suspension was rapidly diluted by approximately a factor of two with phosphate buffered saline and the suspension again shaken for 15 sec.. A 2 ml. aliquot of this diluted suspension was then placed in a second centrifuge tube. Following the immediate centrifugation of these samples, the usual supernatant and corresponding RBC samples were collected and analyzed.

(c) Effect of Red Cell Age on K_{bm} or K: The effect that prolonged incubation of erythrocytes in phosphate buffered saline may have on the magnitude of K_{bm} or K was tested in the following manner. Blood from several donors was pooled to yield 15 ml. of washed red cells. A 1 ml. red cell sample, removed for "zero time" analysis, was put into

12 ml. of phosphate buffered saline containing radioactive digitoxin. The suspension was then subjected to the same procedure as that described in (a). The remaining 14 ml. of red cells were suspended in 25 ml. of phosphate buffered saline. The flask containing the suspension was agitated with a Burrell shaker and kept at 30 °C. Subsequently, the suspension was centrifuged at 800 x g for 10 minutes several times over a 12 hour period. After each centrifugation step, the suspension medium was decanted, a 1 ml. RBC sample removed and the remaining packed red cells resuspended in 25 ml. of phosphate buffered saline. The abstracted 1 ml. red cell sample was immediately introduced into 12 ml. of buffered saline containing digitoxin - ^{3}H. The resulting suspension was again treated as described in (a).

(d) Evaluation of K_{bm} or K and K_b (equations 35 or 78): One ml. aliquots of washed red cells from different donors were injected into 12 ml. of media. These media, kept at 30 °C, contained various FBS concentrations and digitoxin - ^{3}H. Again, neomycin sulfate (0.5 mg./ml.) was added to some of the media. The cell suspensions were subsequently treated as described in (a).

(e) Interaction Between Digitoxin and Erythrocyte Ghosts: In order to at least partially resolve the question of whether the instantaneous and linear digitoxin uptake component by erythrocytes was due to either membrane adsorption or to diffusion of the drug into the cell interior, the magnitude of K_{bm} or K for the glycoside - erythrocyte ghost system was determined.

The erythrocyte ghosts were prepared in this manner (41). Five 3 ml. samples of washed red cells were each suspended in 15 ml. of phosphate

buffered saline. A freezing and thawing of these suspensions resulted in the release of hemoglobin from the cells and the production of ghosts. The RBC ghost suspensions were washed five times with 15 ml. of buffered saline in order to remove most of the hemoglobin from the medium. The suspensions were then frozen and thawed a second time and the ghosts washed two more times. Microscopic analysis of the RBC ghosts indicated that the size of the ghosts was identical to that of the original erythrocytes. The RBC ghosts were subsequently used for experiments identical to those described in (b).

Equilibrium Dialysis

The equilibrium binding constants for the digitoxin - fetal bovine serum, the ouabain - fetal bovine serum and the digitoxin - human hemoglobin interaction were evaluated at 30 ^{o}C under sterile conditions using equilibrium dialysis experiments.

(a) Digitoxin - Fetal Bovine Serum Binding: Six dialysis chambers[1] with a total capacity of 4 ml. were used simultaneously. One such dialysis chamber is shown in Figure 9. After being boiled in water for 1 hour, a cellulose dialysis membrane[2], permeable to water and low molecular weight compounds but impermeable to higher molecular weight compounds such as proteins, was placed between the donor and receiver side of the dialysis chamber. Two ml. samples of cell suspension media containing tritiated digitoxin and 5, 10, 20, 30 40 or 50% FBS were put into the donor side and 2 ml. samples of medium without FBS were pipetted into the receiver side of the six dialysis chambers. At various times, 0.01 ml. samples were aseptically removed from the receiver and the donor side and kept in scintillation vials for assay. By this method, the increase and

---

1. Bellco Glass Inc., Vineland, N.J.
2. Union Carbide Corp., Chicago, Ill. 60638.

decrease of the digitoxin concentrations in the receiver and donor sides, respectively, could be followed simultaneously until equilibrium was reached.

(b) Ouabain - Fetal Bovine Serum Binding: The adsorption equilibrium constant for the ouabain - fetal bovine serum system, K_{bo}, was determined by the same procedure outlined in (a), except that only two fetal bovine serum levels (20 and 50%) were used.

(c) Digitoxin - Human Hemoglobin Binding: Hemoglobin comprises more than 90 per cent of the total solid red cell mass and has a concentration of 328 gm. per liter of erythrocytes (56). Hence, if digitoxin rapidly permeates the plasma membrane, as proposed in Model 6, it is reasonable to assume that the drug may well interact with the hemoglobin in the cell interior. The extent of this possible drug - protein interaction was appraised using equilibrium dialysis experiments.

Two solutions containing 100% and 50% of hemoglobin were prepared by dissolving 3.28 gm. and 1.64 gm. of the protein, respectively, in 10 ml. of phosphate buffered saline. Three dialysis experiments were carried out with each of the solutions according to the procedure described in (a).

Purity Determination of Ouabain -^{3}H and Digitoxin -^{3}H

In order to check for possible biodegradation of the tritium labelled ouabain and digitoxin in the presence of erythrocytes and fetal bovine serum, the purity and stability of these drugs was determined before and after uptake experiments.

Four ml. of red cells were incubated in 15 ml. of media containing ouabain -^{3}H or digitoxin -^{3}H and 15% FBS for 10 hours. At the end of the incubation period, the cell suspensions were centrifuged and the supernatants and erythrocyte sediments placed into separate vials.

Ouabain: The vial containing the supernatant with ouabain -^{3}H was placed in an oven at 70 °C and the water evaporated under a stream of nitrogen gas. The erythrocyte - associated ouabain was removed from the 4 ml. of cells with five successive extractions using a total of 75 ml. of ethanol. The extraction procedure of ouabain from the cells was better than 85% effective. The radiochemical purity of ouabain in these two vials and that of fresh ouabain was checked using thin layer chromatography.

Three TLC glass plates[1], pre-coated with Silica Gel 60F - 254, were first spotted at the origin with a solution containing nonradioactive ouabain[2] (approximately 0.1 mg. of nonradioactive ouabain per spot). The nonradioactive ouabain samples to be assayed were placed on top of the nonradioactive ouabain spots. The plates were then developed using the chloroform: methanol: water (65 : 30 : 5 V/V/V) solvent system.

Digitoxin: The tritiated digitoxin was extracted from the cells and the supernatant using chloroform. Five successive extractions were carried out with both vials utilizing a total of 75 ml. of chloroform for each. Better than 95% of digitoxin was recovered from the cells and the supernatant by the extraction procedure.

After first spotting the origin of three Silica Gel precoated TLC glass plates with nonradioactive digitoxin[3] in chloroform (approximately 0.1 mg. nonradioactive digitoxin per spot), the digitoxin -^{3}H samples were placed on top of the nonradioactive digitoxin spot. The plates were subsequently chromatographed using the benzene: 95% ethanol

---

1. Brinkmann Instruments, Inc. Des Plaines, Ill. 60016
2. Sigma Chem. Corp., St. Louis, Mo. 63178
3. Mann Research Laboratories, Inc., N.Y., N.Y. 10006

(6:1 V/V) solvent system.

The purities of the two glycosides were determined by the use of a radiochromatogram scanner[1].

Specific Activity Determination of Ouabain -^{3}H and Digitoxin -^{3}H

The specific activity values for the two glycosides were determined utilizing the saturation binding property that erythrocytes exhibit with these drugs. In order to reduce the error due to variation in the drug - erythrocyte affinity, the same pool of erythrocytes was used for all experiments.

Ouabain: A constant aliquot of tritiated ouabain was added to four vials. The amount of radioactive drug was sufficient to saturate all erythrocyte binding sites. Ten ml. of phosphate buffered saline containing 0, 2, 4 or 6 x 10^{-8}M nonradioactive ouabain and 1 ml. of red cells were then added to each vial. After incubating the cell suspensions for ten hours, four 0.1 ml. RBC samples and four 0.1 ml. samples of the supernatant were collected from each suspension and analyzed for radioactivity. The decrease of the cell associated radioactivity with increasing concentration of the nonradioactive ouabain in the suspension medium allowed for the estimation of the specific activity of the tritiated ouabain that was present in the suspension medium.

Digitoxin: A constant amount of tritiated digitoxin, sufficient to saturate all the cell-associated Langmuir binding sites, was added to four vials. Ten ml. of phosphate buffered saline containing 0, 1, 2 or 4 x 10^{-8}M nonradioactive digitoxin and 1 ml. of red cells were then introduced into each vial. The suspensions were vigorously shaken for

---

1. Packard Instrument Co., Inc. Downers Grove, Ill. 60515. Model 7201

15 sec. and an aliquot from each suspension was then removed for analysis of the "zero time" drug uptake by the cells. The remaining suspensions were incubated for six hours, after which time, four 0.1 ml. RBC samples and four 0.1 ml. samples of the supernatant were collected from each vial to be analyzed for their radioactivity.

RESULTS OF THE COMPLEMENTAL STUDIES

Intercellular Red Cell Plug Error and Efficiencies

The error due to drug trapped between the compacted red blood cell plugs was evaluated with four samples using PEG - 4,000 - ^{14}C. Since this compound does not interact with erythrocytes, any radioactivity that is present in the RBC plugs must be attributed to intercellular entrapment of the suspension medium containing the radioactive compound. The data collected from the analysis, adjusted for quenching and background radiation of each sample, are listed in Table I. From this data, a mean value of 4.75% was calculated for the intercellular red cell plug error. An appropriate correction was subsequently applied to all 0.1 ml. RBC plug samples, as will be shown later.

The efficiencies of samples containing either medium or red blood cells were evaluated by

$$\% \text{ Efficiency} = \frac{DPM_{after} - DPM_{before}}{\Delta \text{ Vol.}_{std.} \times DPM_{std.}} \times 100 \qquad \text{(Eq. 80)}$$

where $DPM_{std.}$ is the number of disintegrations per minute of 1 ml. of internal standard (water - ^{3}H or toluene - ^{14}C). DPM_{before} and DPM_{after} are the disintegrations per minute of the samples before and after the addition of a Δ Vol. of the internal standard, respectively.

Background radiation counts ($DPM_{bkgd.}$) and efficiency factors for all samples permitted the evaluation of the absolute DPM values for the medium, $DPM_{med.,abs.}$, and the red cell plug samples, $DPM_{RBC,abs.}$, using these equations:

$$DPM_{med.,abs.} = \frac{DPM_{med.} - DPM_{med.,bkgd.}}{\text{Efficiency}_{med.}} \times 100 \qquad \text{(Eq. 81)}$$

and

$$DPM_{RBC,abs.} = A + 0.0475\ A \qquad \text{(Eq. 82)}$$

Table I. Results of the analysis for the intercellular red blood cell plug error using PEG - 4,000 - ^{14}C.

Sample	DPM*/0.1 ml. Medium	DPM*/0.1 ml. RBC	% Error
1	69,429	3,124	4.50
2	72,655	3,545	4.88
3	70,870	3,368	4.75
4	71,813	3,482	4.85
	Mean Intercellular Red Cell Plug Error :		4.75

* Efficiency and background radiation corrections were applied to all samples.

where

$$A = \frac{DPM_{RBC} - DPM_{RBC,bkgd.}}{Efficiency_{RBC}} - 0.0475\ DPM_{med.,abs.}$$

$DPM_{med.}$ and DPM_{RBC} represent the disintegrations per minute of the "raw" data obtained for the medium and red cell samples, respectively. The determination of the absolute DPM values for the RBC plugs with equation (82) takes into account the 4.75% intercellular red cell plug error.

The scintillation counter efficiencies for the tritiated glycosides ranged between 18 and 23 per cent for the samples containing erythrocytes and between 29 and 31 per cent for the samples containing medium.

Calibration of Centrifuge Tube and Hematocrit Tube

The cell counts, measured for each of the centrifuge and hematocrit 0.1 ml. RBC plugs and their respective diluted suspensions, were normalized with respect to the dilution factor and are summarized in Table II. The small differences in cell count that were observed with the suspensions of the two highest dilutions indicate that coincidence and dead-time error in these systems were minimal. Therefore, the absolute number of cells in the 0.1 ml. RBC plugs could be estimated from the suspensions with the highest dilution. The average number of erythrocytes in these four 0.1 ml. RBC plugs was computed to be 1.07×10^9. This number compares favorably with that of 1.15×10^9 which is computed using the reported average red cell volume of 87×10^{-12} cm^3. The difference between the experimentally determined number of erythrocytes in the 0.1 ml. red cell plugs and the theoretical value, in fact, can almost entirely be attributed to the intercellular red cell plug error.

Stability of Erythrocyte Suspensions with Time

The results obtained for the various transport related parameters

Table II. Determination of absolute number of red blood cells in 0.1 ml. RBC plugs from two centrifuge and two hematocrit tubes. By successive dilution of the cell suspensions with saline, coincidence and dead-time Coulter counter errors were eliminated allowing the estimation of the absolute number of red cells in the original RBC plugs.

Suspension	Dilution Factor *	Number of Erythrocytes x 10^{-8}/0.1 ml. RBC plug**			
		Hematocrit Tube #1	Hematocrit Tube #2	Centrifuge Tube #1	Centrifuge Tube #2
A	0	6.76	6.89	6.68	6.71
B	2.5	7.82	8.21	7.84	7.96
C	5	8.40	8.80	8.49	8.63
D	10	8.96	9.36	8.90	9.04
E	25	9.70	9.93	9.78	9.83
F	50	10.47	10.84	10.11	10.42
G	100	10.91	11.22	10.15	10.59

* Dilution factor applied to suspension A
** Mean value for ten readings

that were tested for their time dependent constancy are listed in Table III. These results clearly indicate that the pH and the number of cells in suspension remain constant over a twelve hour period. The complementary tests of the hematocrit and number of cells per 0.1 ml. of red cell plug show that the cell volume does not change during the same time period. Furthermore, visual observation of the supernatant over the twelve hour period indicated that little or no hemolysis of the erythrocytes occurred. It should be noted that the overall stability of erythrocytes, particularly in the absence of fetal bovine serum in the suspension medium, was much reduced when the incubation period exceeded fifteen hours. Transport studies that indicated any sign of cellular deterioration were immediately stopped.

Evaluation of Binding Constants from "Zero Time" Measurements

(a) Evaluation of K_{bm} (Models 2 and 5, equation 14) or K (Model 6, equation 8): Figure 10 shows a plot of the instantaneously accumulated cellular digitoxin concentration as a function of the drug concentration in the external phosphate buffered saline medium. The linear regression line for all data points, forced through the origin, gave a slope of 2.26. According to equation (14) in Model 2 or equation (8) in Model 6, the magnitude of the slope is equal to K_{bm} or K, respectively. The correlation coefficient was 0.999. The excellent fit of the experimental data does not only demonstrate the existence of the linear relationship between the cell - associated drug concentration and the free drug concentration in the medium but also indicates that the value of K_{bm} or K is apparently independent of the source of the red cells and the presence of neomycin sulfate in the medium.

(b) Reversibility of Instantaneous Digitoxin - Erythrocyte Inter-

Table III. Stability determination of pH, hematocrit, number of cells in 0.1 ml. of suspension and 0.1 ml. RBC plug with two cell suspensions containing 0 and 30% FBS. The cell counts were determined with a Coulter counter, Model A.

Time hrs.	FBS %	pH	#of cells* x 10^{-8}/0.1 ml. suspn.	Hematocrit** %	#of cells*** x 10^{-8}/0.1 ml.RBC plug
0	0	7.42	7.420	7.50	6.820
4	0	7.37	7.372	7.50	6.804
8	0	7.35	7.407	7.55	6.812
12	0	7.36	7.354	7.60	6.807
0	30	7.39	7.126	7.35	6.734
4	30	7.34	7.068	7.40	6.735
8	30	7.38	7.093	7.30	6.719
12	30	7.36	7.123	7.30	6.709

* mean value from ten readings
** mean of two readings
*** values are not adjusted for coincidence and dead-time error

action (equation 14 or 8): The rapid reversibility of the instantaneous digitoxin - erythrocyte interaction is clearly shown in Figure 11. Linear regression analysis of all data points gave a slope of 2.28 which is also equal to the value of K_{bm} or K. The correlation coefficient for all data points was 0.999.

(c) Effect of Red Cell Age on K_{bm} or K: The data collected for the digitoxin - erythrocyte binding constant, K_{bm} or K, as a function of red cell incubation time are given in Table IV. The mean value for K_{bm} or K, listed in Table IV, is 2.28. The magnitude of K_{bm} or K, within experimental error, does not change over a twelve hour period of incubation of the erythrocytes in phosphate buffered saline.

(d) Evaluation of K_{bm} or K and K_b (equations 35 or 78): The plot of $(C_T/C_s)_{t=0}$ or $(C_T/C_i)_{t=0}$ <u>versus</u> FBS concentration used for the evaluation of the digitoxin - fetal bovine serum and the digitoxin - erythrocyte equilibrium binding constants is shown in Figure 12. Linear regression analysis of the data gave a slope and intercept of 2.41 and 0.44, respectively. The digitoxin - erythrocyte binding constant, K_{bm} or K was computed from the intercept as 2.27 and the FBS binding constant, K_b, was evaluated from the slope and intercept to be 5.47.

(e) Interaction Between Digitoxin and Erythrocyte Ghosts: Figure 13 shows that the amount of digitoxin that is instantaneously taken up by RBC ghosts is linearly related to the concentration of the drug in the medium and that the instantaneous drug uptake is also readily reversible. Linear regression analysis of the data shown in Figure 13 gave a slope of 1.07, which is identical to the digitoxin - RBC ghost binding constant.

The composition of the RBC ghost interior, except for a small amount of residual hemoglobin, is expected to be identical to that of the in-

Table IV. Data collected for the digitoxin - erythrocyte equilibrium binding constant as a function of erythrocyte incubation time and determined from "zero time" measurements. The cells were incubated in phosphate buffered saline. The temperature was 30 °C. The values for K_{bm} or K were calculated with equations (14 and 8), respectively.

Incubation Time, hrs.	K_{bm} or K^*	Standard Deviation
0	2.27	0.026
1	2.30	0.042
2	2.24	0.018
3	2.28	0.022
4	2.33	0.044
6	2.31	0.024
8	2.26	0.046
10	2.29	0.037
12	2.28	0.069
	Mean : 2.28	

* Mean value from four determinations

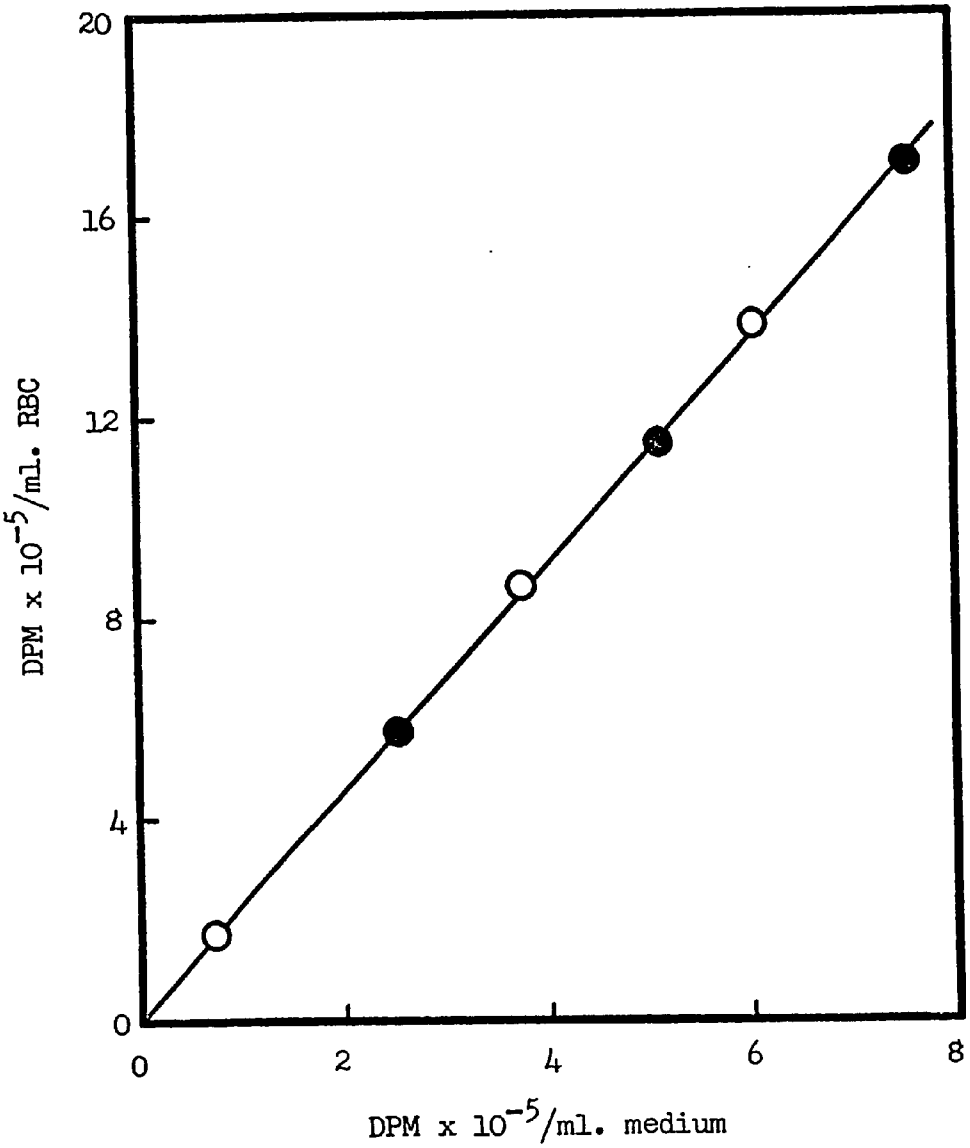


Figure 10. Amount of digitoxin taken up by 1 ml. of RBC versus concentration of digitoxin in the external phosphate buffered saline at "zero time". The slope is 2.26 and is equal to the digitoxin - erythrocyte binding constant, K_{bm} or K. The temperature was 30 °C. The presence (O) or absence (●) of 0.5 mg. neomycin sulfate per ml. of medium is inconsequential.

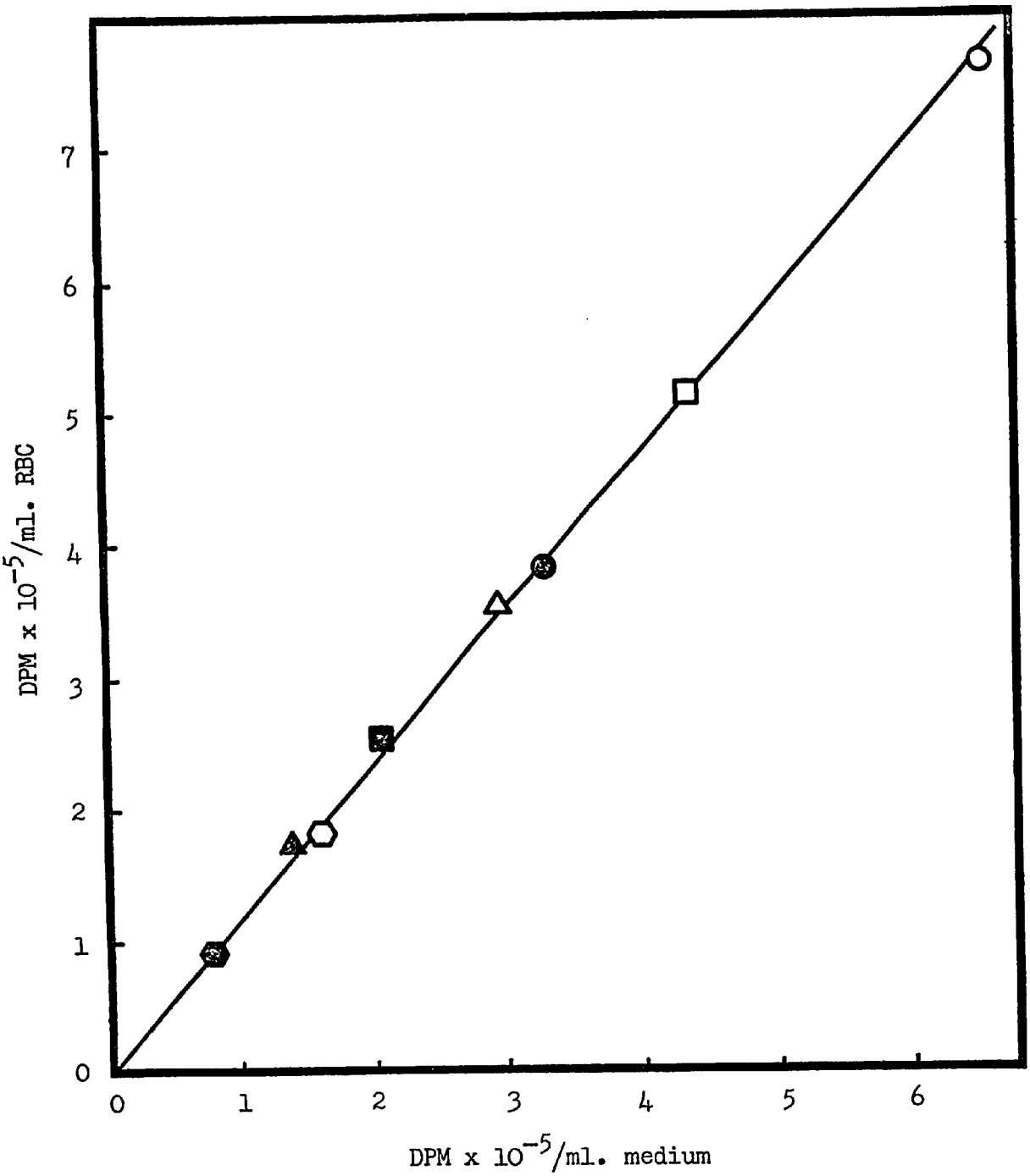


Figure 11. Amount of digitoxin taken up by 1 ml. RBC versus concentration of digitoxin in the external phosphate buffered saline at "zero time". Plot demonstrates the rapid reversibility of the instantaneous cellular drug uptake. Open and identical closed symbols represent the data collected from one particular suspension system before and after rapid dilution, respectively. The slope is 2.28 and is equal to the digitoxin - erythrocyte binding constant K_{bm} or K. The temperature was 30 °C.

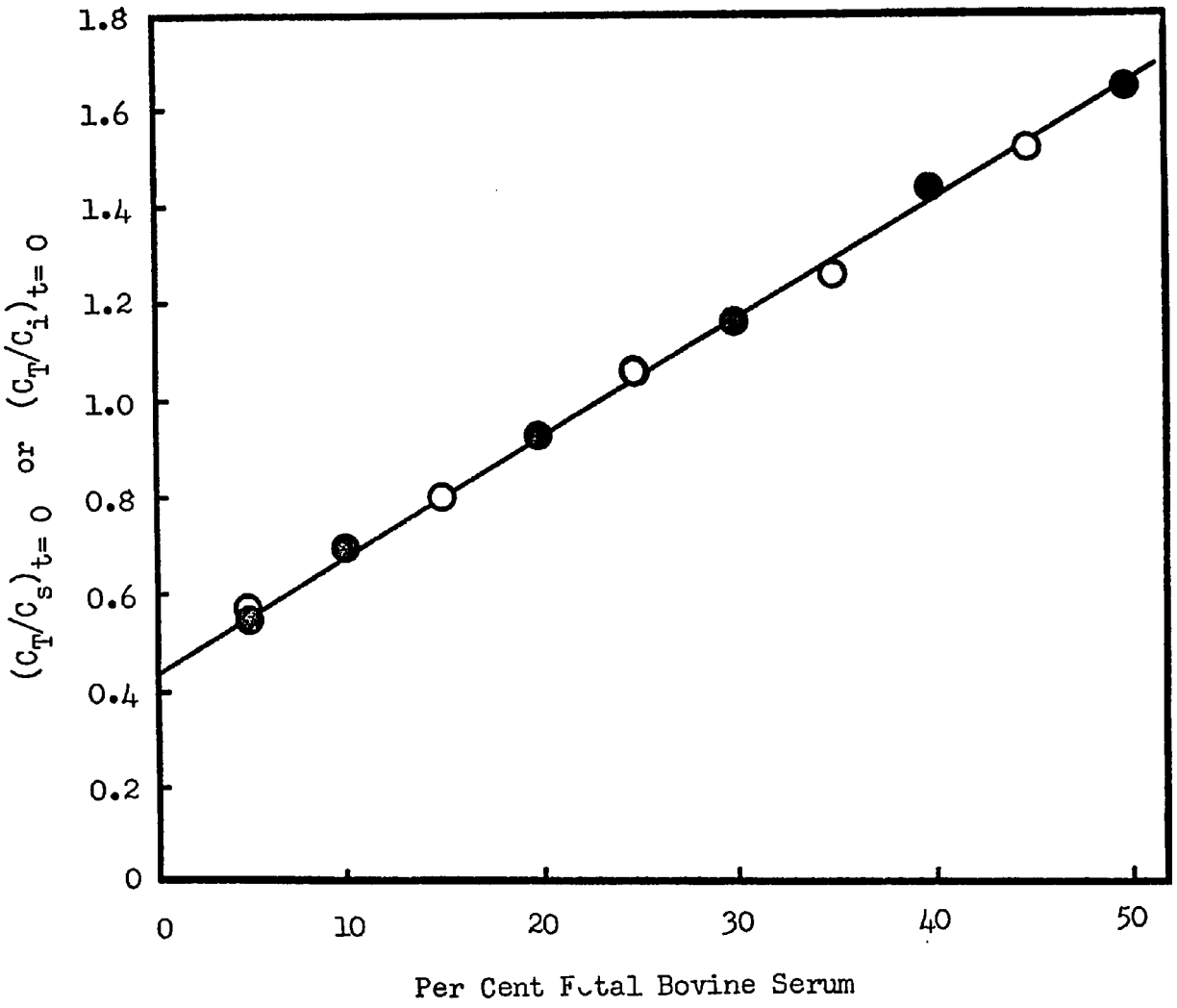


Figure 12. "Zero time" data for the ratio of total digitoxin concentration in media to the RBC concentration versus FBS levels in the suspension media. The slope is 2.41 and the intercept is 0.44. With equations (35 and 73), the digitoxin - erythrocyte binding constant, K_{bm} or K, and the digitoxin - FBS binding constant, K_b, are computed from the slope and intercept as 2.27 and 5.47, respectively. The temperature was 30 °C. The absence (o) or presence (●) of 0.5 mg. neomycin sulfate in the suspension media was inconsequential.

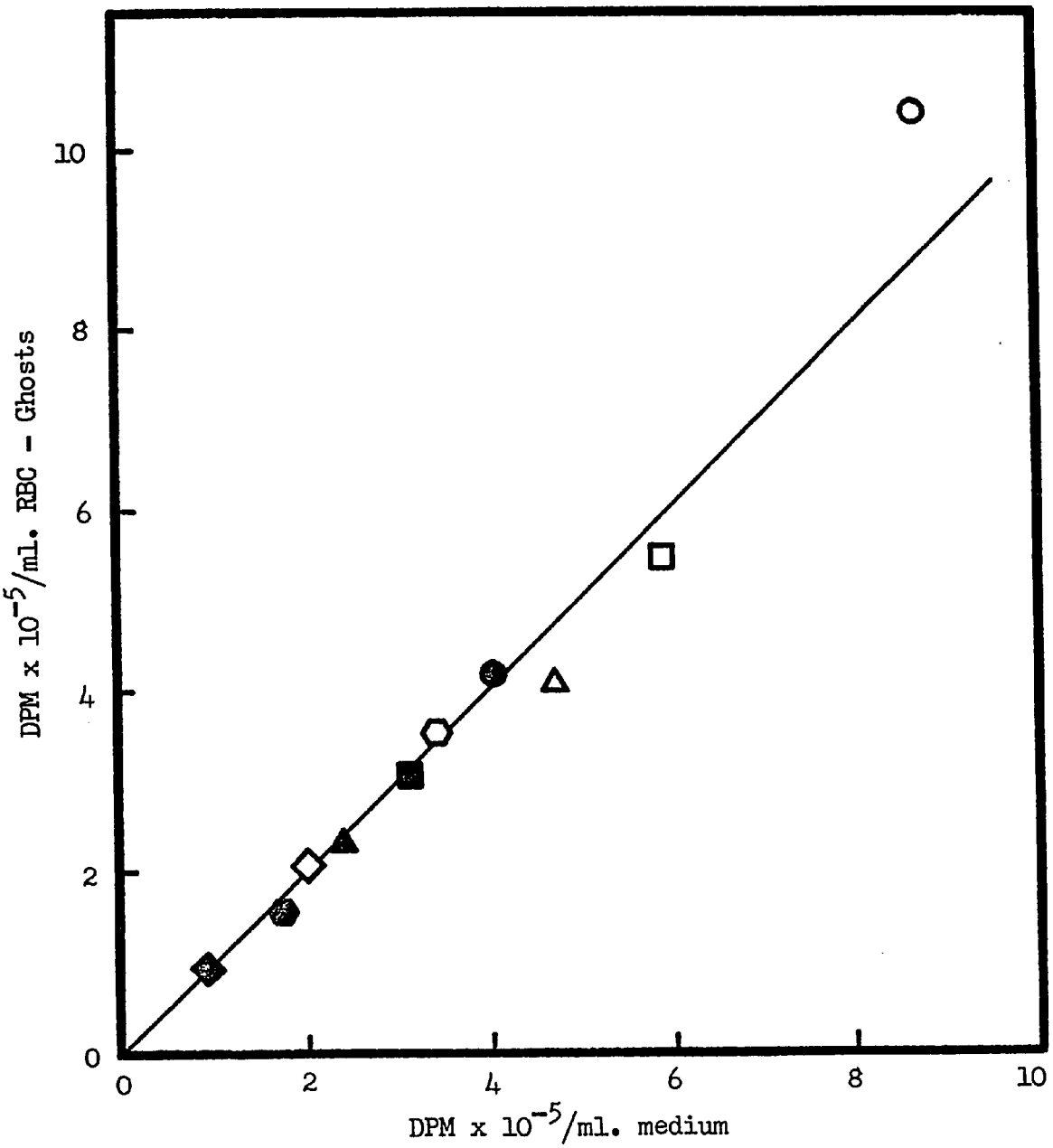


Figure 13. Amount of digitoxin taken up by 1 ml. RBC - ghosts versus concentration of external phosphate buffered saline at "zero time". Plot demonstrates the rapid reversibility of the instantaneous drug uptake. The temperature was 30 °C. Open and identical closed symbols represent data obtained from one particular suspension before and after rapid dilution, respectively. The slope is 1.07 and is equal to the digitoxin - RBC - ghost binding constant.

cubation medium. Hence, if the instantaneous digitoxin uptake is the result of diffusion of the drug into the cell interior, as proposed in Model 6, it would be expected that the digitoxin - RBC ghost binding constant is near unity. On the other hand, it could be argued that the presumed linear membrane binding property, discussed in Models 2 and 5, could have been partially destroyed during the freezing and thawing process of the erythrocytes. The present data for the digitoxin - RBC ghost interaction, therefore, favors the hypothesis of rapid permeation of the drug into the cell interior. However, more information is required before a definitive conclusion can be drawn regarding the mechanism of the instantaneous digitoxin uptake by erythrocytes.

Equilibrium Dialysis

The data collected from the different equilibrium dialysis experiments was analyzed with

$$K_D = \frac{C_D - C_R}{C_R S} \qquad (t=\infty) \qquad \text{(Eq. 77)}$$

where K_D typifies the respective drug - substrate equilibrium binding constant, C_D represents the equilibrium concentration of the donor side containing FBS or human hemoglobin of fraction S and C_R is the equilibrium concentration of the receiver side containing no substrate.

(a) Digitoxin - Fetal Bovine Serum Binding: A summary of the data that was obtained for the digitoxin - FBS systems is given in Table V. The mean value for the digitoxin - FBS binding constant, K_b, calculated from the data listed in Table V, is 5.65 with a standard deviation of 0.38. This value is in good agreement with that determined from "zero time" kinetic data listed in Table VIII.

The apparent loss of digitoxin -^{3}H from the systems may be the

result of adsorption of the compound to the cellulose dialysis membrane or it may be due to partitioning of the drug into the silicone grease that was used to seal the dialysis chambers. The apparent loss of digitoxin should, however, have no influence on the magnitude of the equilibrium values.

A summary of the equilibrium binding constants determined for the digitoxin - erythrocyte and digitoxin - fetal bovine serum interactions using the different experimental methods is given in Table VIII. A mean value of 2.27 and 5.52 was found for the digitoxin - erythrocyte and digitoxin - FBS binding equilibrium constants, K_{bm} or K and K_b, respectively.

(b) Ouabain - Fetal Bovine Serum Binding: Table VI lists the results that were obtained for the dialysis of ouabain and fetal bovine serum. The data indicates that there is essentially no interaction between ouabain and FBS.

(c) Digitoxin - Human Hemoglobin Binding: The data for the digitoxin - human hemoglobin dialysis experiments are given in Table VII. The extent of the digitoxin - hemoglobin interaction appears to be protein concentration dependent. The mean equilibrium binding constant, K_{bh}, in the presence of 100% and 50% hemoglobin was 1.86 and 3.50, respectively. The reduction in the equilibrium adsorption constant value with 100% hemoglobin could be attributed to increased hemoglobin - hemoglobin interaction at the higher protein concentration which, in turn, may decrease the affinity of hemoglobin for digitoxin.

The cell water of erythrocytes available for diffusing solutes is generally considered to comprise 66% of the total cell volume. The total amount of digitoxin that can instantaneously be taken up by

Table V. Data obtained from equilibrium dialysis experiments for the estimation of the digitoxin - FBS binding constant, K_b. The basic medium was phosphate buffered saline and the temperature 30 °C. The equilibrium binding constant, K_b, was determined from the equilibrium dialysis data using equation (83).

Time (hrs.)	5% FBS		10% FBS		20% FBS	
	C_D	C_R	C_D	C_R	C_D	C_R
0	4,323	23	4,370	25	4,395	21
8	2,734	608	2,821	507	3,346	462
25	2,055	1,237	2,404	963	2,865	891
46	1,894	1,396	2,160	1,101	2,595	1,037
67	1,909	1,510	2,134	1,280	2,574	1,198
80	1,887	1,484	2,171	1,307	2,572	1,184
96	1,880	1,490	2,152	1,362	2,500	1,223
Equilibrium*:	1,892	1,495	2,152	1,316	2,549	1,202
K_b	5.31		6.35		5.60	

Time (hrs.)	30% FBS		40% FBS		50% FBS	
	C_D	C_R	C_D	C_R	C_D	C_R
0	5,009	23	4,477	25	4,261	25
8	3,955	444	3,729	397	3,806	376
25	3,498	866	3,379	732	3,493	711
46	3,216	1,069	3,151	898	3,188	797
67	3,179	1,176	3,105	957	3,098	832
80	3,242	1,198	3,088	936	3,119	854
96	3,182	1,237	3,124	931	3,127	848
Equilibrium*:	3,201	1,204	3,106	941	3,115	845
K_b	5.53		5.75		5.37	

* Mean value calculated from equilibrium data (67, 80 and 96 hrs.). C_D and C_R represent concentrations in DPM/0.01 ml. medium of the donor and receiver sides of the dialysis chamber, respectively.

Table VI. Equilibrium dialysis data for the ouabain - FBS system. The basic medium was phosphate buffered saline and the temperature 30 °C. The donor side of the dialysis chamber contained the human hemoglobin. The equilibrium binding constant, K_{bo}, was evaluated with equation (77).

Time (hrs.)	20% FBS		50% FBS	
	C_D	C_R	C_D	C_R
24	9,863	9,591	5,442	5,003
48	9,775	9,686	5,409	5,274
72	9,695	9,701	5,368	5,298
96	9,723	9,734	5,423	5,317
Equilibrium* :	9,709	9,718	5,385	5,308
K_{bo}	0		0.03	

* Mean value calculated from 72 and 96 hours data.

C_D and C_R represent concentrations in DPM/0.01 ml. medium of the donor and receiver side of the dialysis chamber, respectively.

Table VII. Equilibrium dialysis data for the digitoxin - human hemoglobin system. The basic medium was phosphate buffered saline. The donor side of the dialysis chamber contained the human hemoglobin. The temperature was 30 °C. The equilibrium binding constant, K_{bh}, was evaluated with equation (77).

100% Human Hemoglobin						
Time (hrs.)	C_D	C_R	C_D	C_R	C_D	C_R
24	6,270	1,638	8,210	1,772	9,268	2,442
48	5,936	2,022	7,723	2,147	8,832	2,903
72	5,754	2,216	7,536	2,387	8,599	3,134
96	5,862	2,140	7,496	2,413	8,721	3,104
Equilibr.*:	5,808	2,178	7,516	2,400	8,660	3,119
K_{bh}	1.67		2.13		1.78	

50% Human Hemoglobin						
Time (hrs.)	C_D	C_R	C_D	C_R	C_D	C_R
24	4,995	917	6,698	1,367	9,534	2,584
48	4,597	1,253	6,252	1,823	9,066	3,023
72	4,375	1,492	5,851	2,100	8,827	3,300
96	4,321	1,156	6,111	2,196	8,865	3,508
Equilibr.*:	4,348	1,504	5,981	2,148	8,756	3,404
K_{bh}	3.79		3.57		3.14	

* Mean value calculated from 72 and 96 hours data.
C_D and C_R represent concentrations in DPM/0.01 ml. medium of the donor and receiver side of the dialysis chamber, respectively.

Table VIII. Mean values determined for the instantaneous, linear and reversible digitoxin - erythrocyte and digitoxin - fetal bovine serum binding constants K_{bm} or K and K_b, as determined by different experimental methods.

Experimental Method	K_{bm} or K	K_b	Equation
"Zero time" analysis (no FBS)	2.26		14 or 8
"Zero time" analysis (reversibility check, no FBS)	2.28		14 or 8
"Zero time" analysis (RBC incubation effect)	2.28		14 or 8
"Zero time" analysis (different FBS levels)	2.27	5.47	35 or 78
Equilibrium dialysis		5.56	83
Mean:	2.27	5.52	

erythrocytes as a result of diffusion is the sum of the drug that has permeated into the aqueous cell phase plus the fraction of drug which is bound to hemoglobin in the cell interior. Hence, the digitoxin - erythrocyte equilibrium binding constant due to diffusion, i.e. K, would be approximately 2.52. This number is close to the value of 2.27 which was determined for K_{bm} or K from "zero time" experiments.

Thus, it appears reasonable to conclude from the above consideration as well as from the information gathered for the digitoxin - RBC ghost interaction that the instantaneous, linear and reversible digitoxin - erythrocyte interaction previously defined by K_{bm} or K is, in fact, the result of rapid diffusion of the drug into the cell interior and therefore is best represented by the intrinsic partition coefficient, K.

Purity Determination of Ouabain -^{3}H and Digitoxin -^{3}H

The radiochromatogram scanner recordings for the different ouabain -^{3}H and digitoxin -^{3}H samples are shown in Figure 14 and Figure 15, respectively. The single peaks on these radiochromatograms clearly show that neither of the two glycosides were chemically degraded to any large extent by either the erythrocytes or the fetal bovine serum present in the suspension media.

Specific Activity Determination of Ouabain -^{3}H and Digitoxin -^{3}H

Ouabain: The value determined for the cellular concentration when there was no nonradioactive ouabain in the medium was taken to represent 100% cellular saturation and served as a reference point in the specific activity computations. The addition of nonradioactive ouabain to the suspension medium resulted in a reduction of binding of tritiated ouabain to the cells. Relating the percent decrease of cellular radioactivity to the known concentration of nonradioactive ouabain in the suspension medium as well as the DPM measured for the ouabain -^{3}H in

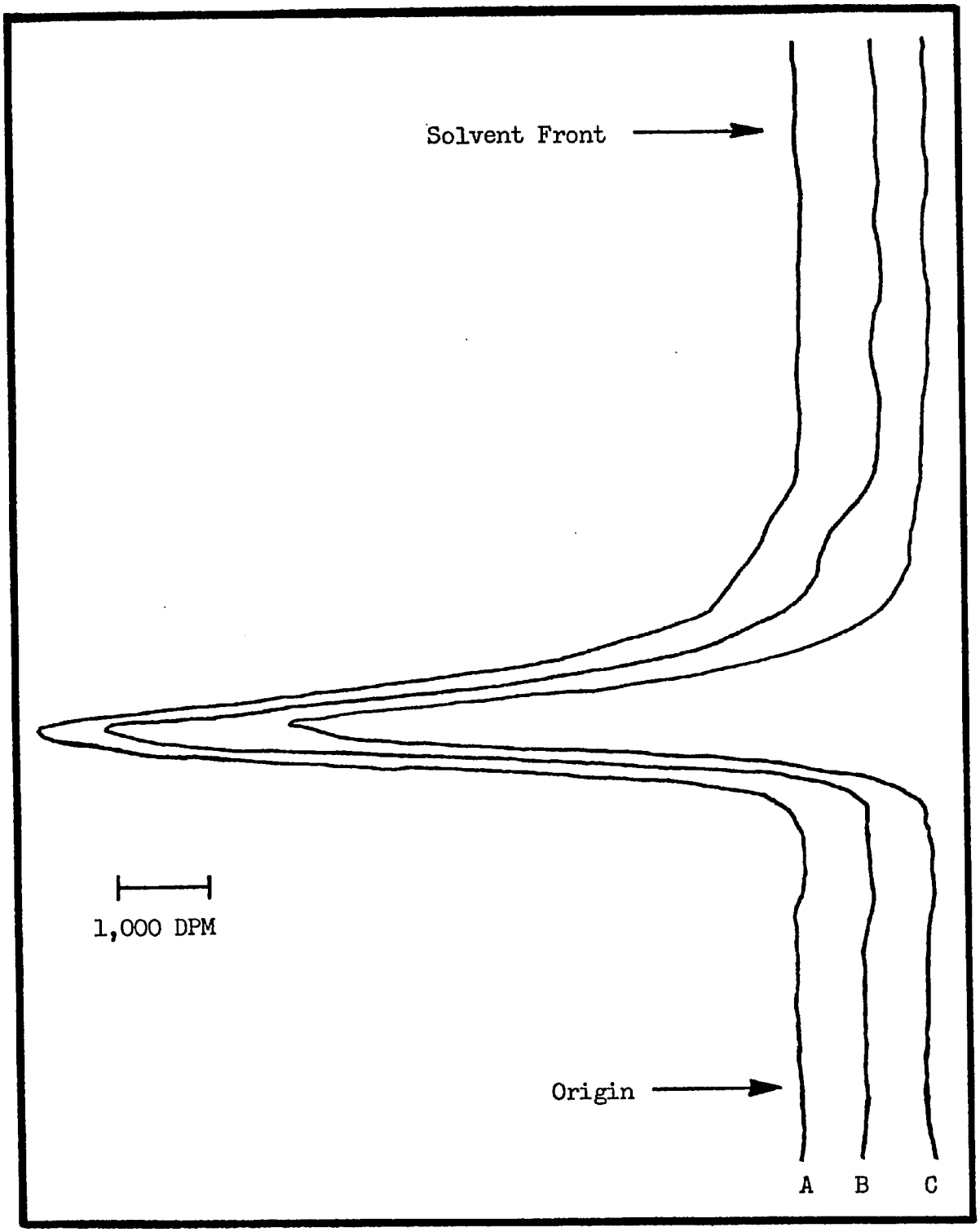


Figure 14. Radiochromatogram scanner recordings obtained for the different ouabain - ^{3}H samples. Curve A represents the cell extracted ouabain, curve B represents the ouabain from the medium and curve C represents the radiochemically pure ouabain provided by the commercial supplier. The background radiation was the same for all three recordings. The single, superimposed peaks demonstrate that the drug remained stable in the presence of erythrocytes and FBS.

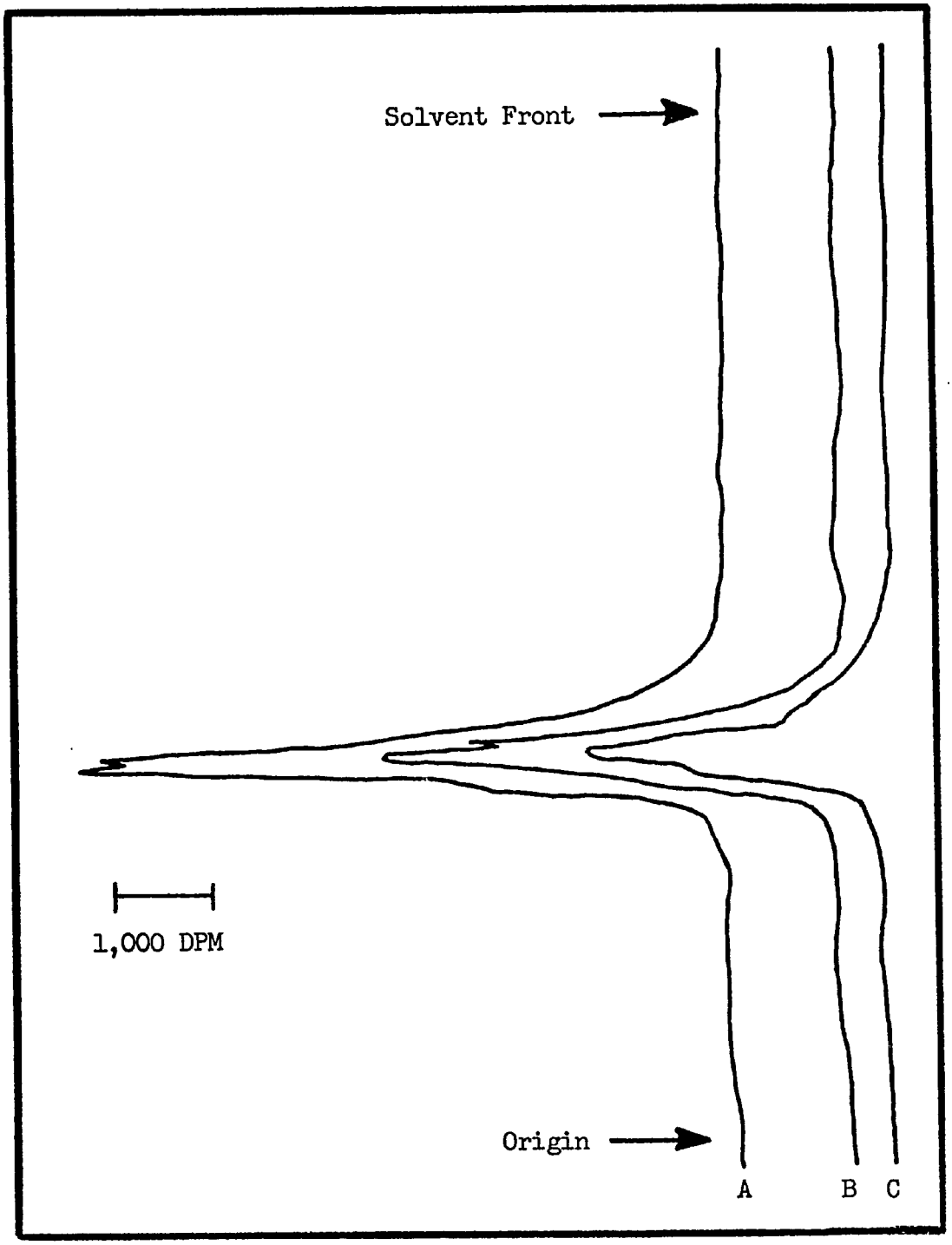


Figure 15. Radiochromatogram scanner recordings obtained for the different digitoxin - ^{3}H samples. Curve A represents the cell extracted digitoxin, curve B represents the digitoxin extracted from the suspension medium and curve C represents the radiochemically pure digitoxin provided by the commercial supplier. The background radiation was the same for all three recordings. The single, superimposed peaks demonstrate that the drug remained stable in the presence of erythrocytes and FBS.

the medium allowed for the calculation of the specific activity of the drug for each suspension system.

The data obtained for the specific activity determination of ouabain -^{3}H is shown in Table IX. The average specific activity of ouabain was found to be 10.2 Ci/mM. This value is in close agreement with that of 11.7 Ci/mM given by the comercial supplier.

Digitoxin: The calculation of the specific activity of digitoxin -^{3}H from the experimental data was carried out in the same manner as that of ouabain. The results of the specific activity determination of digitoxin are listed in Table X. The average specific activity of digitoxin -^{3}H was 15.7 Ci/mM.

Table IX. Determination of the specific activity of ouabain -^{3}H in the presence of a known concentration of nonradioactive ouabain in the suspension medium. The DPM/ml. RBC saturation value with no nonradioactive ouabain in the medium acted as a reference point.

Nonradioactive Ouabain in Medium, M	DPM*/ml. Medium	DPM*/ml. RBC	Specific Activity Ci/mM
0	793,131	347,143	
2×10^{-8}	800,377	224,806	9.88
4×10^{-8}	765,791	159,183	10.25
6×10^{-8}	808,404	128,341	10.42
		Mean Specific Activity :	10.20

* Mean value for four samples

Table X. Determination of the specific activity of digitoxin -^{3}H in the presence of a known concentration of nonradioactive digitoxin in the suspension medium. The DPM/ml. RBC saturation value with no nonradioactive digitoxin in the medium served as a reference point in the computation of the specific activity.

Nonradioactive Digitoxin in Medium, M	DPM*/ml. Medium	DPM*/ml. RBC **	Specific Activity Ci/mM
0	505,181	563,164	
1×10^{-8}	495,444	330,503	16.20
2×10^{-8}	483,051	245,059	14.25
4×10^{-8}	514,725	146,747	16.60
		Mean Specific Activity :	15.70

* Mean value for four samples

** The linear cellular drug uptake component was subtracted prior to the tabulation.

Using the respective specific activities that were determined for the ouabain -^{3}H and digitoxin -^{3}H, the radioactivity that was measured for the different transport samples was converted to the molar unit.

The mathematical solutions for all physical models previously described were programmed for the analysis of the transport data with a digital calculator[1]. The transport parameters for the different uptake and release experiments were then evaluated with the various models by adjusting the magnitude of these parameters until the best visual fit of the theory with the experimental data was obtained. In this section, the analysis of the transport data will be discussed only with the model that was found to give the best correlation between the theory and the kinetic data for the respective glycoside - erythrocyte transport system. The unsuitability and process of elimination of the other models is described in the next section.

Ouabain Uptake and Release Experiments

As will be seen, excellent agreement was found for the uptake and release data for all ouabain and fetal bovine serum concentrations with Model 4. Figures 16 and 17 show the kinetic data for the cellular ouabain uptake from media containing 0% FBS and different drug concentrations. The solid lines, representing the best theoretical fit to the data, were computed with equation (64). The magnitudes of the transport parameters determined for the different plots in these figures are listed in Table XI.

---

1. Hewlett - Packard, Loveland, Colorado 80537. Model 10.

Figure 18 shows the kinetic data that was collected for the release of the cellular ouabain into media containing 0% FBS and the theoretical curves that were obtained using Model 4. The Langmuir binding sites of the cells in both release experiments were completely saturated with ouabain during the preincubation period. The values of the transport parameters determined from the theory and the experimental data for these release experiments are given in Table XII. The mean value for the adsorption rate constant, determined from the uptake experiments, was $k_f = 5.75 \times 10^{-9}$ cm./sec. and the mean value for the desorption rate constant, evaluated from the release experiments was $k_r = 3.37 \times 10^{-21}$ moles/cm.^{2} sec.. The value of the dissociation constant for the ouabain - erythrocyte complex, computed from the ratio of the desorption rate constant to the adsorption rate constant, was 5.8×10^{-13} moles/ml.RBC. The maximum number of molecular ouabain binding sites per cell was evaluated using the mean value of Q and found to be 753 ± 96. Figure 19 gives the equilibrium data that was obtained from the transport experiments with media containing 0% FBS. This plot clearly demonstrates the nonlinear binding and saturation characteristic of the ouabain - erythrocyte interaction. The theoretical plot in Figure 19 was computed with equation (67) using the average values that were determined for k_f, k_r and Q.

Tables XI and XII show that in the theoretical analysis of the experimental uptake studies, the mean value for the desorption rate constant was held constant and taken to be that determined from release experiments; whereas in the analysis of the release data, the mean adsorption rate constant, determined from the uptake experiments, was utilized and held constant. The reason for doing this was that

the theory of Model 4 for drug uptake is quite sensitive to changes in the magnitudes of k_f and Q but rather insensitive to k_r. For release experiments, on the other hand, the theory is quite sensitive to the variations in the magnitudes of k_r and Q but quite insensitive to k_f. This particular aspect of Model 4 (and, as will be seen, Model 6) will be discussed in more detail in the next chapter.

Figures 20 and 21 show Model 4 plots of the kinetic data for the cellular ouabain uptake from media containing different concentrations of the drug and 5% FBS. The values of the transport parameters determined for these plots with equation (64) and the experimental data are listed in Table XIII. Release data and Model 4 plots for three release experiments are given in Figures 22 and 23. All three release experiments were carried out in media containing 5% FBS and with cells that were completely saturated with ouabain at the beginning of the release experiments. The theoretically evaluated transport parameters and experimental data for these figures are listed in Table XIV. The mean rate constants for these transport systems containing 5% FBS in the media were $k_f = 3.26 \times 10^{-9}$ cm./sec. and $k_r = 2.99 \times 10^{-21}$ moles/cm.^{2} sec.. The dissociation constant for the ouabain - erythrocyte complex in the presence of 5% FBS was calculated to be 9.2×10^{-13} moles/ml.RBC and the maximum number of molecular ouabain binding sites per cell, computed from the mean value of Q, was 783 ± 78. Figure 24 shows the equilibrium data of the cell - associated ouabain as a function of the ouabain concentration in the medium containing 5% FBS and the theoretical Langmuir isotherm computed with the mean values of k_f, k_r and Q.

Figures 25 and 26 show data of the cellular ouabain uptake from media containing different concentrations of ouabain and 15% FBS as

well as the best fitting theoretical plots for the uptake data. The transport parameters determined from the data in these figures and the experimental data are given in Table XV. Model 4 plots for ouabain release data are shown in Figure 27. The media contained 15% FBS. The release experiments shown in this figure were carried out with cells that were completely saturated with ouabain as well as cells which were only partially saturated with the drug. The analysis of the data in this figure clearly demonstrates that Model 4 is well capable of explaining the kinetic data, irrespective of the level of cellular saturation at the beginning of the release experiment. The transport data for this figure are listed in Table XVI. The data of two more release experiments in 15% FBS medium are shown in Figure 28. These experiments were carried out in the presence of 1×10^{-5} M and 1×10^{-3} M nonradioactive ouabain in the suspension medium. The analysis of the data in this figure with Model 4 yielded transport parameters which were similar to those determined for the systems containing 15% FBS in the medium but no nonradioactive ouabain. The transport parameters for the data in Figure 28 are listed in Table XVI. The purpose and significance of the release experiments in the presence of the nonradioactive ouabain in the suspension medium will be discussed in the next chapter.

The mean rate constants for the ouabain transport in the presence of 15% FBS in the suspension medium were $k_f = 1.32 \times 10^{-9}$ cm./sec. and $k_r = 2.40 \times 10^{-21}$ moles/cm.^{2} sec.. The dissociation constant for the ouabain - erythrocyte complex was computed to be 1.82×10^{-12} moles/ml.RBC. By using the average value for Q obtained from the uptake and the release data, the maximum number of molecular ouabain binding sites

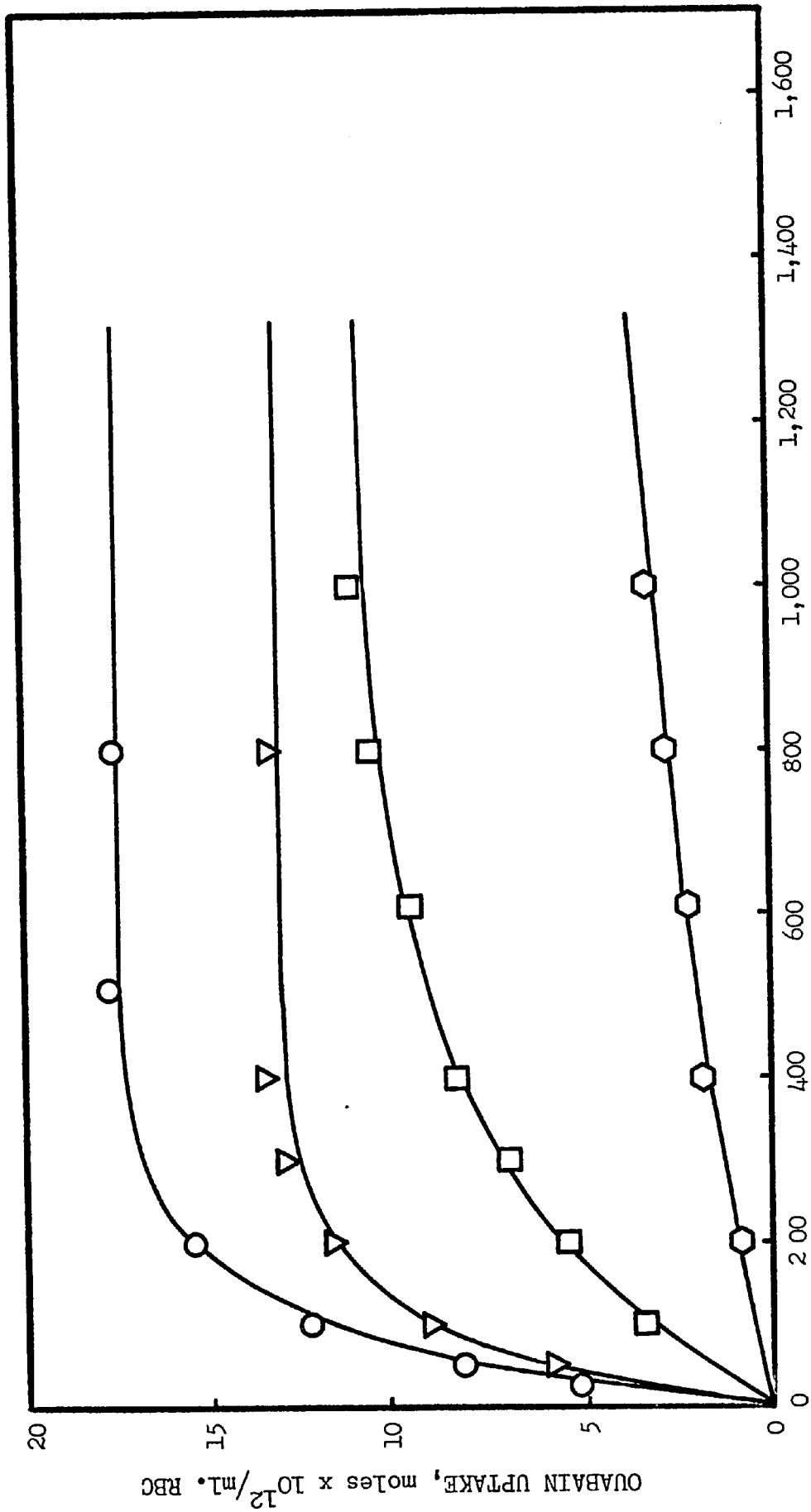


Figure 16. Model 4 plots of the cellular ouabain uptake from media containing different concentrations of ouabain and no FBS. The temperature was 30 °C. The theoretical transport parameters k_f, k_r and Q, determined with equation (64), and the experimental data for this figure are listed in Table XI.

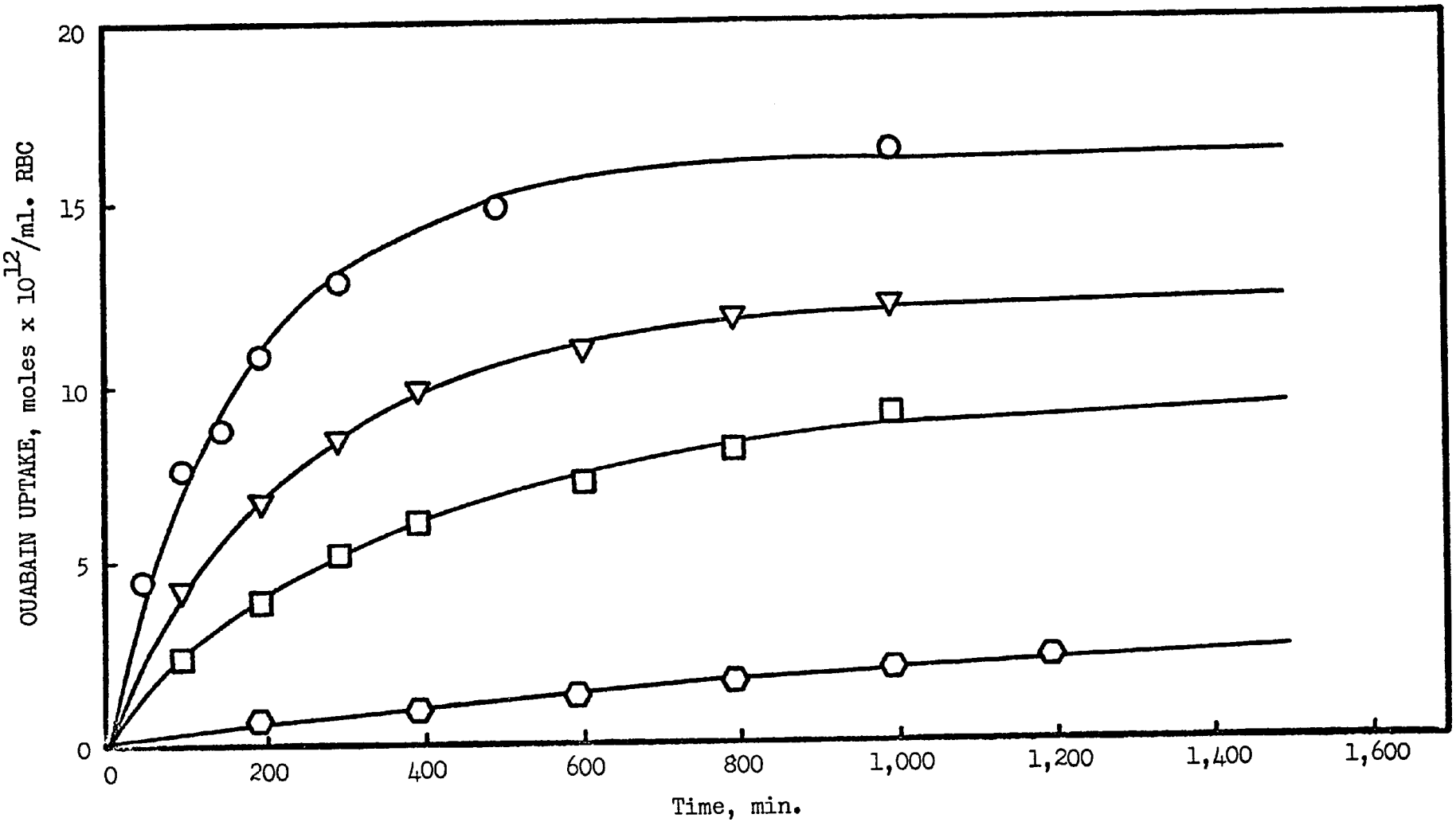


Figure 17. Model 4 plots of the cellular ouabain uptake from media containing different concentrations of ouabain and no FBS. The temperature was 30 °C. The theoretical transport parameters k_f, k_r and Q, determined with equation (64), and the experimental data for this figure are listed in Table XI.

Table XI. Summary of transport parameters evaluated with Model 4, equation (64), and the experimental data for the ouabain uptake experiments. The suspension media were phosphate buffered saline with 0% FBS. The temperature was 30 °C.

Figure	Symbol	T ($\frac{\text{moles/ml.}}{\text{suspension}}$)	H ($\frac{\text{ml.RBC/ml.}}{\text{suspension}}$)	Q (moles/RBC)	k_f (cm./sec.)	k_r (moles/cm.^{2} sec.)
16	○	3.00×10^{-11}	0.054	1.55×10^{-21}	5.80×10^{-9}	3.37×10^{-21}
16	▽	2.20×10^{-11}	0.051	1.16×10^{-21}	5.90×10^{-9}	3.37×10^{-21}
16	□	5.95×10^{-12}	0.059	1.07×10^{-21}	5.80×10^{-9}	3.37×10^{-21}
16	⬡	7.73×10^{-13}	0.055	1.20×10^{-21}	5.50×10^{-9}	3.37×10^{-21}
17	○	1.37×10^{-11}	0.050	1.48×10^{-21}	5.90×10^{-9}	3.37×10^{-21}
17	▽	7.83×10^{-12}	0.056	1.16×10^{-21}	5.60×10^{-9}	3.37×10^{-21}
17	□	3.84×10^{-12}	0.056	1.07×10^{-21}	5.80×10^{-9}	3.37×10^{-21}
17	⬡	4.40×10^{-13}	0.054	1.25×10^{-21}	5.70×10^{-9}	3.37×10^{-21}
Mean:				1.24×10^{-21}	5.75×10^{-9}	3.37×10^{-21}

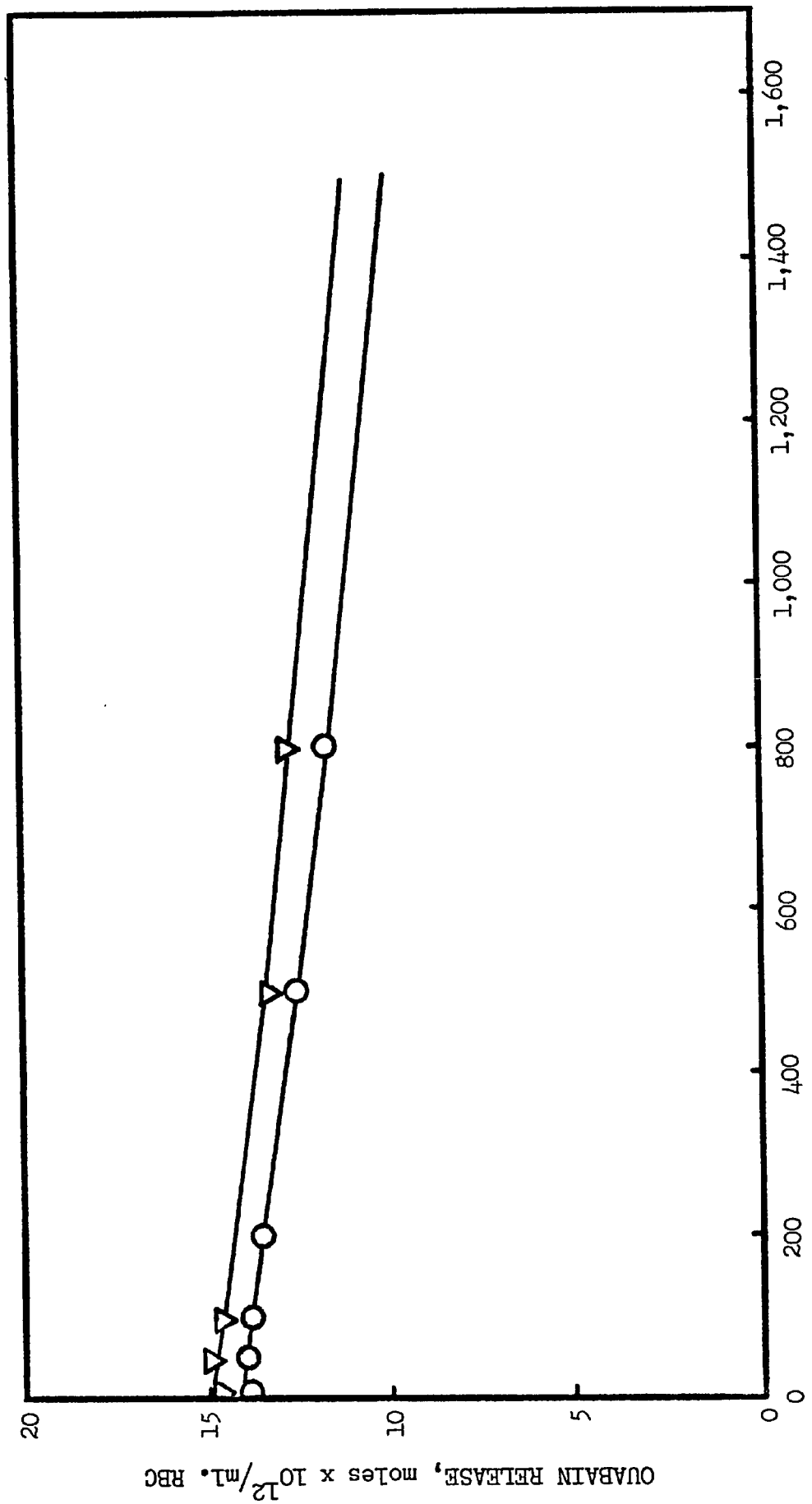


Figure 18. Model 4 plots of the ouabain release data. The media contained no FBS and the temperature was 30 °C. The cells were preincubated in phosphate buffered saline containing ouabain $-^3H$ for 10 hrs. The theoretical transport parameters k_f, k_r and Q, evaluated with equation (64), and the experimental data for this figure are listed in Table XII.

Table XII. Summary of transport parameters evaluated with Model 4, equation (64), and experimental data for the ouabain release experiments. The suspension media were phosphate buffered saline with 0% FBS. The temperature was 30 °C.

Figure	Symbol	T ($\frac{\text{moles/ml.}}{\text{suspension}}$)	H ($\frac{\text{ml.RBC/ml.}}{\text{suspension}}$)	Q (moles/RBC)	k_f (cm./sec.)	k_r (moles/cm.^{2} sec.)
18	▽	1.27×10^{-12}	0.051	1.30×10^{-21}	5.75×10^{-9}	3.48×10^{-21}
18	O	9.33×10^{-13}	0.062	1.24×10^{-21}	5.75×10^{-9}	3.26×10^{-21}
Mean:				1.27×10^{-21}	5.75×10^{-9}	3.37×10^{-21}

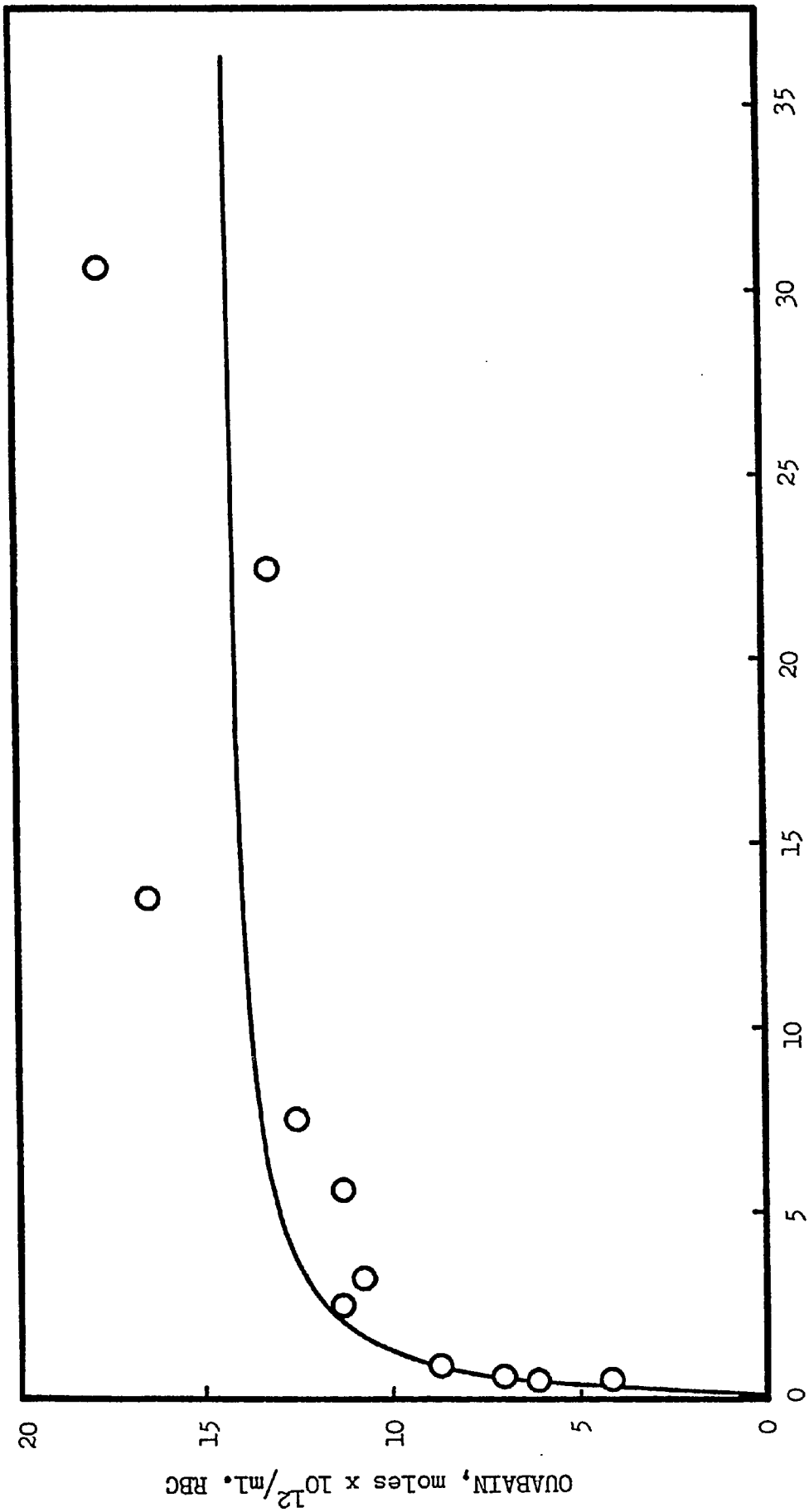


Figure 19. Equilibrium data of the cell - associated ouabain as a function of the ouabain concentration in the medium containing no FBS. The temperature was 30 °C. The theoretical curve was computed with equation (67) using the following average Langmuir parameters determined from uptake and release experiments:

$k_f = 5.75 \times 10^{-9}$ cm./sec., $k_r = 3.37 \times 10^{-21}$ moles/cm.^{2} sec. and $Q = 1.25 \times 10^{-21}$ moles/RBC.

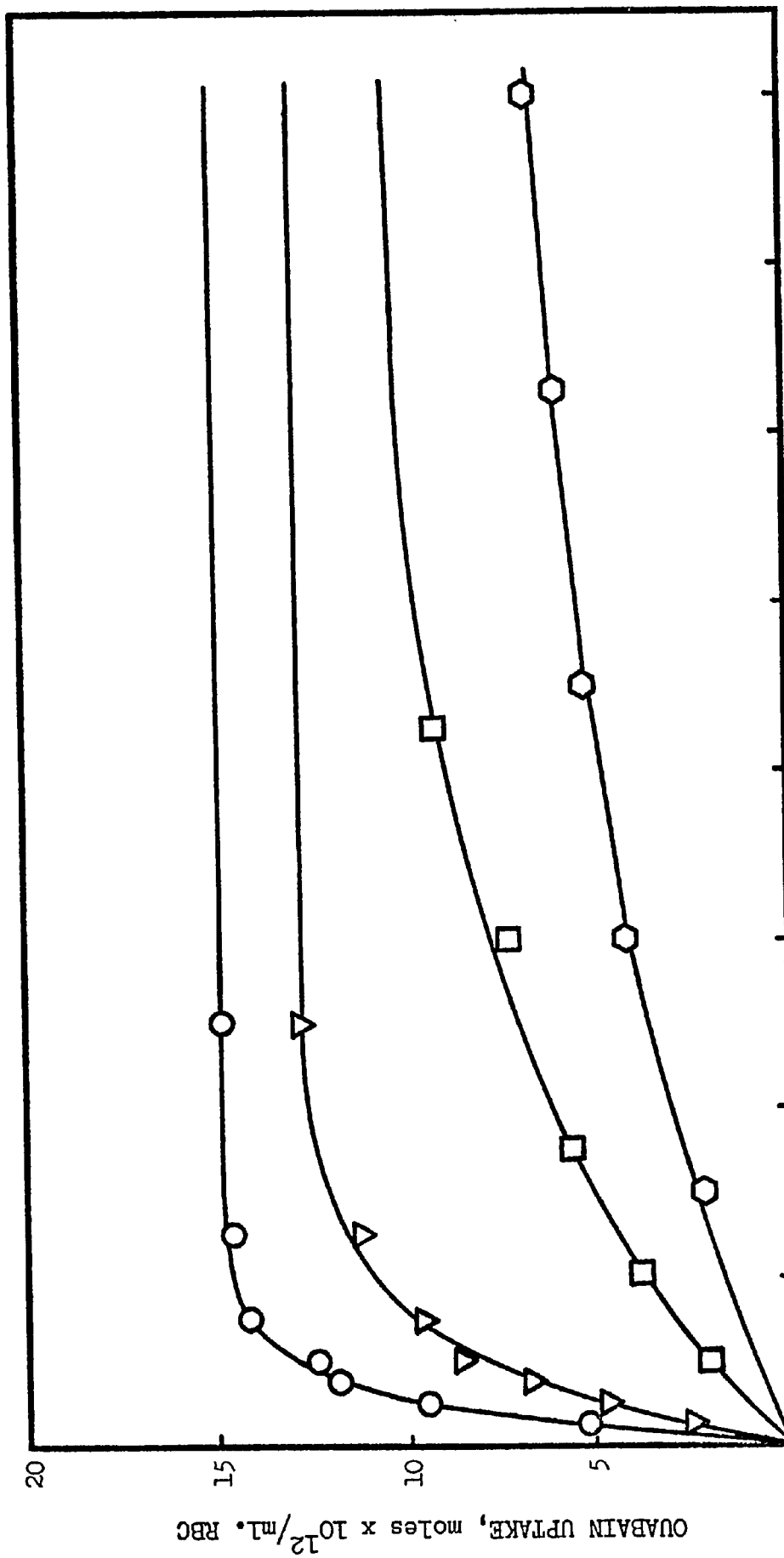


Figure 20. Model 4 plots of the cellular ouabain uptake from media containing different concentrations of ouabain and 5% FBS. The temperature was 30 °C. The theoretical transport parameters k_f, k_r and Q, determined with equation (64), and the experimental data for this figure are listed in Table XIII.

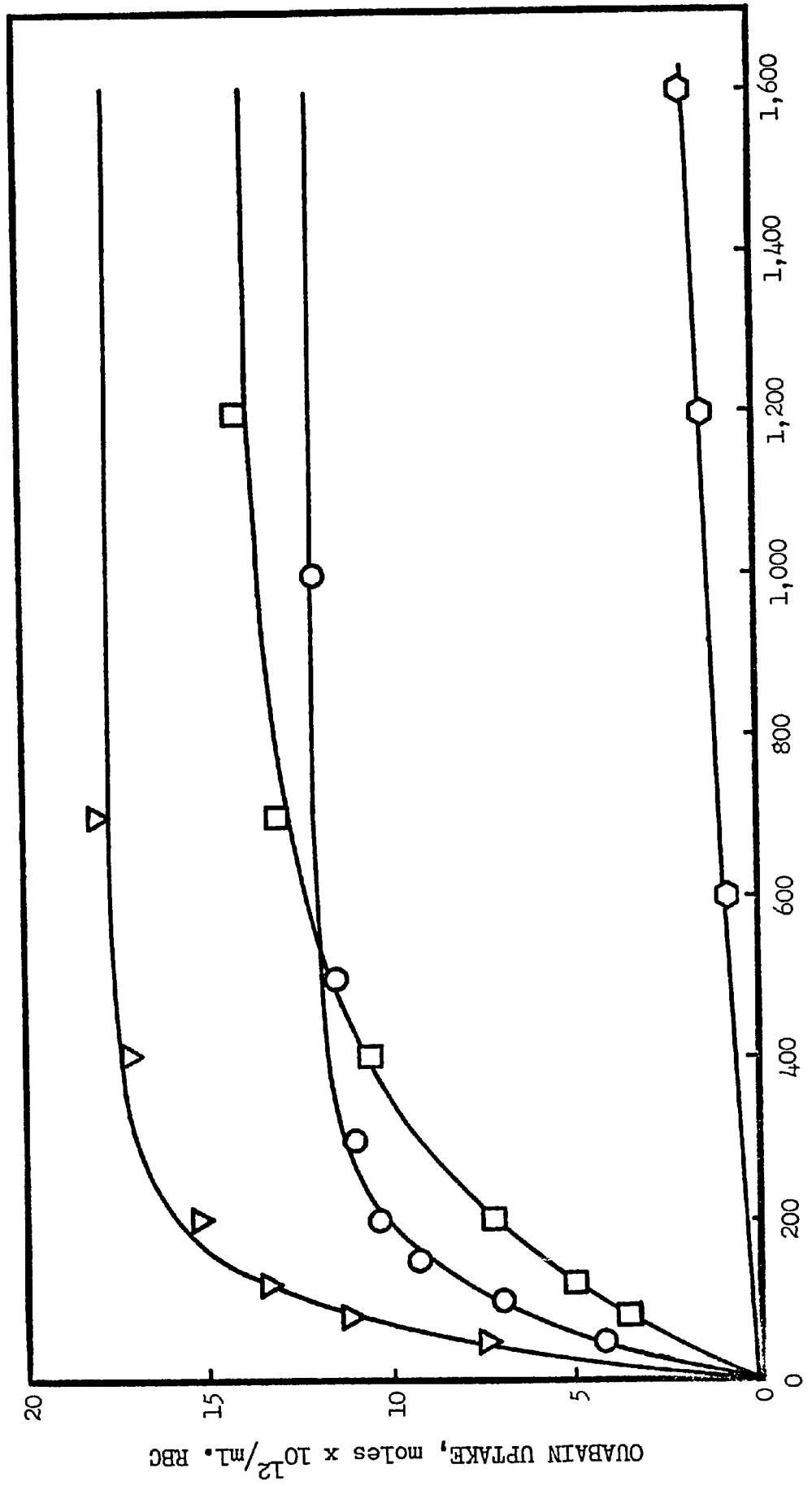


Figure 21. Model 4 plots of the cellular ouabain uptake from media containing different concentrations of ouabain and 5% FBS. The temperature was 30 °C. The theoretical transport parameters k_f, k_r and Q, determined with equation (64), and the experimental data for this figure are listed in Table XIII.

Table XIII. Summary of transport parameters evaluated with Model 4, equation (64), and experimental data for ouabain uptake experiments. The media contained 5% FBS. The temperature was 30°C.

Figure	Symbol	T ($\frac{\text{moles/ml.}}{\text{suspension}}$)	H ($\frac{\text{ml.RBC/ml.}}{\text{suspension}}$)	Q (moles/RBC)	k_f (cm./sec.)	k_r (moles/cm^2 sec.)
20	○	4.05×10^{-11}	0.054	1.32×10^{-21}	3.20×10^{-9}	2.99×10^{-21}
20	▽	1.75×10^{-11}	0.057	1.18×10^{-21}	3.10×10^{-9}	2.99×10^{-21}
20	□	3.18×10^{-12}	0.056	1.34×10^{-21}	3.20×10^{-9}	2.99×10^{-21}
20	⬡	1.28×10^{-12}	0.056	1.40×10^{-21}	3.30×10^{-9}	2.99×10^{-21}
21	▽	5.71×10^{-11}	0.056	1.55×10^{-21}	3.20×10^{-9}	2.99×10^{-21}
21	○	2.92×10^{-11}	0.052	1.07×10^{-21}	3.40×10^{-9}	2.99×10^{-21}
21	□	1.24×10^{-11}	0.052	1.28×10^{-21}	3.70×10^{-9}	2.99×10^{-21}
21	⬡	4.43×10^{-13}	0.054	1.41×10^{-21}	3.00×10^{-9}	2.99×10^{-21}
Mean:				1.32×10^{-21}	3.26×10^{-9}	2.99×10^{-21}

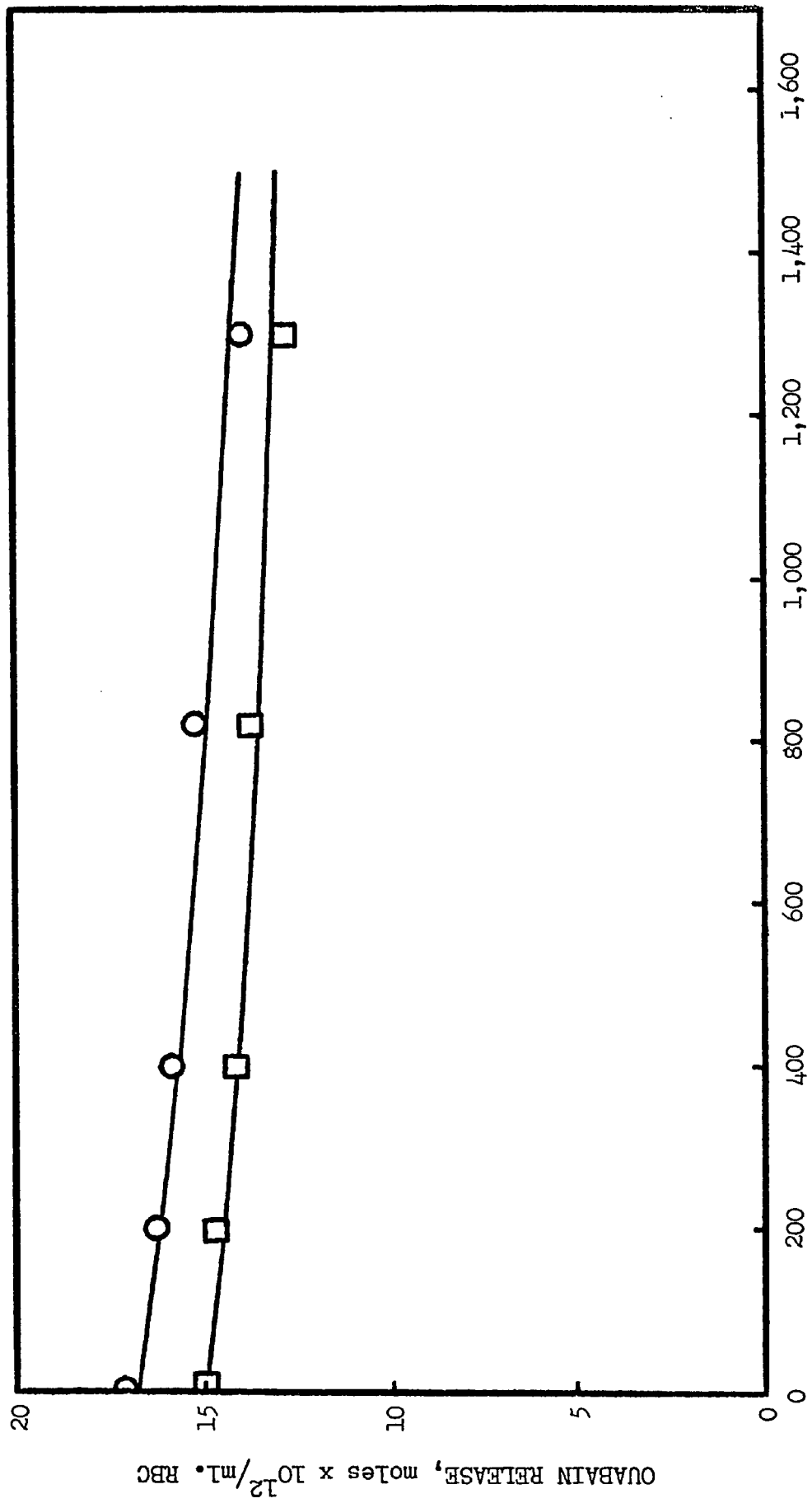


Figure 22. Model 4 plots of the ouabain release data. The media contained 5% FBS and the temperature was 30 °C. The cells were preincubated in media containing 5% FBS and ouabain -^{3}H for 10 hrs. The theoretical transport parameters k_f, k_r and Q, evaluated with equation (64), and the experimental data for this figure are listed in Table XIV.

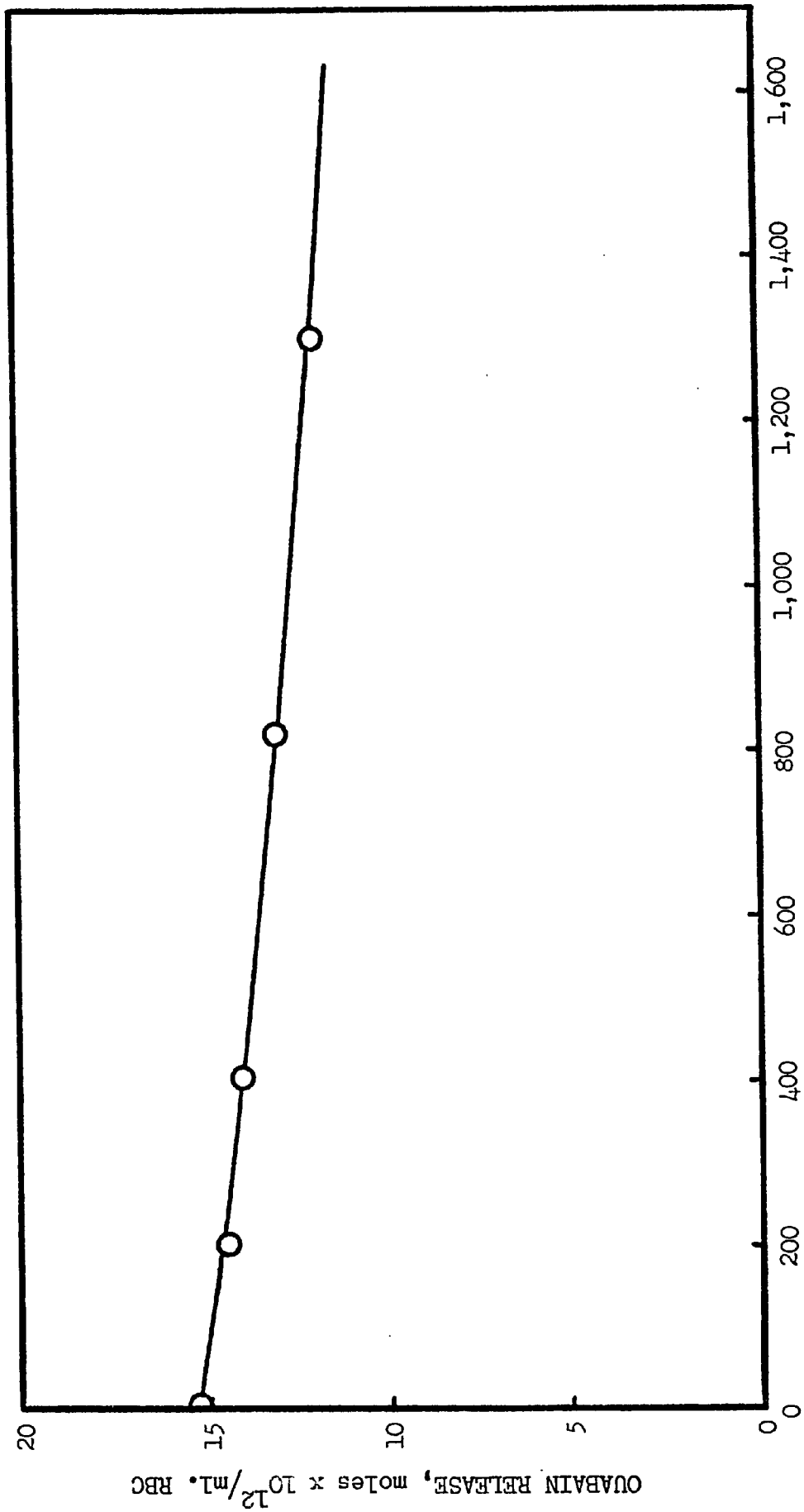


Figure 23. A Model 4 plot of the ouabain release data. The medium contained 5% FBS and the temperature was 30 °C. The cells were preincubated in the medium containing 5% FBS and ouabain -^{3}H for 10 hrs. The theoretical transport parameters k_f, k_r and Q, evaluated with equation (64), and the experimental data for this figure are listed in Table XIV.

Table XIV. Summary of transport parameters evaluated with Model 4, equation (64), and the experimental data for ouabain release experiments. The suspension media contained 5% FBS. The temperature was 30 °C.

Figure	Symbol	T ($\frac{\text{moles/ml.}}{\text{suspension}}$)	H ($\frac{\text{ml.RBC/ml.}}{\text{suspension}}$)	Q (moles/RBC)	k_f (cm./sec.)	k_r (moles/cm.^{2} sec.)
22	○	3.46×10^{-12}	0.055	1.45×10^{-21}	3.26×10^{-9}	2.90×10^{-21}
22	□	5.44×10^{-12}	0.056	1.30×10^{-21}	3.26×10^{-9}	2.90×10^{-21}
23	○	2.09×10^{-12}	0.055	1.32×10^{-21}	3.26×10^{-9}	3.17×10^{-21}
Mean:				1.36×10^{-21}	3.26×10^{-9}	2.99×10^{-21}

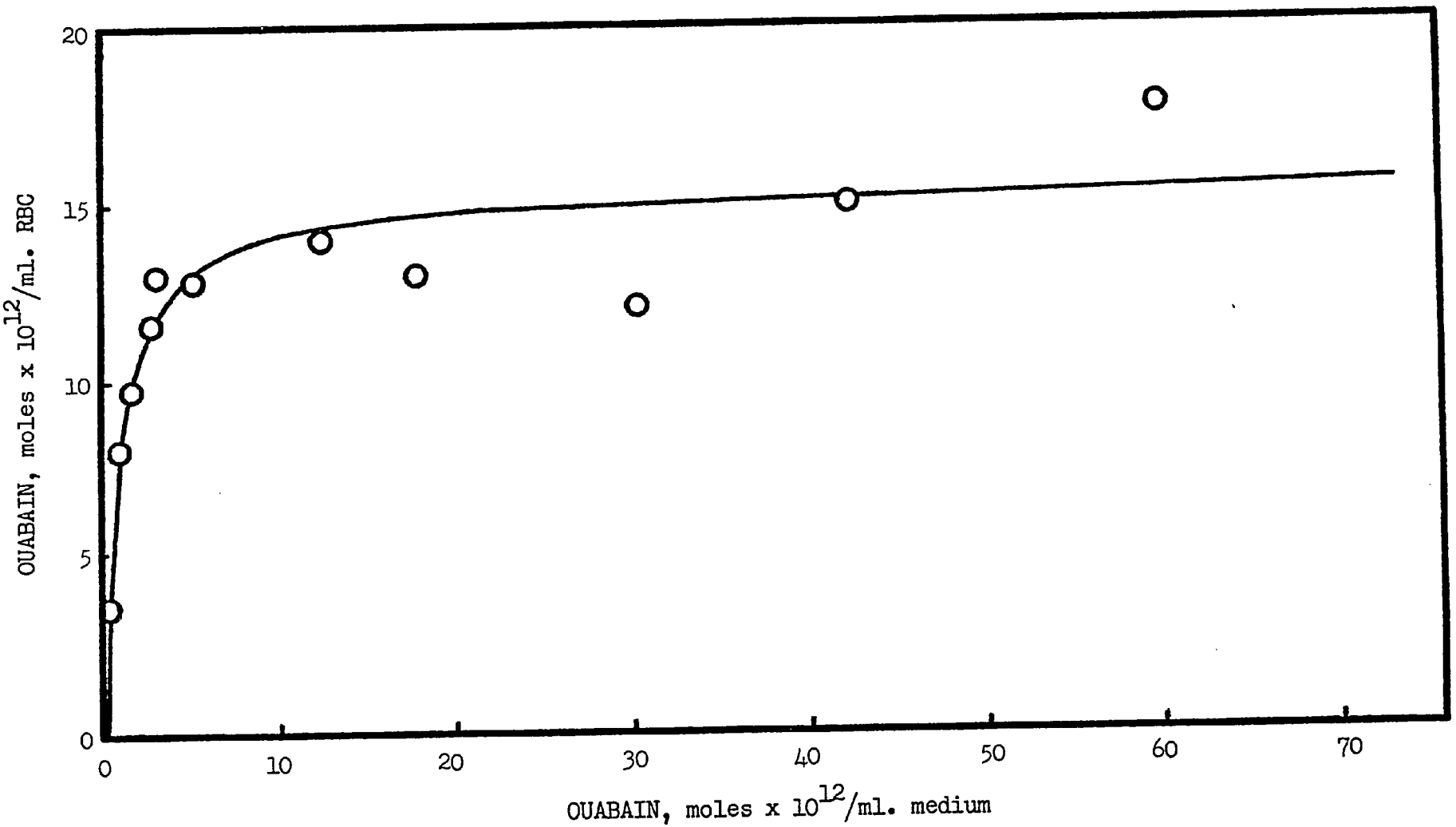


Figure 24. Equilibrium data of the cell - associated ouabain as a function of the ouabain concentration in the medium containing 5% FBS. The temperature was 30 °C. The theoretical curve was computed with equation (67) using the following average Langmuir parameters determined from uptake and release experiments: $k_f = 3.26 \times 10^{-9}$ cm./sec., $k_r = 2.99 \times 10^{-21}$ moles/cm.^{2} sec. and $Q = 1.30 \times 10^{-21}$ moles/RBC.

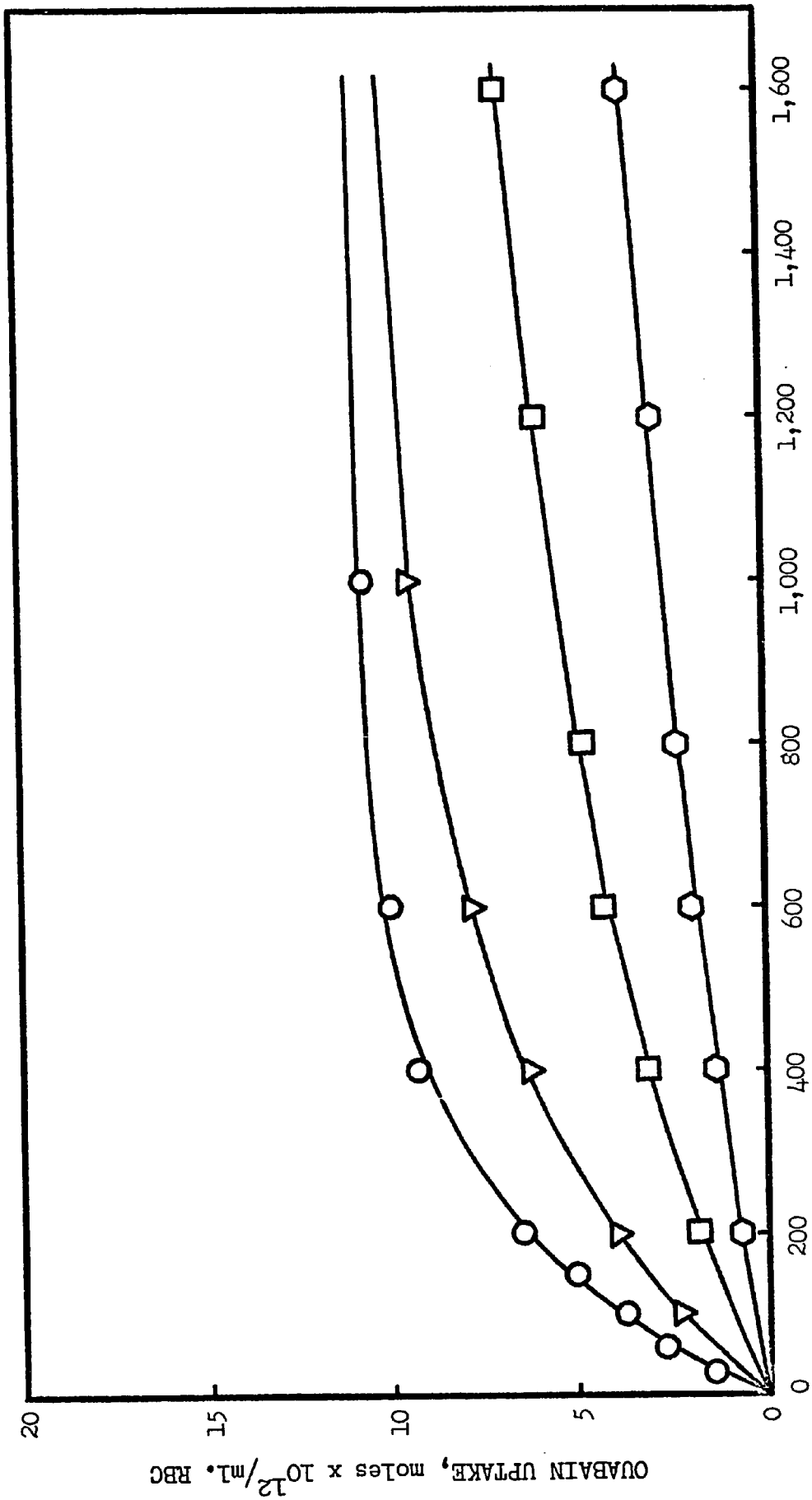


Figure 25. Model 4 plots of the cellular ouabain uptake from media containing 15% FBS and different concentrations of ouabain -^{3}H. The temperature was 30 °C. The theoretical transport parameters k_f, k_r and Q, determined with equation (64), and the experimental data for this figure are listed in Table XV.

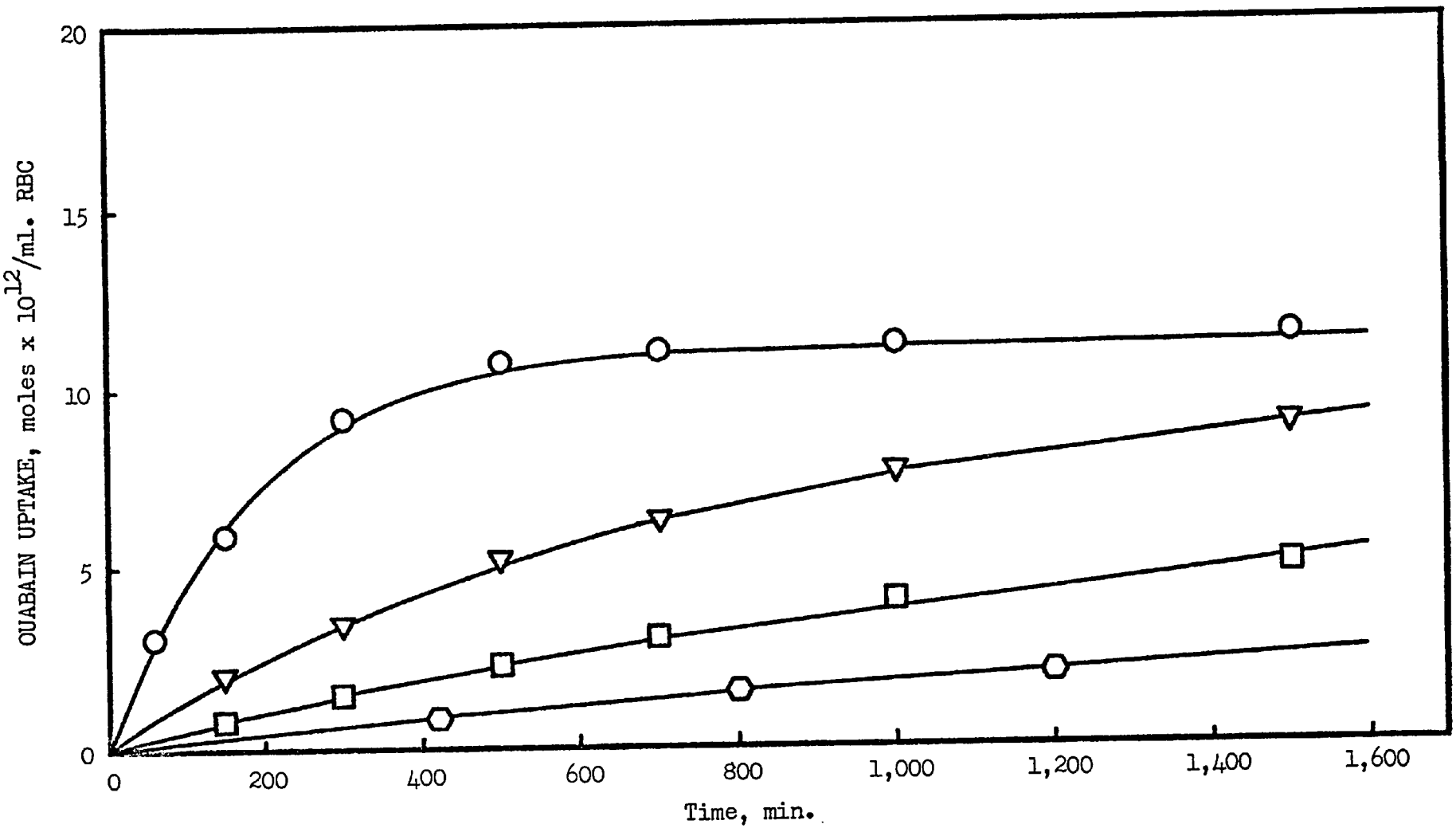


Figure 26. Model 4 plots of the cellular ouabain uptake from media containing 15% FBS and different concentrations of ouabain -^{3}H. The temperature was 30 °C. The theoretical transport parameters k_f, k_r and Q, determined with equation (64), and the experimental data for this figure are listed in Table XV.

Table XV. Summary of transport parameters evaluated with Model 4, equation (64), and the experimental data for ouabain uptake experiments. The media contained 15% FBS and the temperature was 30 °C.

Figure	Symbol	T ($\frac{\text{moles/ml.}}{\text{suspension}}$)	H ($\frac{\text{ml.RBC/ml.}}{\text{suspension}}$)	Q (moles/RBC)	k_f (cm./sec.)	k_r (moles/cm.^{2} sec.)
25	○	3.12×10^{-11}	0.054	10.00×10^{-22}	1.35×10^{-9}	2.40×10^{-21}
25	▽	1.72×10^{-11}	0.055	9.90×10^{-22}	1.30×10^{-9}	2.40×10^{-21}
25	□	6.77×10^{-12}	0.054	8.92×10^{-22}	1.30×10^{-9}	2.40×10^{-21}
25	⬡	2.42×10^{-12}	0.057	9.37×10^{-22}	1.30×10^{-9}	2.40×10^{-21}
26	○	3.85×10^{-11}	0.055	10.10×10^{-22}	1.40×10^{-9}	2.40×10^{-21}
26	▽	9.50×10^{-12}	0.054	10.70×10^{-22}	1.30×10^{-9}	2.40×10^{-21}
26	□	3.70×10^{-12}	0.053	10.26×10^{-22}	1.30×10^{-9}	2.40×10^{-21}
26	⬡	1.70×10^{-12}	0.053	9.37×10^{-22}	1.20×10^{-9}	2.40×10^{-21}
		5.68×10^{-13}	0.054	9.81×10^{-22}	1.45×10^{-9}	2.40×10^{-21}
Mean:				9.83×10^{-22}	1.32×10^{-9}	2.40×10^{-21}

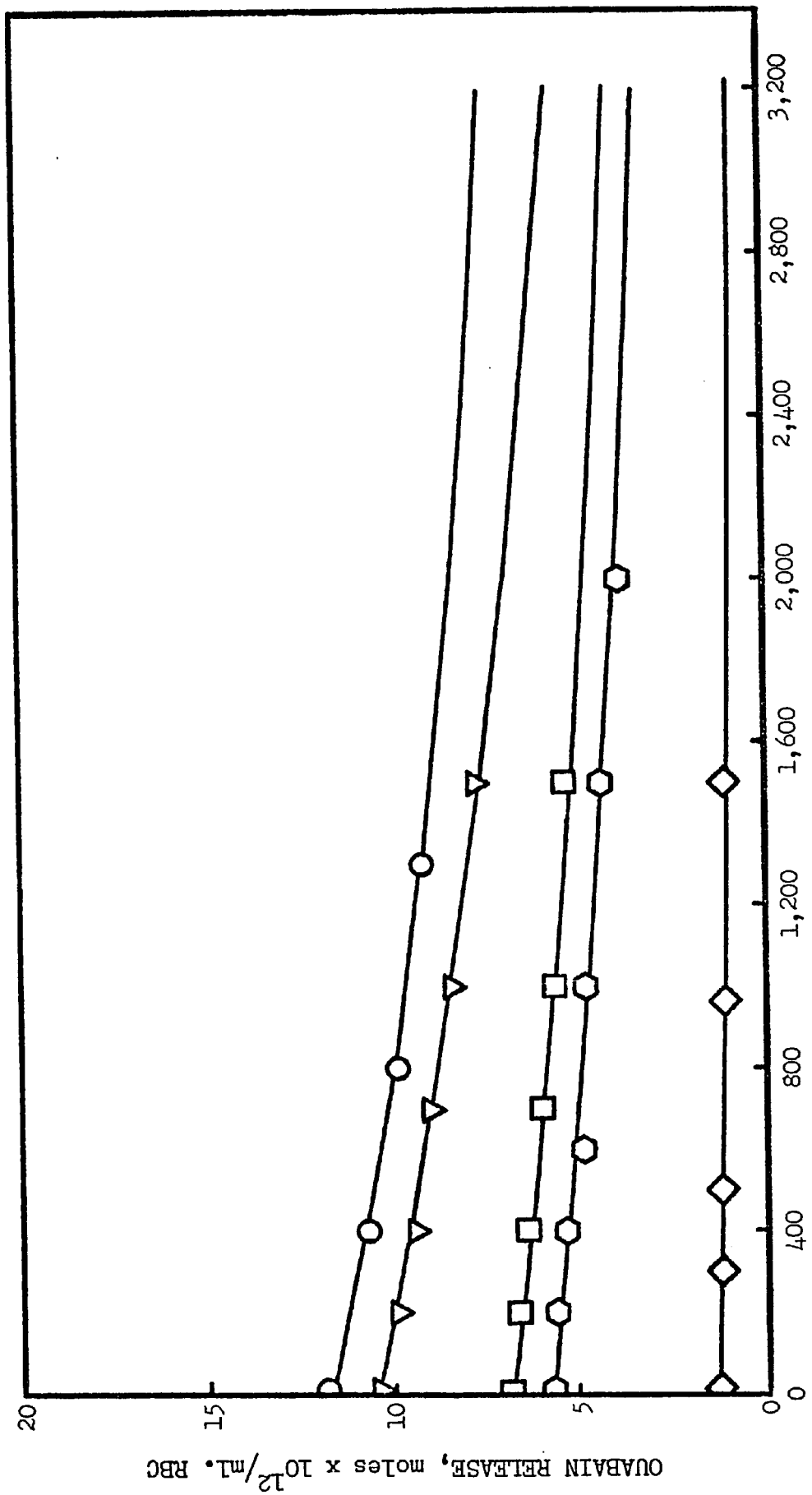


Figure 27. Model 4 plots of the ouabain release data. The media contained 15% FBS. The temperature was 30 °C. The cells were preincubated in media containing 15% FBS and ouabain — ^3H from 1 to 10 hrs. The theoretical transport parameters k_f, k_r and Q, evaluated with equation (64), and the experimental data for this figure are listed in Table XVI.

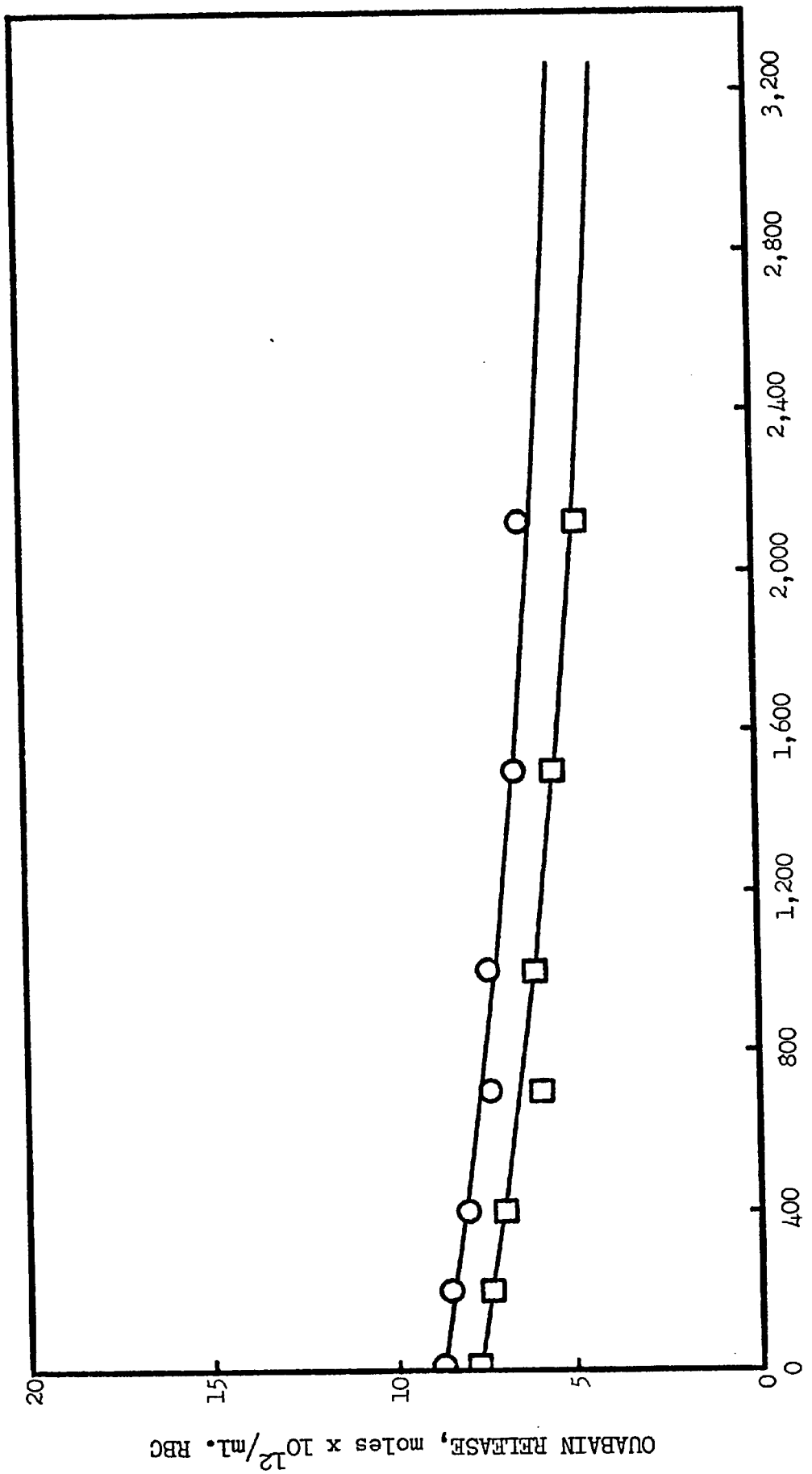


Figure 28. Model 4 plots of the ouabain release data. The media contained 15% FBS. The temperature was 30 °C. The cells were preincubated in media containing 15% FBS and ouabain - ^{3}H for 8 hrs. The theoretical transport parameters k_f, k_r and Q, evaluated with equation (64), and the experimental data for this figure are listed in Table XVI.

Table XVI. Summary of transport parameters evaluated with Model 4, equation (64), and the experimental data for ouabain release experiments. The suspension media contained 15% FBS and the temperature was 30 °C.

Figure	Symbol	T ($\frac{\text{moles/ml.}}{\text{suspension}}$)	H ($\frac{\text{ml.RBC/ml.}}{\text{suspension}}$)	Q (moles/RBC)	k_f (cm./sec.)	k_r (moles/cm.^{2} sec.)
27	○	1.93×10^{-12}	0.055	10.10×10^{-22}	1.32×10^{-9}	2.23×10^{-21}
27	▽	4.50×10^{-12}	0.052	9.68×10^{-22}	1.32×10^{-9}	2.05×10^{-21}
27	□	1.06×10^{-12}	0.055	9.68×10^{-22}	1.32×10^{-9}	2.45×10^{-21}
27	⬡	6.81×10^{-13}	0.054	9.72×10^{-22}	1.32×10^{-9}	2.32×10^{-21}
27	◇	1.81×10^{-21}	0.052	9.72×10^{-22}	1.32×10^{-9}	2.68×10^{-21}
28	○	1.12×10^{-12}	0.055	9.72×10^{-22}	1.32×10^{-9}	2.36×10^{-21}
28	□	1.14×10^{-12}	0.054	9.72×10^{-22}	1.32×10^{-9}	3.21×10^{-21}
Mean:				9.76×10^{-22}	1.32×10^{-9}	2.40×10^{-21}

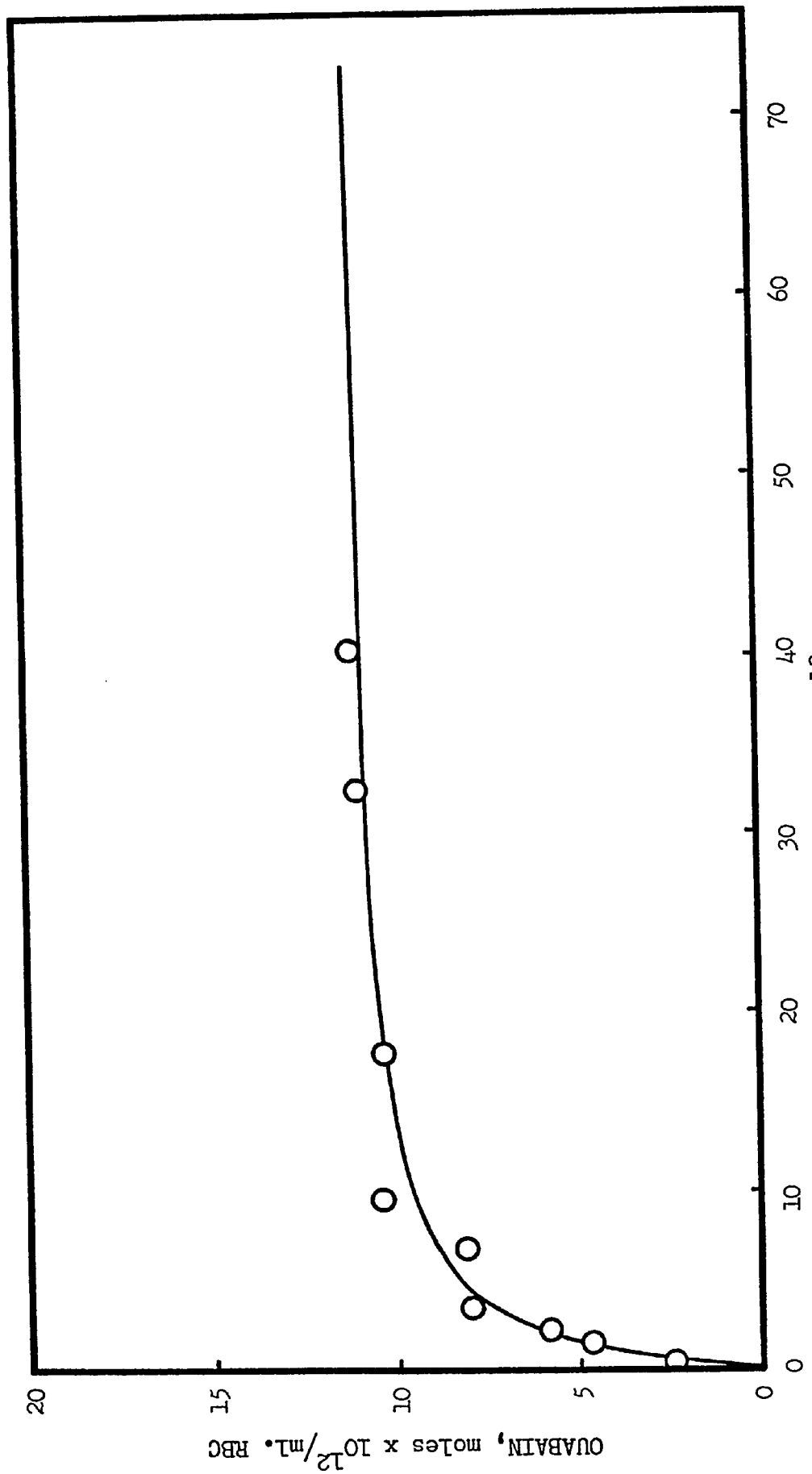


Figure 29. Equilibrium data of the cell – associated ouabain as a function of the ouabain concentration in the medium containing 15% FBS. The temperature was 30 °C. The theoretical curve was computed with equation (67) using the following average Langmuir parameters determined from uptake and release experiments:

$k_f = 1.32 \times 10^{-9}$ cm./sec., $k_r = 2.40 \times 10^{-21}$ moles/cm.^{2} sec. and $Q = 9.80 \times 10^{-21}$ moles/RBC.

per cell in the presence of 15% FBS in the media was calculated as 590 ± 23.

Figure 29 shows the equilibrium data of the cell - associated ouabain as a function of the ouabain concentration in the medium containing 15% FBS. The theoretical Langmuir isotherm was computed using the average values of k_f, k_r and Q, that were determined from the uptake and release experiments.

Summary of Ouabain Transport

The close association observed between the theoretical plots and the experimental data presented for the uptake and release of ouabain in suspension media containing different drug and fetal bovine serum concentrations very satisfactorily demonstrates the suitability of Model 4. The mean values of the transport parameters that were evaluated for the systems containing 0, 5 and 15% FBS are summarized in Table XVII.

The experimental data shown in the different Langmuir isotherm plots indicate that, in the absence of fetal bovine serum in the suspension medium, there is some scatter, whereas with increasing FBS levels in the media the experimental precision is much improved. Thus, it appears that the presence of fetal bovine serum in the suspension media acts upon the erythrocytes in a stabilizing manner.

The theoretical plots for all the ouabain uptake and release data in the presence of different FBS concentrations were obtained by adjusting the rate parameters k_f and k_r as well as the cellular saturation value, Q, for each particular experiment until the best fit between the theory and the experimental data was obtained. It should be noted, however, that because of the rather small deviations

Table XVII. Summary of the mean values of the transport parameters and standard deviations evaluated from the ouabain uptake and release experiments at 30 °C for the systems containing 0, 5 and 15% FBS using Model 4.

% FBS	Q (moles/RBC)	S.D.* (moles/RBC)	k_f (cm./sec.)	S.D.* (cm./sec.)	k_r (moles/cm.^{2} sec.)	S.D.* (moles/cm.^{2} sec.)
0	1.25×10^{-21}	0.16×10^{-21}	5.75×10^{-9}	0.14×10^{-9}	3.37×10^{-21}	0.16×10^{-21}
5	1.30×10^{-21}	0.13×10^{-21}	3.26×10^{-9}	0.21×10^{-9}	2.99×10^{-21}	0.16×10^{-21}
15	9.80×10^{-22}	0.39×10^{-22}	1.32×10^{-9}	0.07×10^{-9}	2.40×10^{-21}	0.23×10^{-21}

* Standard deviation for the data listed in Tables XI through XVI.

per cell in the presence of 15% FBS in the media was calculated as 590 ± 23.

Figure 29 shows the equilibrium data of the cell - associated ouabain as a function of the ouabain concentration in the medium containing 15% FBS. The theoretical Langmuir isotherm was computed using the average values of k_f, k_r and Q, that were determined from the uptake and release experiments.

Summary of Ouabain Transport

The close association observed between the theoretical plots and the experimental data presented for the uptake and release of ouabain in suspension media containing different drug and fetal bovine serum concentrations very satisfactorily demonstrates the suitability of Model 4. The mean values of the transport parameters that were evaluated for the systems containing 0, 5 and 15% FBS are summarized in Table XVII.

The experimental data shown in the different Langmuir isotherm plots indicate that, in the absence of fetal bovine serum in the suspension medium, there is some scatter, whereas with increasing FBS levels in the media the experimental precision is much improved. Thus, it appears that the presence of fetal bovine serum in the suspension media acts upon the erythrocytes in a stabilizing manner.

The theoretical plots for all the ouabain uptake and release data in the presence of different FBS concentrations were obtained by adjusting the rate parameters k_f and k_r as well as the cellular saturation value, Q, for each particular experiment until the best fit between the theory and the experimental data was obtained. It should be noted, however, that because of the rather small deviations

that were observed between the individual values of k_f and k_r for any particular FBS concentration, reasonably good theoretical fits for all the ouabain transport data could also be obtained by using the average values of the rate constants for the respective FBS levels and the experimentally determined values of Q.

A statistically significant decrease in the magnitudes of both the adsorption rate constant and desorption rate constant with increasing FBS concentrations in the media was observed. This decrease in affinity of the erythrocytes for ouabain with increasing FBS levels may be attributed to electrolytes that are present in the fetal bovine serum. Gardner and Conlon (53) reported that the rate of ouabain uptake by erythrocytes was reduced when some of the sodium in the suspension medium was replaced by potassium or choline. It could be postulated that the reduced affinity of erythrocytes for ouabain is the result of a competitive binding effect. The erythrocyte - glycoside binding sites may also have an affinity for certain cations and possibly anions that are present in the fetal bovine serum. When sodium ions occupy the receptor site, they may be replaced by ouabain at a certain rate, whereas if some other ions such as potassium occupy the sites, the rate of displacement is slower because of stronger interaction of the ions with the receptor sites resulting in a decreased value for the adsorption rate constant in the presence of different fetal bovine serum concentrations in the media. A stronger argument, that the change in affinity is attributed to electrolyte effects, will be presented in the summary of the digitoxin transport data. Congruent with the decrease in the rate constants, the dissociation constant for the ouabain - erythrocyte complex in-

creased with higher FBS levels in the suspension media.

The number of molecular ouabain binding sites per cell in the absence of FBS in the media is approximately 750 and appears to decrease with increasing levels of FBS in the media. The small decrease in binding sites with the higher FBS concentrations suggests that a small fraction of the ions in the fetal bovine serum responsible for the decrease in the ouabain - erythrocyte affinity may be irreversibly bound to the erythrocyte receptor sites.

The cellular saturation equilibrium data that were observed with the ouabain uptake experiments raised the question as to whether the permeability coefficient for the transport of ouabain into the cells was so small that the diffusional uptake component could experimentally not be resolved or whether the drug did not partition into the cell interior because of insufficient solvent water in the cell interior. This question was resolved by equilibrium dialysis[1]. At equilibrium, the ouabain concentrations of the donor side containing 100% human hemoglobin and the receiver side containing phosphate buffered saline were nearly identical. The results then suggest that the absence of a linear cellular ouabain uptake component is not the result of unfavorable thermodynamic properties of the cell interior but rather that the permeability coefficient for the diffusional ouabain uptake must be very low.

Digitoxin Uptake and Release Experiments

As will be seen, excellent agreement was found for all the

---

1. The interaction between ouabain and human hemoglobin was evaluated using two equilibrium dialysis studies which were experimentally analogous to the procedure outlined on p. 66 for the digitoxin - human hemoglobin interaction.

digitoxin transport data with Model 6. In the theoretical analysis of the digitoxin uptake and release experiments, the value of the digitoxin - fetal bovine serum equilibrium binding constant, K_b, was taken to be 5.52. For uptake experiments, the digitoxin - erythrocyte equilibrium binding constant, K, was determined by extrapolating the kinetic data to zero time, whereas in the analysis of release experiments, the mean value of K = 2.27 was utilized.

Figure 30 shows the kinetic data that was obtained for the cellular digitoxin uptake from media containing 0% FBS and different concentrations of the drug. The theoretical plots shown in this figure represent the best fit obtained with Model 6. The experimental data for the different experiments clearly illustrate the instantaneous drug uptake. The transport parameters evaluated with equation (75) and the experimental data for this figure are listed in Table XVIII. Figures 31, 32 and 33 show digitoxin release data and the best fitting Model 6 plots. The release experiments were carried out in media containing 0% FBS and the cells were completely saturated with the drug during the preincubation period. The rapid initial loss of drug from the cells is the result of drug release from the cell interior, whereas the slow cellular drug release that follows is the result of digitoxin desorbing from the Langmuir binding sites. The values of the transport parameters determined for the release experiments shown in Figures 31, 32 and 33 and the experimental data are given in Table IXX. The mean value of the adsorption rate constant, determined from uptake experiments, was 1.93×10^{-8} cm./sec. and the average value of the desorption rate constant, evaluated from the release data, was 3.92×10^{-21} moles/cm.^{2} sec.. The dis-

sociation constant for the digitoxin - erythrocyte complex in the absence of FBS in the media was computed from the ratio of k_r to k_f as 2.0×10^{-13} moles/ml.RBC. The maximum number of molecular digitoxin binding sites per cell was calculated from the maximum cellular saturation concentration Q as 729 ± 60.

Figure 34 shows the equilibrium data of the total cell - associated digitoxin concentration as a function of the digitoxin concentration in the medium containing 0% FBS. The data clearly show the linear and nonlinear drug uptake components. The theoretical curve was obtained with equation (79) using the average values of k_f, k_r, Q and K that were determined from the uptake and release experiments. Figure 35 shows the equilibrium data of the cellular digitoxin bound to Langmuir sites as a function of the digitoxin concentration in the media containing 0% FBS. The theoretical curve in this figure was computed with equation (67) using the average values of k_f, k_r and Q as determined with Model 6 for the uptake and release data. The data in Figure 35 clearly demonstrates the nonlinear binding and saturation characteristic of the digitoxin - erythrocyte interaction.

Figures 36 and 37 show digitoxin uptake data and the best fitting Model 6 plots. The suspension media contained 5% FBS and different concentrations of digitoxin. The transport parameters determined with Model 6 and the experimental data for these figures are given in Table XX. Figures 38, 39 and 40 give digitoxin release data and Model 6 plots which gave the best fit to the data. The suspension media contained 5% FBS and the cells in the transport systems were completely saturated with digitoxin during the preincubation period. The transport parameters and experimental data for these figures are listed

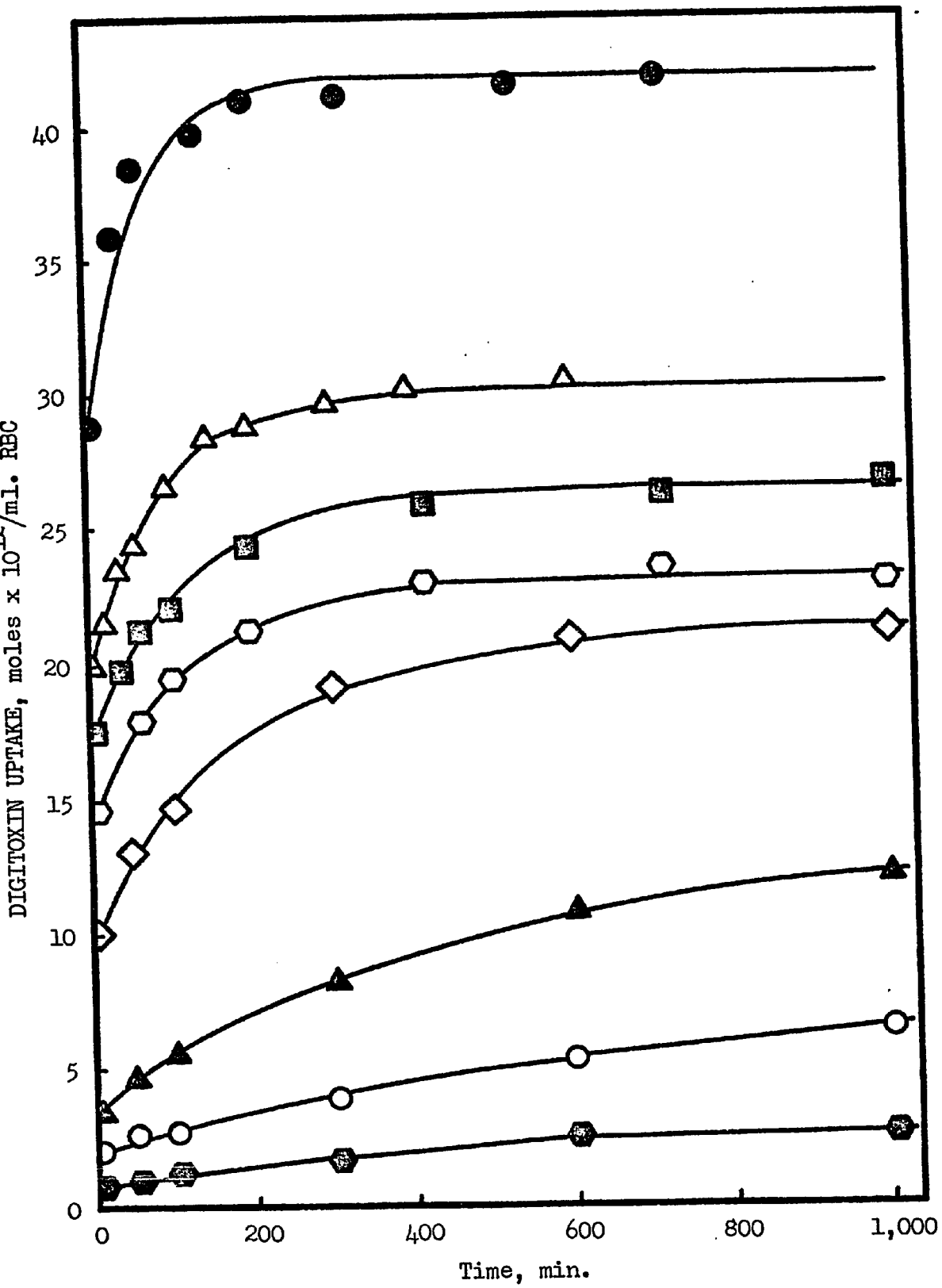


Figure 30. Model 6 plots of the cellular digitoxin uptake data. The media contained different concentrations of digitoxin and no FBS. The temperature was 30 °C. The theoretical transport parameters k_f, k_r and Q, determined with equation (75), and the experimental data for this figure are listed in Table XVIII.

Table XVIII. Summary of transport parameters evaluated with Model 6, equation (75), and the experimental data for digitoxin uptake experiments at 30 °C. The suspension media contained 0% FBS.

Figure	Symbol	T ($\frac{\text{moles/ml.}}{\text{suspension}}$)	H ($\frac{\text{ml.RBC/ml.}}{\text{suspension}}$)	K*	Q (moles/RBC)	k_f (cm./sec.)	k_r (moles/cm.^{2} sec.)
30	●	1.06×10^{-11}	0.052	2.16	1.07×10^{-21}	1.80×10^{-8}	3.91×10^{-21}
30	△	8.62×10^{-12}	0.053	2.38	1.13×10^{-21}	1.80×10^{-8}	3.91×10^{-21}
30	■	6.38×10^{-12}	0.056	2.27	1.34×10^{-21}	2.00×10^{-8}	3.91×10^{-21}
30	○	5.17×10^{-12}	0.055	2.25	1.26×10^{-21}	2.20×10^{-8}	3.91×10^{-21}
30	◇	4.38×10^{-12}	0.055	2.19	1.28×10^{-21}	1.80×10^{-8}	3.91×10^{-21}
30	▲	1.47×10^{-12}	0.054	2.21	1.30×10^{-21}	2.10×10^{-8}	3.91×10^{-21}
30	○	6.27×10^{-13}	0.051	2.30	1.22×10^{-21}	2.00×10^{-8}	3.91×10^{-21}
30	○	2.74×10^{-13}	0.057	2.25	1.19×10^{-21}	1.90×10^{-8}	3.91×10^{-21}
		7.92×10^{-12}	0.061	2.26	1.01×10^{-21}	2.00×10^{-8}	3.91×10^{-21}
		1.02×10^{-11}	0.057	2.31	1.17×10^{-21}	1.70×10^{-8}	3.91×10^{-21}
		9.94×10^{-12}	0.059	2.26	1.22×10^{-21}	2.00×10^{-8}	3.91×10^{-21}
		8.76×10^{-12}	0.061	2.27	1.18×10^{-21}	1.80×10^{-8}	3.91×10^{-21}
Mean:					1.20×10^{-21}	1.93×10^{-8}	3.91×10^{-21}

* Evaluated by extrapolating kinetic data to zero time.

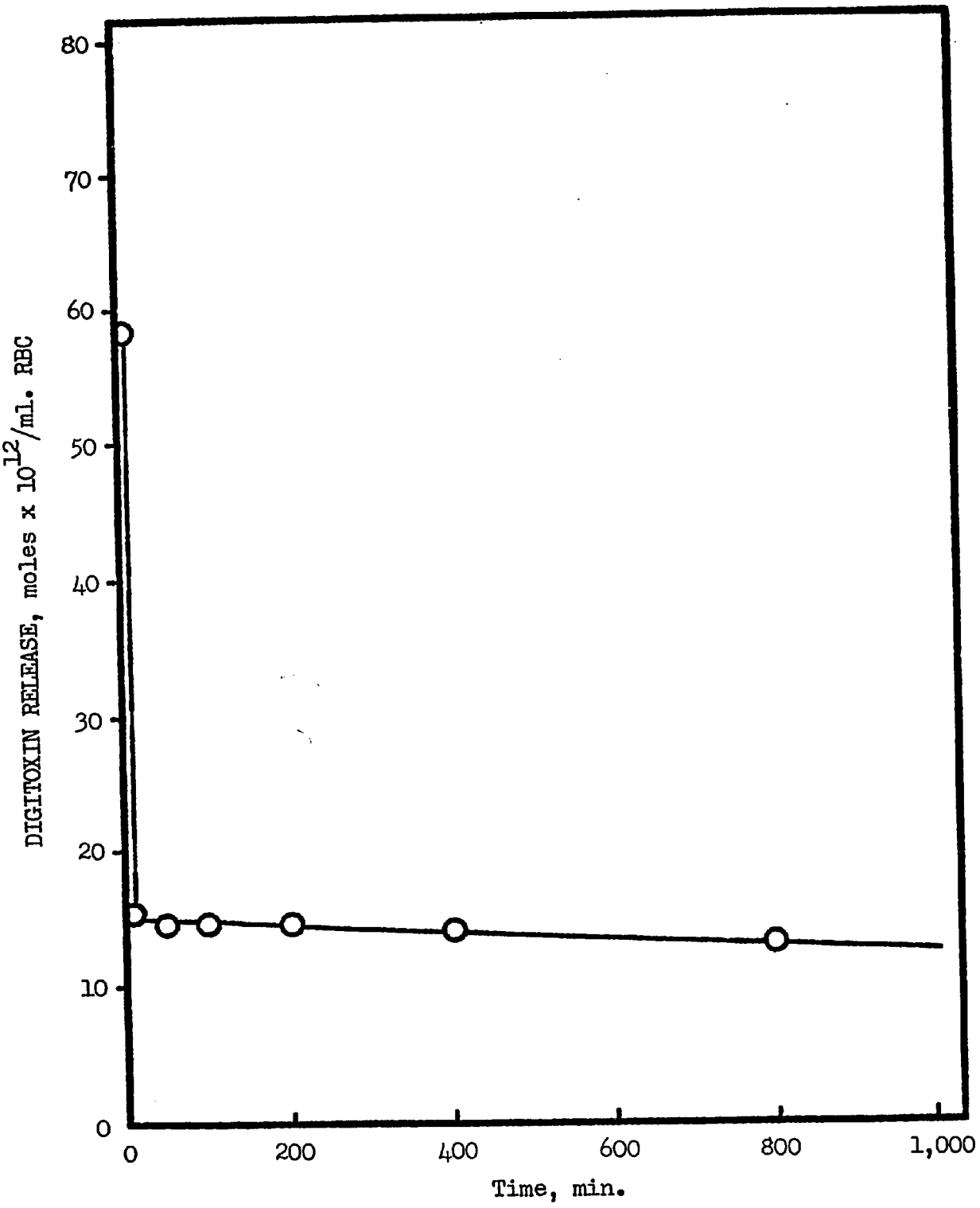


Figure 31. Model 6 plot of the cellular digitoxin release data. The medium contained no FBS and the temperature was 30 °C. The cells were preincubated in phosphate buffered saline containing digitoxin -^{3}H for 8 hrs. The theoretical transport parameters k_f, k_r and Q, determined with equation (75), and the experimental data for this figure are listed in Table IXX.

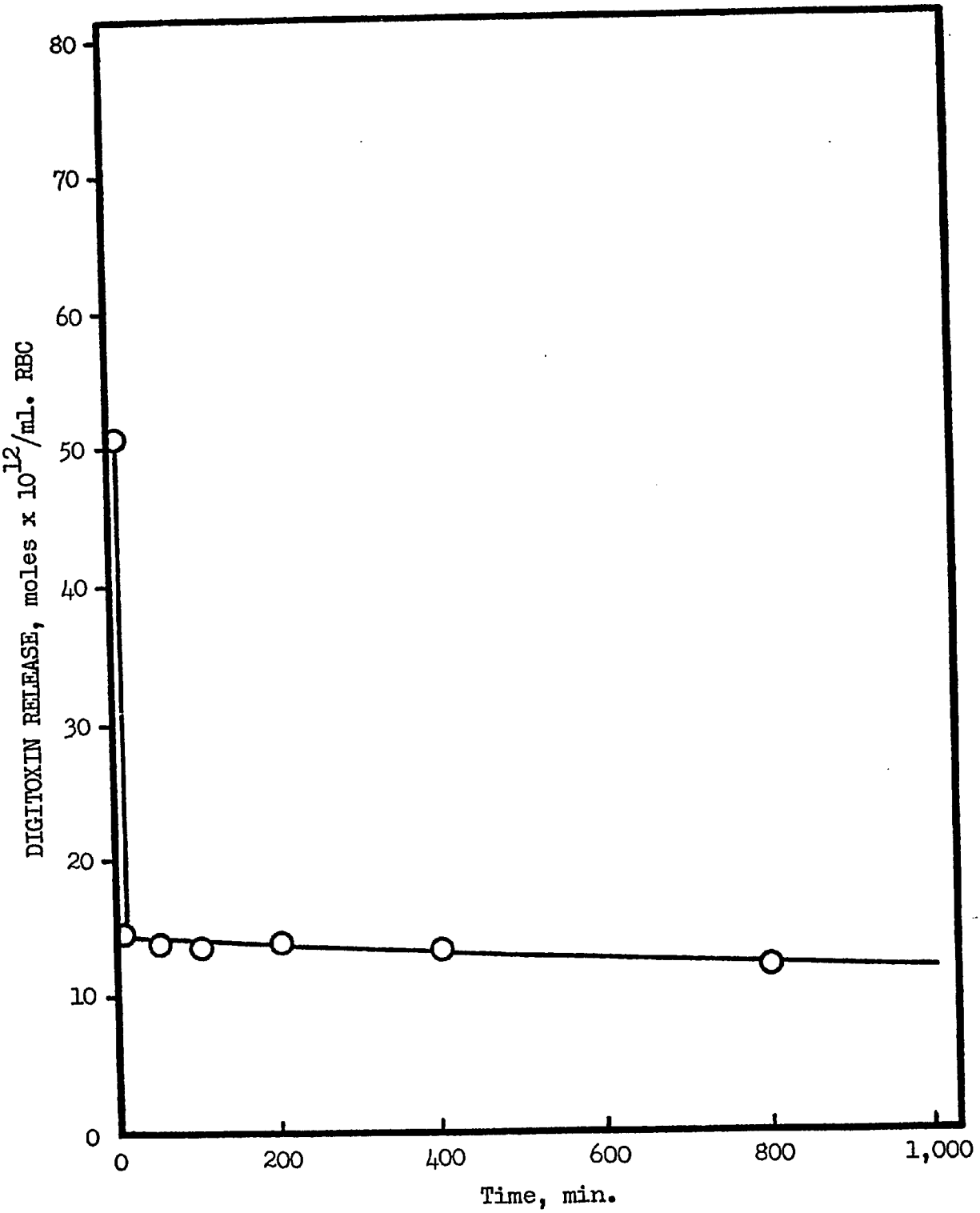


Figure 32. Model 6 plot of the cellular digitoxin release data. The medium contained no FBS and the temperature was 30 °C. The cells were preincubated in phosphate buffered saline containing digitoxin -^{3}H for 8 hrs. The theoretical transport parameters kf, k_r and Q, determined with equation (75), and the experimental data for this figure are listed in Table IXX.

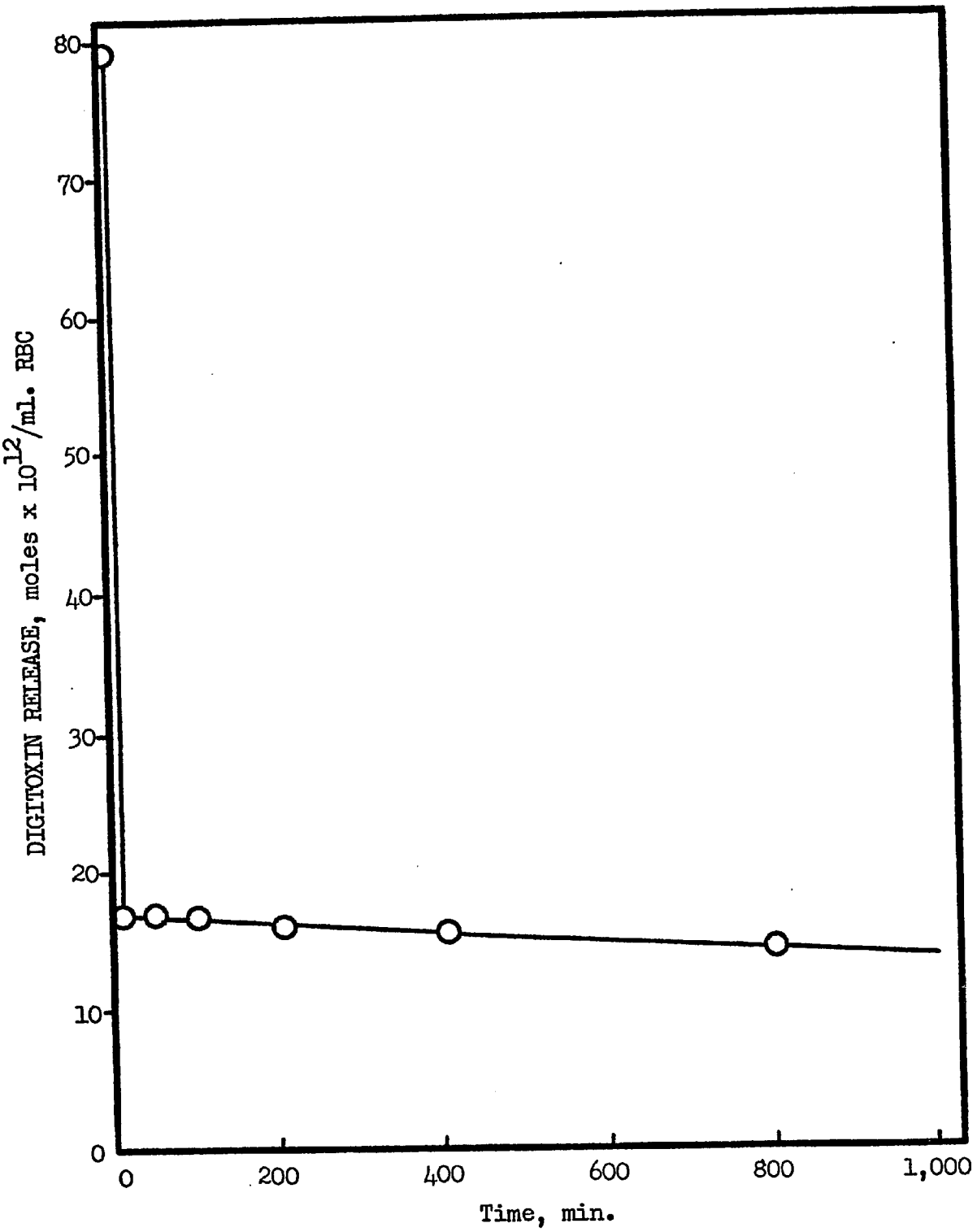


Figure 33. Model 6 plot of the cellular digitoxin release data. The medium contained no FBS and the temperature was 30 °C. The cells were preincubated in phosphate buffered saline containing digitoxin -^{3}H for 8 hrs. The theoretical transport parameters k_f, k_r and Q, determined with equation (75), and the experimental data for this figure are listed in Table IXX.

Table IXX. Summary of transport parameters evaluated with Model 6, equation (75), and the experimental data for digitoxin release experiments at 30 °C. The media contained 0% FBS.

Figure	Symbol	T (moles/ml. suspension)	H (ml.RBC/ml. suspension)	K	Q (moles/RBC)	k_f (cm./sec.)	k_r (moles/cm.^{2} sec.)
31	O	1.12×10^{-12}	0.065	2.27	1.30×10^{-21}	1.93×10^{-8}	3.68×10^{-21}
32	O	9.91×10^{-13}	0.059	2.27	1.18×10^{-21}	1.93×10^{-8}	4.09×10^{-21}
33	O	1.29×10^{-12}	0.056	2.27	1.37×10^{-21}	1.93×10^{-8}	3.97×10^{-31}
Mean:					1.28×10^{-21}	1.93×10^{-8}	3.91×10^{-21}

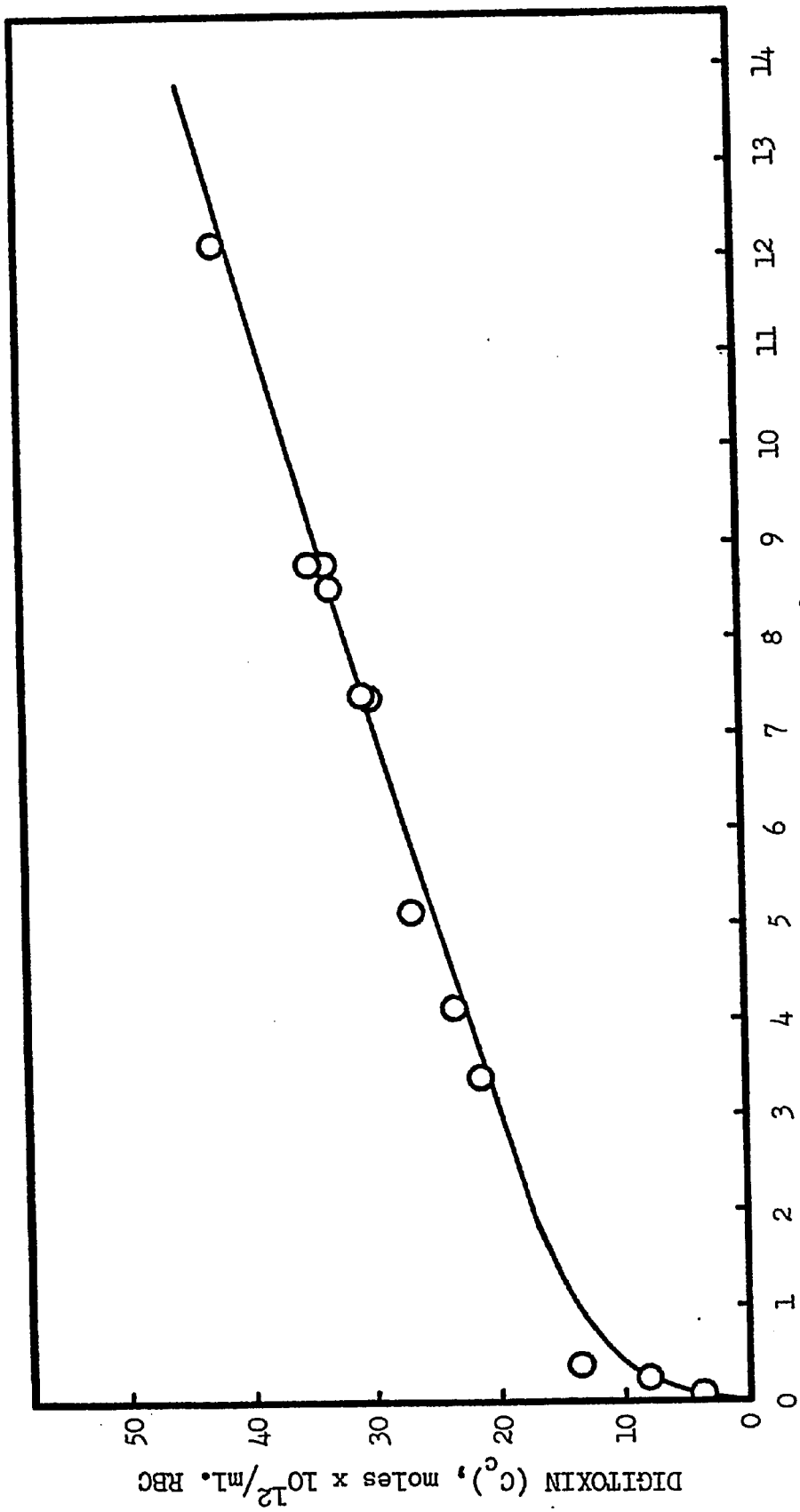


Figure 34. Equilibrium data of the total cell - associated digitoxin as a function of the digitoxin concentration in the media containing no FBS. The temperature was 30 °C. The theoretical curve was computed with equation (79) using the following mean parameters determined from uptake and release experiments: $k_f = 1.93 \times 10^{-8}$ cm./sec., $k_r = 3.91 \times 10^{-21}$ moles/cm.^{2} sec., Q = 1.21 x 10^{-21} moles/RBC and K = 2.26.

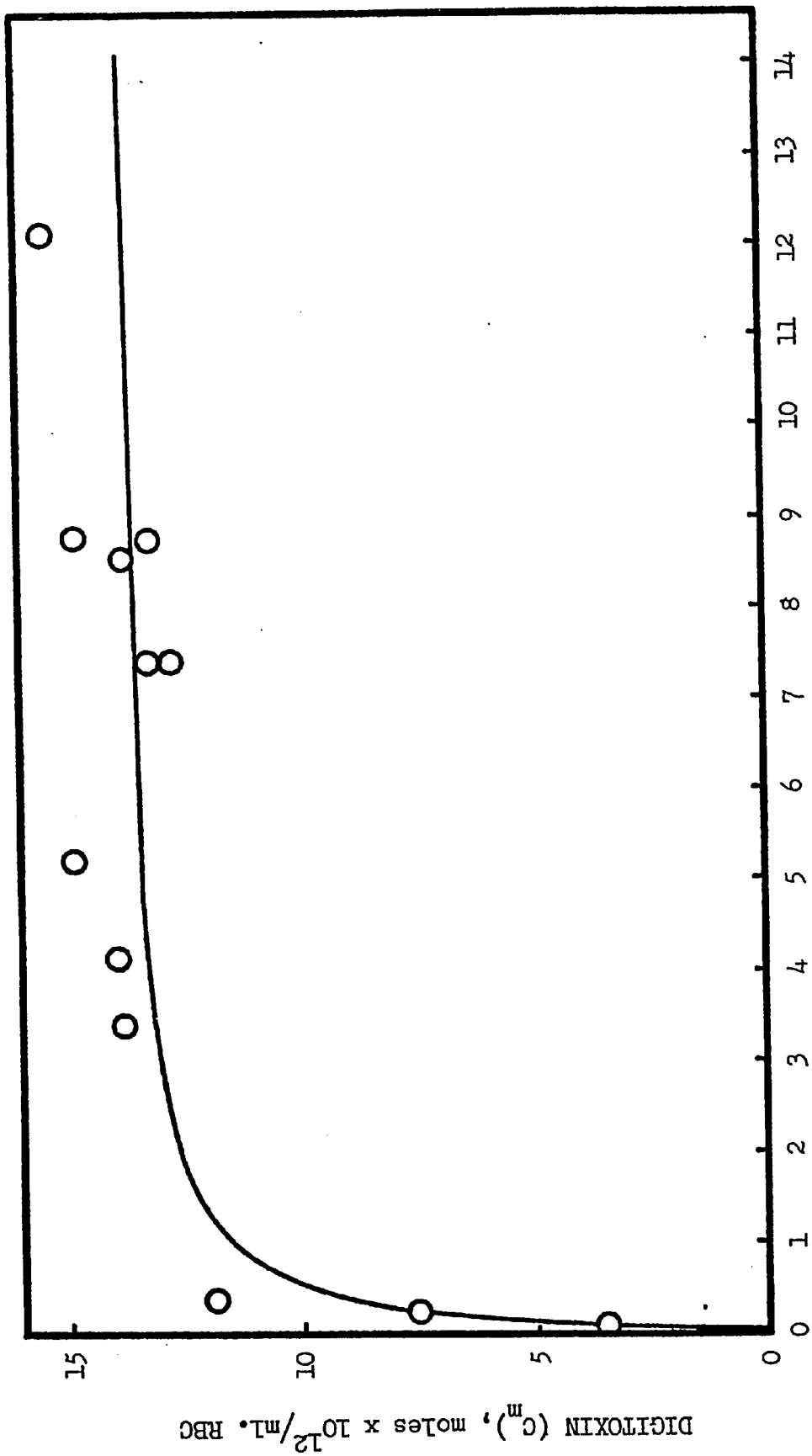


Figure 35. Equilibrium data of the cellular digitoxin bound to Langmuir sites as a function of the digitoxin concentration in the media containing no FBS. The temperature was 30 °C. The theoretical curve was computed with equation (67) using the following mean parameters determined from uptake and release experiments: $k_f = 1.93 \times 10^{-8}$ cm./sec., $k_r = 3.91 \times 10^{-21}$ moles/cm.^{2} sec. and $Q = 1.21 \times 10^{-21}$ moles/RBC.

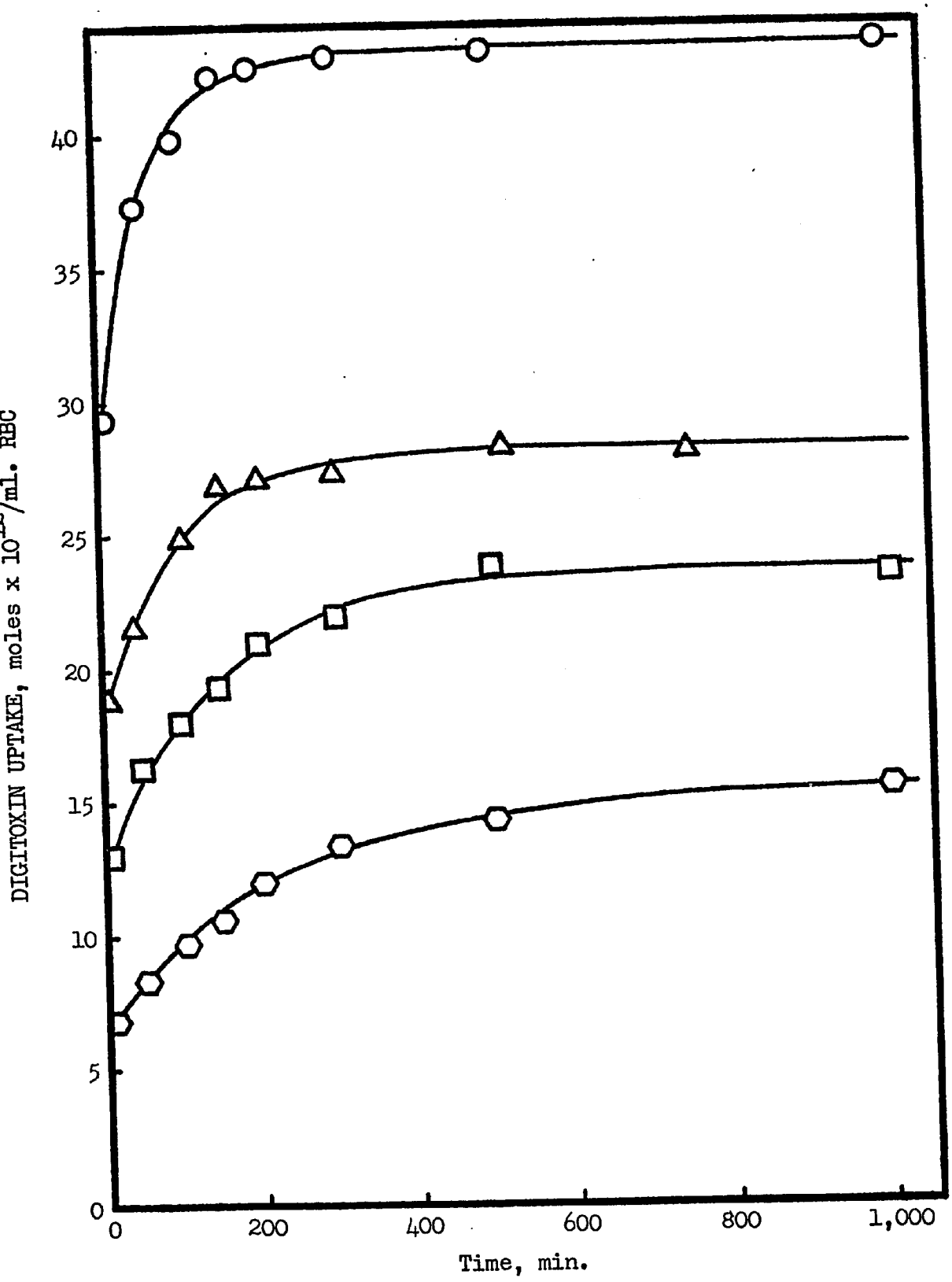


Figure 36. Model 6 plots of the cellular digitoxin uptake data. The media contained 5% FBS and different concentrations of digitoxin. The temperature was 30 °C. The theoretical transport parameters k_f, k_r and Q, evaluated with equation (75), and the experimental data for this figure are given in Table XX.

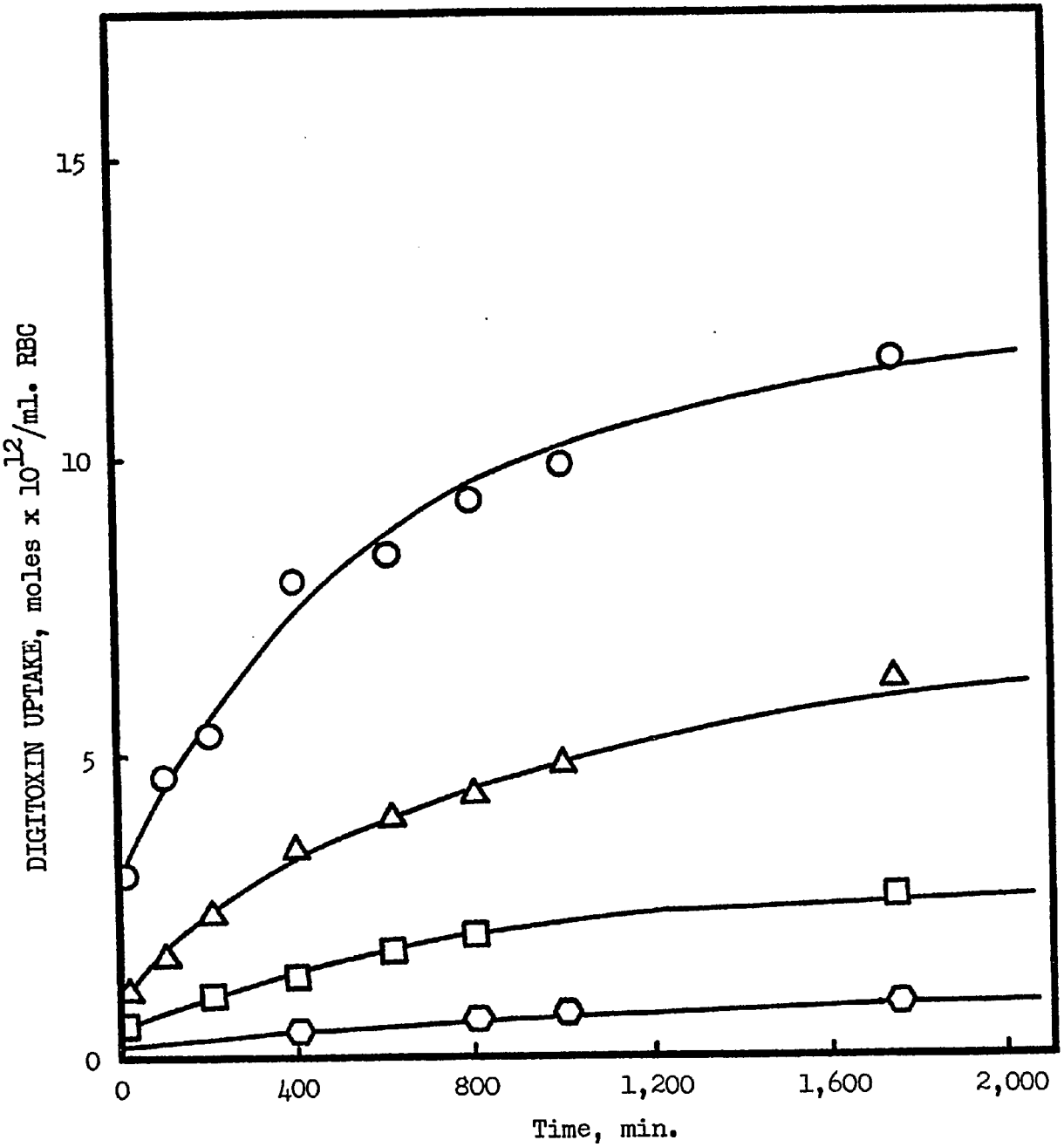


Figure 37. Model 6 plots of the cellular digitoxin uptake data. The media contained 5% FBS and different concentrations of digitoxin. The temperature was 30 °C. The theoretical transport parameters k_f, k_r and Q, evaluated with equation (75), and the experimental data for this figure are given in Table XX.

Table XX. Summary of transport parameters evaluated with Model 6, equation (75), and the experimental data for digitoxin uptake experiments at 30 °C. The media contained 5% FBS.

Figure	Symbol	T ($\frac{\text{moles/ml.}}{\text{suspension}}$)	H ($\frac{\text{ml.RBC/ml.}}{\text{suspension}}$)	K*	Q (moles/RBC)	k_f (cm./sec.)	k_r (moles/cm.^{2} sec.)
36	○	1.84×10^{-11}	0.049	2.28	1.12×10^{-21}	1.20×10^{-8}	3.58×10^{-21}
36	△	1.06×10^{-11}	0.065	2.21	1.06×10^{-21}	1.50×10^{-8}	3.58×10^{-21}
36	□	7.82×10^{-12}	0.055	2.19	1.09×10^{-21}	1.30×10^{-8}	3.58×10^{-21}
36	⬡	4.00×10^{-12}	0.053	2.24	9.28×10^{-22}	1.30×10^{-8}	3.58×10^{-21}
37	○	1.76×10^{-12}	0.052	2.29	1.13×10^{-21}	1.20×10^{-8}	3.58×10^{-21}
37	△	6.53×10^{-13}	0.054	2.22	1.15×10^{-21}	1.50×10^{-8}	3.58×10^{-21}
37	□	2.97×10^{-13}	0.054	2.15	1.02×10^{-21}	1.30×10^{-8}	3.58×10^{-21}
37	⬡	9.48×10^{-14}	0.051	2.31	9.86×10^{-22}	1.20×10^{-8}	3.58×10^{-21}
		1.06×10^{-11}	0.058	2.15	1.04×10^{-21}	1.20×10^{-8}	3.58×10^{-21}
		1.06×10^{-11}	0.060	2.23	1.03×10^{-21}	1.50×10^{-8}	3.58×10^{-21}
		1.05×10^{-11}	0.062	2.23	1.07×10^{-21}	1.50×10^{-8}	3.58×10^{-21}
Mean:				2.23	1.06×10^{-21}	1.34×10^{-8}	3.58×10^{-8}

* Evaluated by extrapolating kinetic data to zero time.

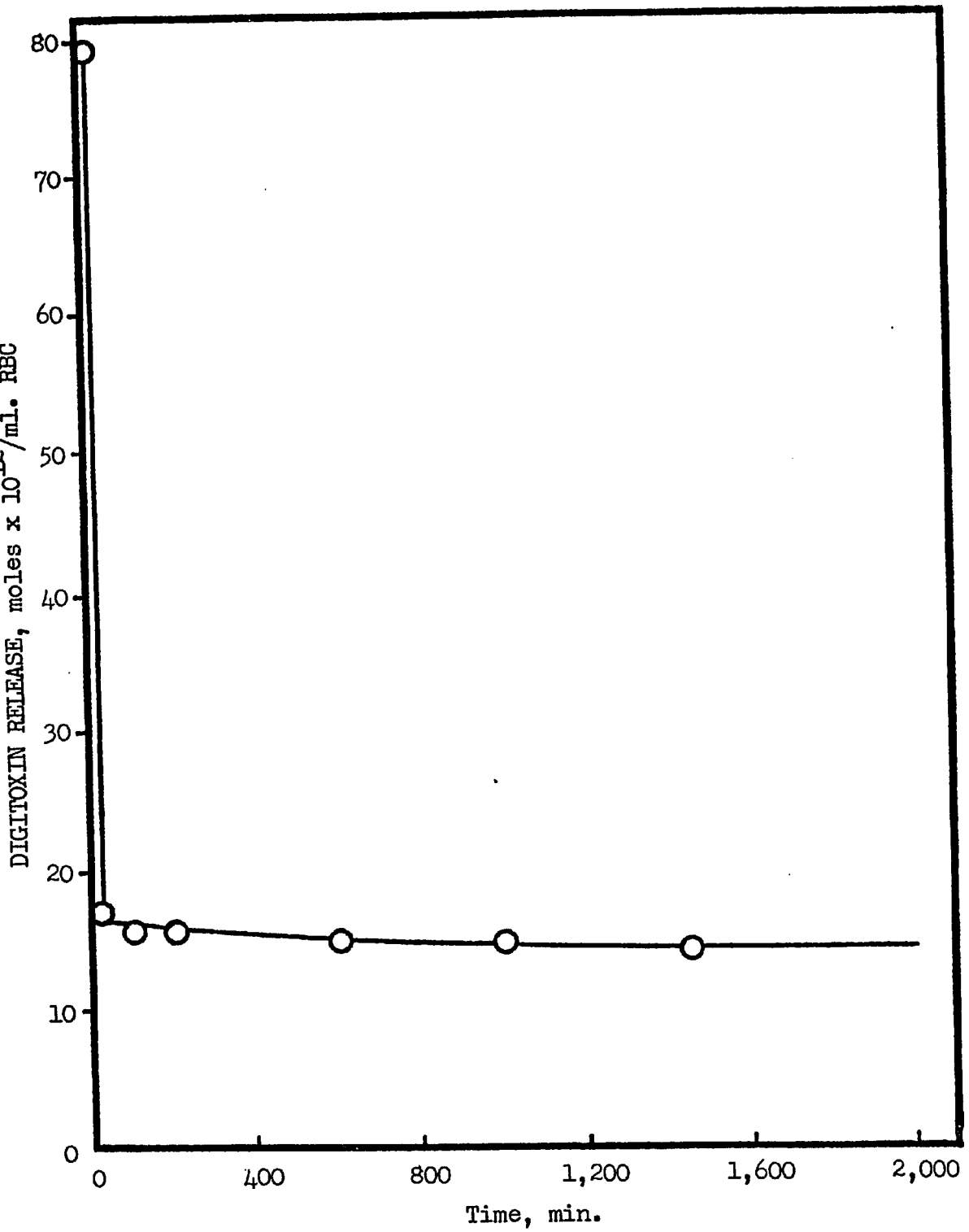


Figure 38. Model 6 plot of the cellular digitoxin release data. The medium contained 5% FBS and the temperature was 30 °C. The cells were preincubated in media containing 5% FBS and digitoxin $-^{3}H$ for 8 hrs. The theoretical transport parameters k_f, k_r and Q, evaluated from the experimental data using equation (75), and the experimental data are given in Table XXI.

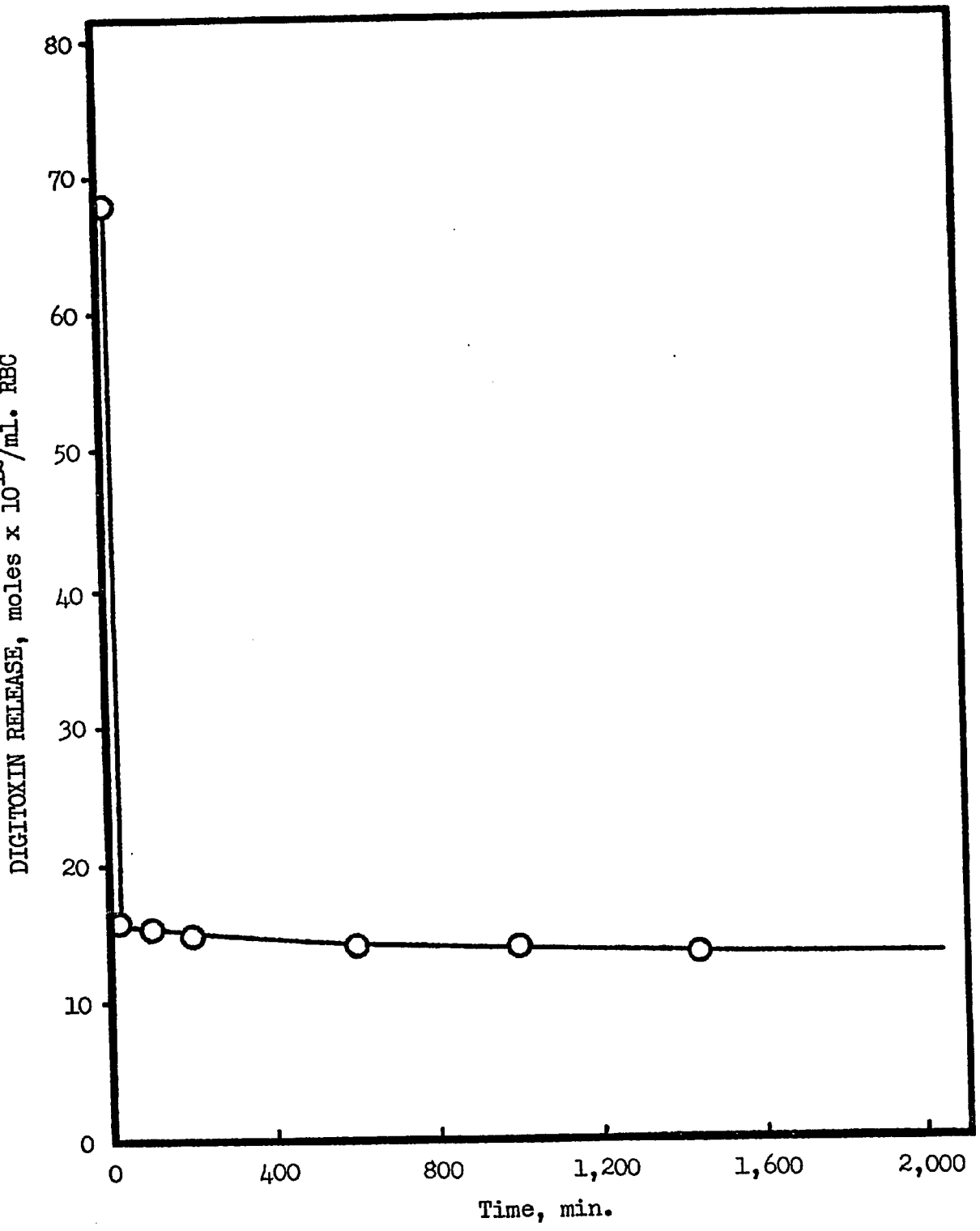


Figure 39. Model 6 plot of the cellular digitoxin release data. The medium contained 5% FBS and the temperature was 30 °C. The cells were preincubated in media containing 5% FBS and digitoxin -^{3}H for 8 hrs. The theoretical transport parameters k_f, k_r and Q, evaluated from the experimental data using equation (75), and the experimental data are given in Table XXI.

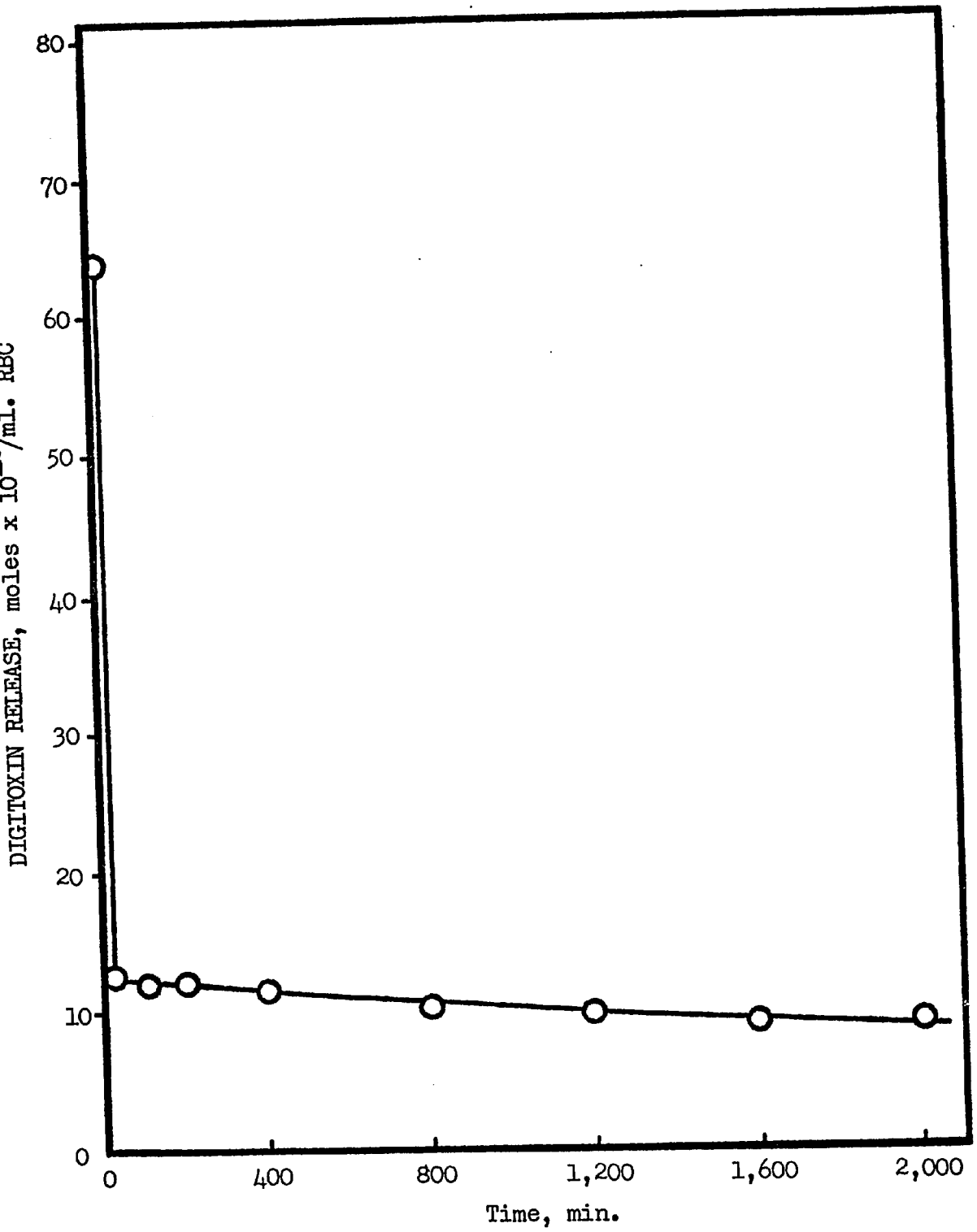


Figure 40. Model 6 plot of the cellular digitoxin release data. The medium contained 5% FBS and the temperature was 30 °C. The cells were preincubated in media containing 5% FBS and digitoxin $-^{3}H$ for 8 hrs. The theoretical transport parameters k_f, k_r and Q, evaluated from the experimental data using equation (75), and the experimental data are given in Table XXI.

Table XXI. Summary of transport parameters evaluated with Model 6, equation (75), and experimental data for digitoxin release at 30 °C. The suspension media contained 5% FBS.

Figure	Symbol	T ($\frac{\text{moles/ml.}}{\text{suspension}}$)	H ($\frac{\text{ml.RBC/ml.}}{\text{suspension}}$)	K	Q (moles/RBC)	k_f (cm./sec.)	k_r (moles/cm^2 sec.)
38	O	2.26×10^{-12}	0.051	2.27	1.15×10^{-21}	1.34×10^{-8}	3.77×10^{-21}
39	O	2.24×10^{-12}	0.053	2.27	1.15×10^{-21}	1.34×10^{-8}	3.48×10^{-21}
40	O	9.52×10^{-13}	0.056	2.27	1.01×10^{-21}	1.34×10^{-8}	3.48×10^{-21}
Mean:					1.10×10^{-21}	1.34×10^{-8}	3.58×10^{-21}

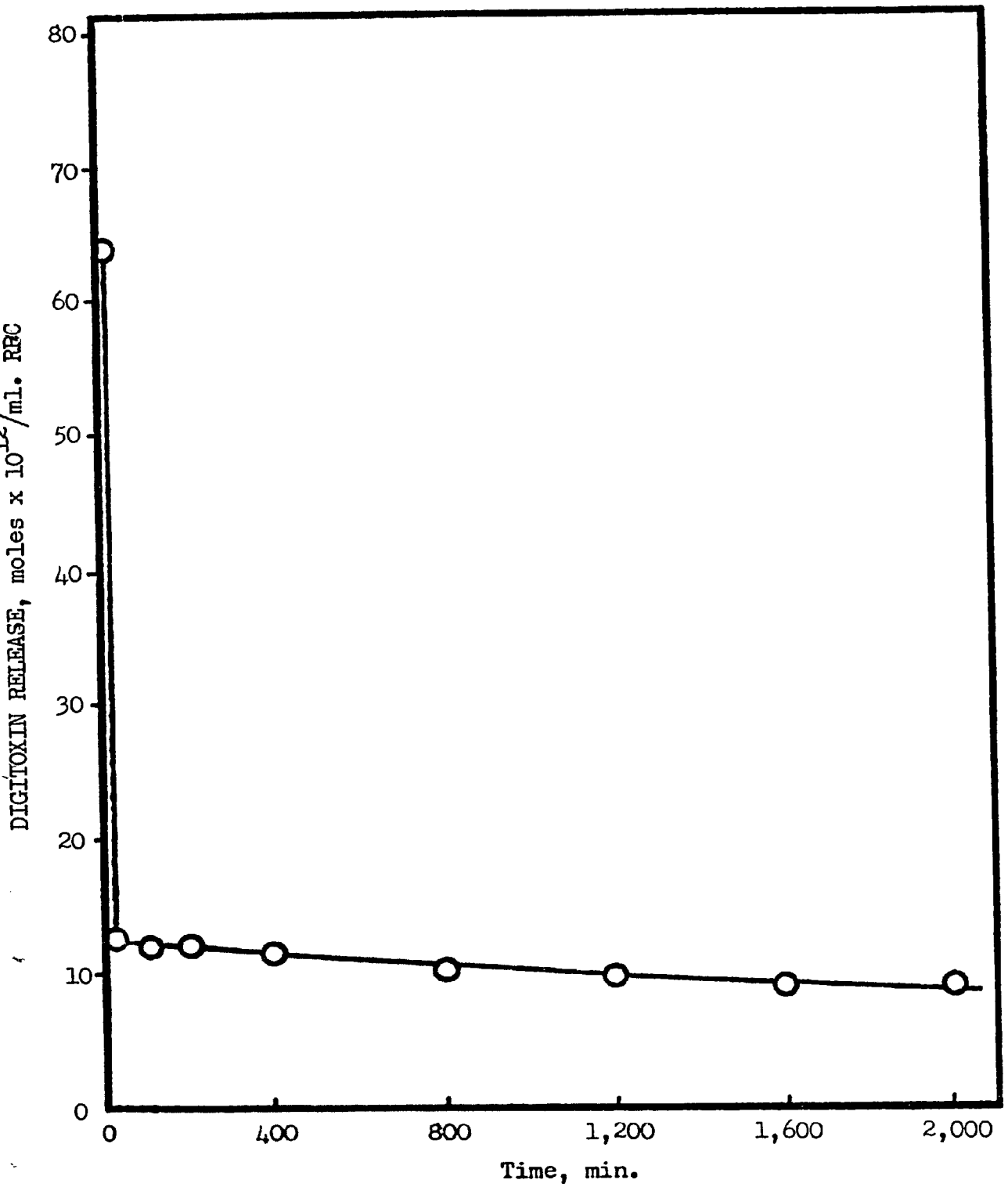


Figure 40. Model 6 plot of the cellular digitoxin release data. The medium contained 5% FBS and the temperature was 30 °C. The cells were preincubated in media containing 5% FBS and digitoxin -^{3}H for 8 hrs. The theoretical transport parameters k_f, k_r and Q, evaluated from the experimental data using equation (75), and the experimental data are given in Table XXI.

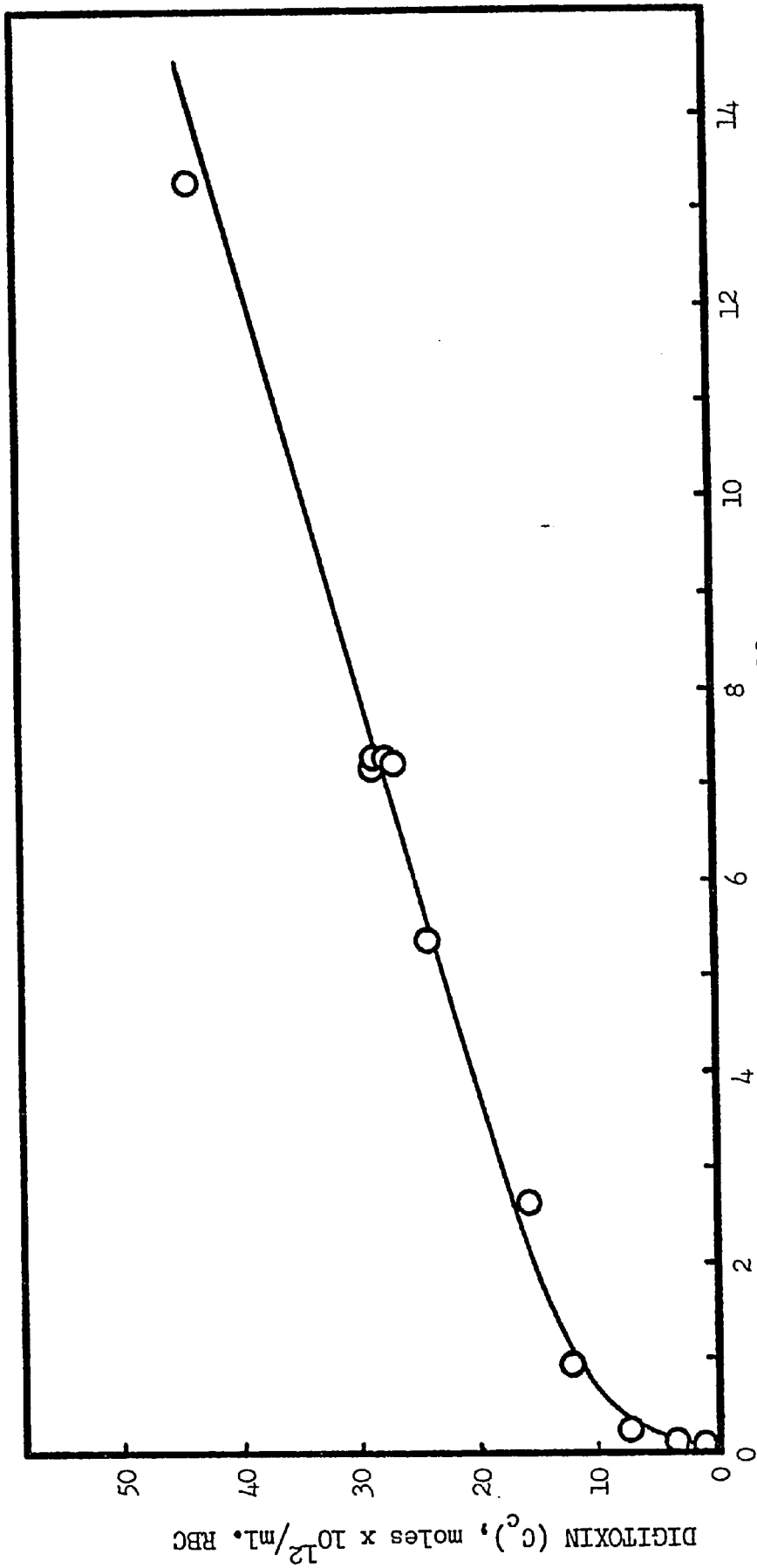


Figure 41. Equilibrium data of the total cell - associated digitoxin as a function of the unbound digitoxin concentration in the media containing 5% FBS. The temperature was 30 °C. The theoretical curve was computed with equation (79) using the following mean parameters determined from uptake and release experiments:

k_f = 1.34 x 10^{-8} cm./sec., k_r = 3.58 x 10^{-21} moles/cm.^{2} sec., Q = 1.07 x 10^{-21} moles/RBC and K = 2.23.

Figure 42. Equilibrium data of the cellular digitoxin bound to Langmuir sites as a function of the unbound digitoxin concentration in the media containing 5% FBS. The temperature was 30 °C. The theoretical curve was computed with equation (67) using the following mean parameters determined from uptake and release experiments: k_f = 1.34 x 10^{-8} cm./sec., k_r = 3.58 x 10^{-21} moles/cm.^{2} sec. and Q = 1.07 x 10^{-21} moles/RBC.

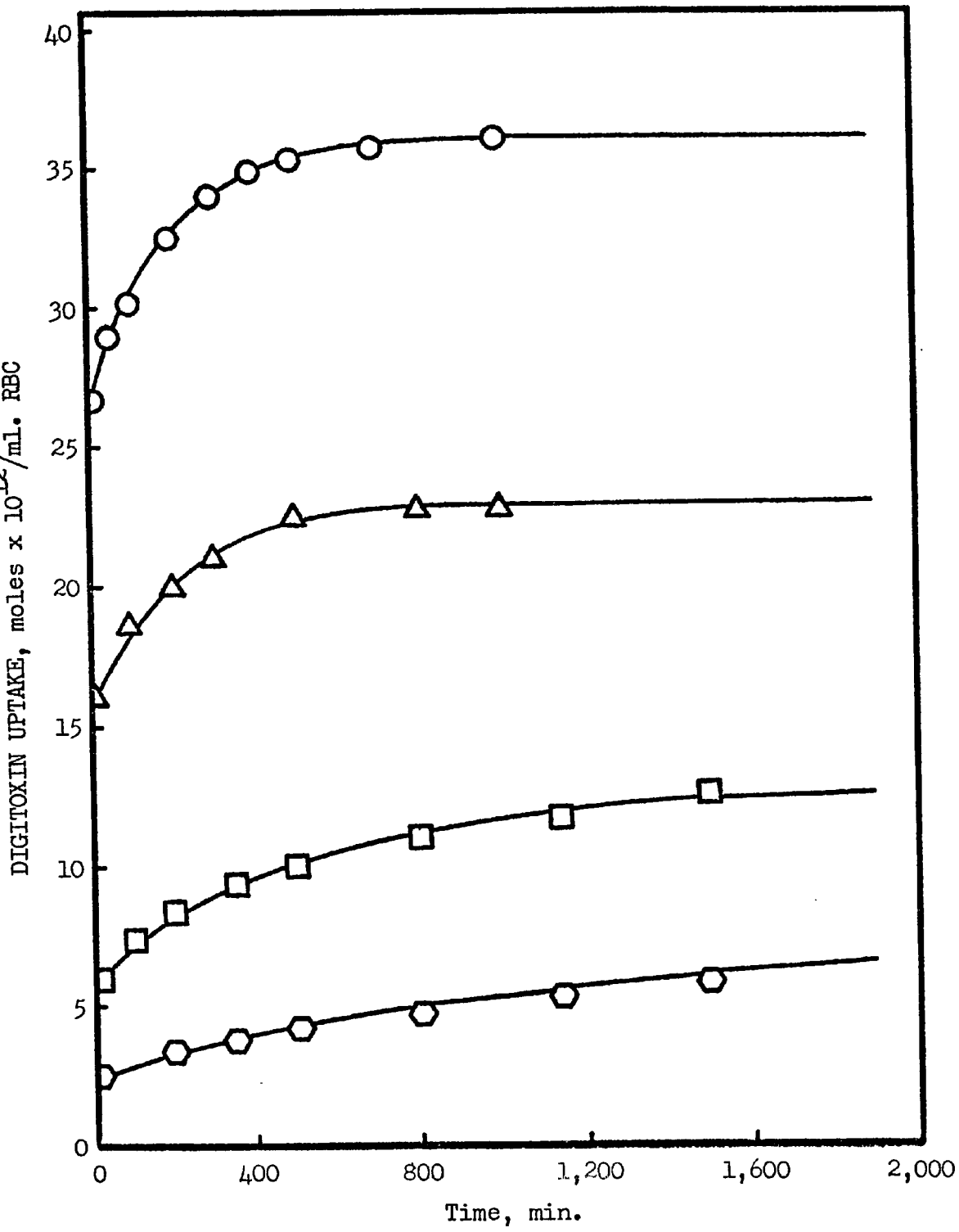


Figure 43. Model 6 plots of the cellular digitoxin uptake data. The media contained 15% FBS and different concentrations of digitoxin. The temperature was 30 °C. The theoretical transport parameters k_f, k_r and Q, evaluated using equation (75), and the experimental data for this figure are given in Table XXIII.

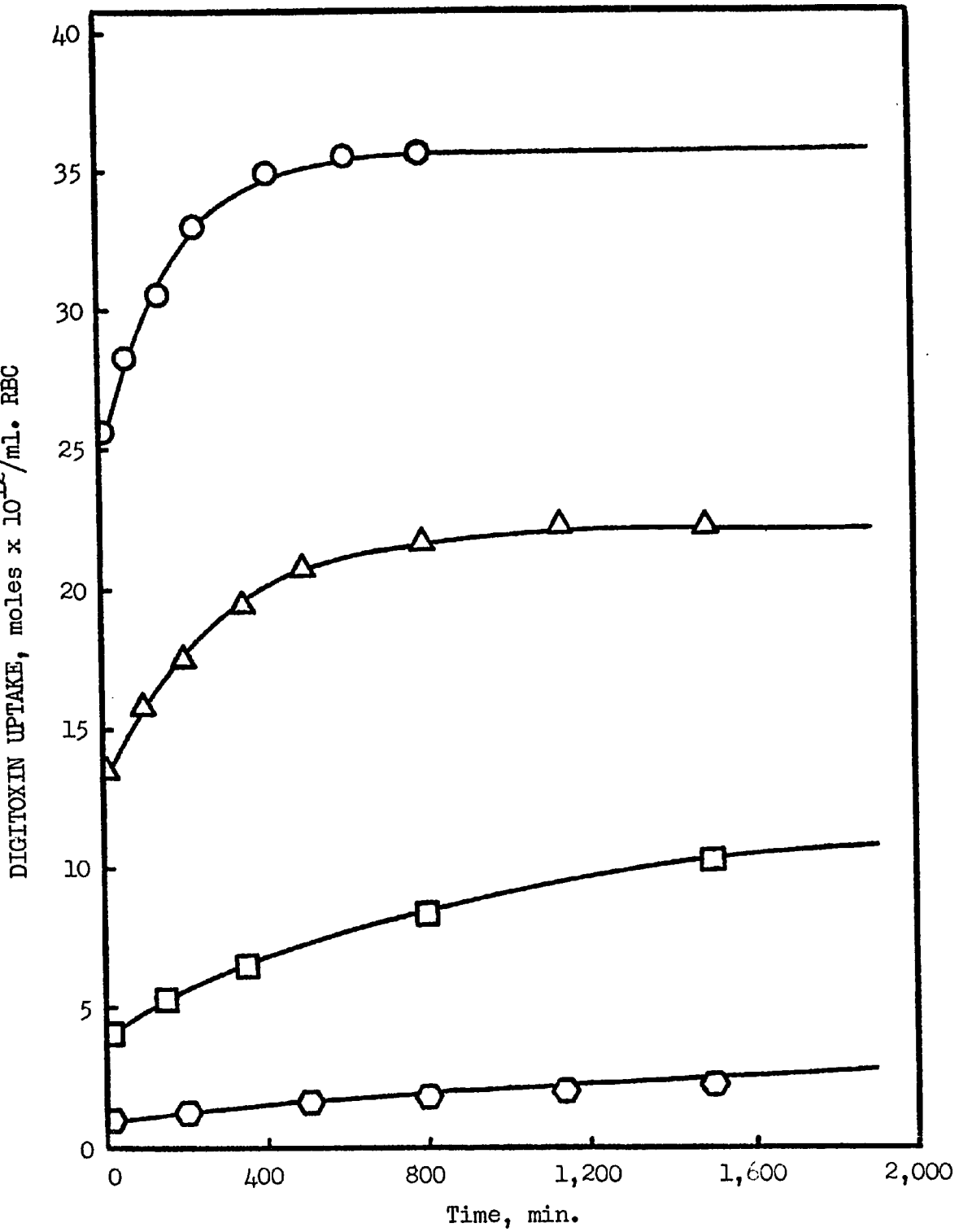


Figure 44. Model 6 plots of the cellular digitoxin uptake data. The media contained 15% FBS and different concentrations of digitoxin. The temperature was 30 °C. The theoretical transport parameters k_f, k_r, and Q, evaluated using equation (75), and the experimental data for this figure are given in Table XXIII.

Table XXII. Summary of transport parameters evaluated with Model 6, equation (75), and the experimental data for digitoxin uptake experiments at 30 °C. The media contained 15% FBS.

Figure	Symbol	T ($\frac{\text{moles/ml.}}{\text{suspension}}$)	H ($\frac{\text{ml.RBC/ml.}}{\text{suspension}}$)	K*	Q (moles/RBC)	k_f (cm./sec.)	k_r (moles/cm.^{2} sec.)
43	○	2.24×10^{-11}	0.062	2.18	9.43×10^{-22}	4.10×10^{-9}	2.97×10^{-21}
43	△	1.31×10^{-11}	0.052	2.24	7.25×10^{-22}	4.60×10^{-9}	2.97×10^{-21}
43	□	5.21×10^{-12}	0.053	2.14	7.98×10^{-22}	4.40×10^{-9}	2.97×10^{-21}
43	⬡	2.11×10^{-12}	0.056	2.21	8.70×10^{-22}	3.90×10^{-9}	2.97×10^{-21}
44	○	2.29×10^{-11}	0.067	2.02	9.69×10^{-22}	4.40×10^{-9}	2.97×10^{-21}
44	△	1.12×10^{-11}	0.051	2.17	9.28×10^{-22}	4.60×10^{-9}	2.97×10^{-21}
44	□	3.24×10^{-12}	0.048	2.24	10.70×10^{-22}	4.60×10^{-9}	2.97×10^{-21}
44	⬡	7.62×10^{-13}	0.055	2.35	8.99×10^{-22}	4.00×10^{-9}	2.97×10^{-21}
		2.26×10^{-11}	0.066	2.04	8.41×10^{-22}	4.40×10^{-9}	2.97×10^{-21}
		2.27×10^{-11}	0.062	2.08	7.83×10^{-22}	4.30×10^{-9}	2.97×10^{-21}
		8.64×10^{-14}	0.060	3.32	9.57×10^{-22}	4.20×10^{-9}	2.97×10^{-21}
Mean:				2.27	8.89×10^{-22}	4.32×10^{-9}	2.97×10^{-21}

* Evaluated by extrapolating kinetic data to zero time.

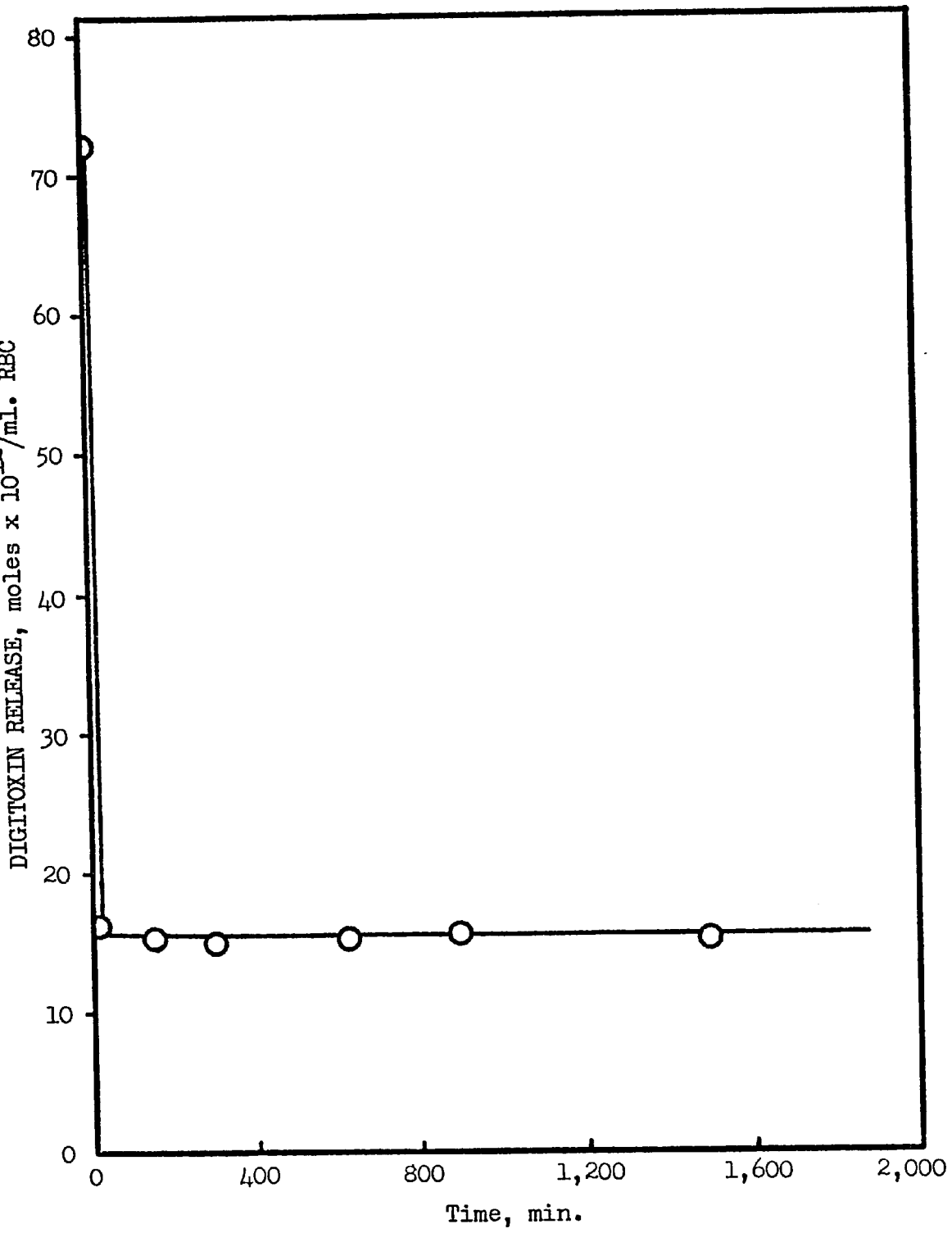


Figure 45. Model 6 plot of cellular digitoxin release data. The media contained 15% FBS. The cells were preincubated for 10 hrs. in media containing 15% FBS and digitoxin $-^{3}H$. The theoretical transport parameters k_f, k_r and Q, determined with equation (75), and the experimental data for this figure are given in Table XXIII.

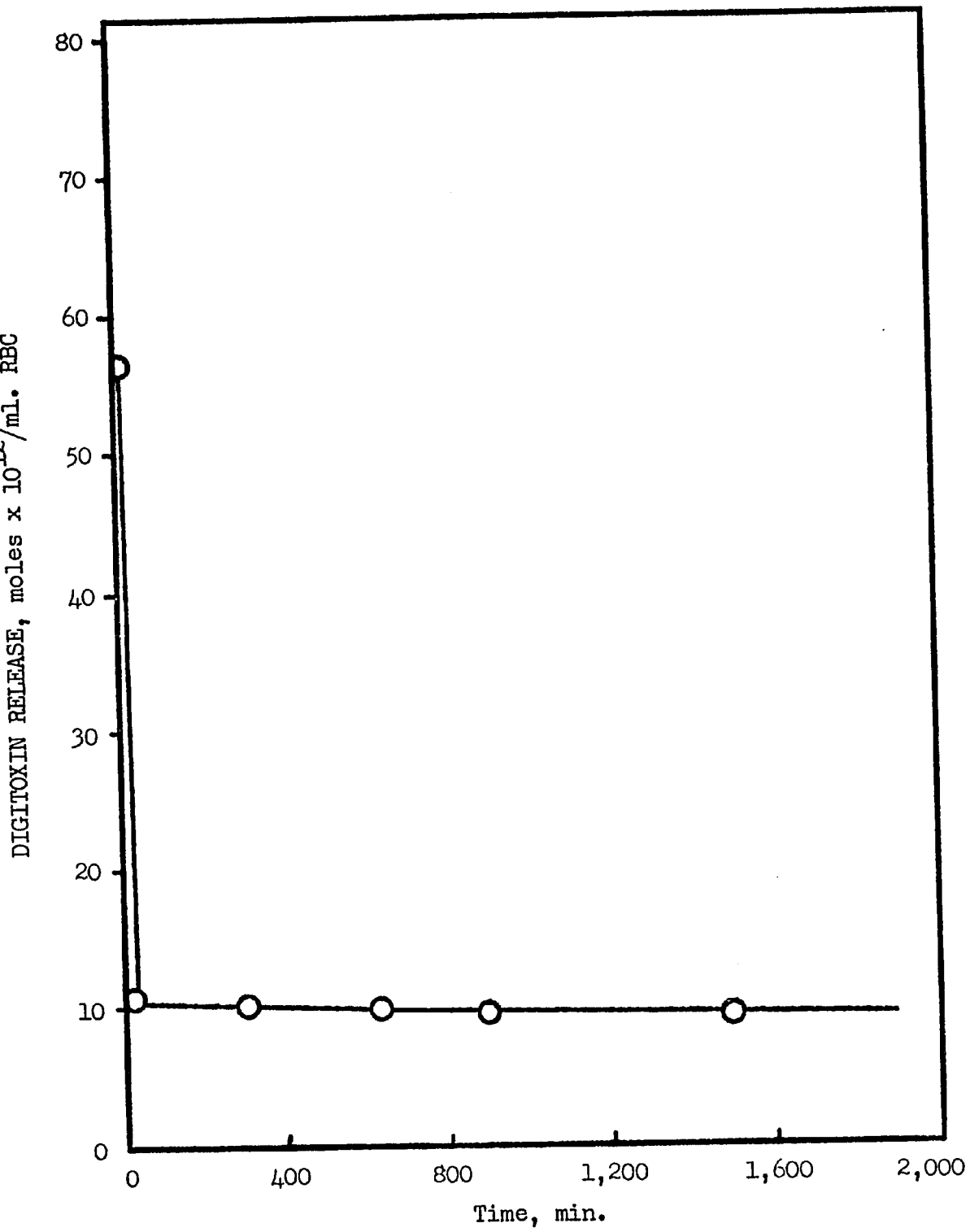


Figure 46. Model 6 plot of cellular digitoxin release data. The media contained 15% FBS. The cells were preincubated for 10 hrs. in media containing 15% FBS and digitoxin -^{3}H. The theoretical transport parameters k_f, k_r and Q, determined with equation (75), and the experimental data for this figure are given in Table XXIII.

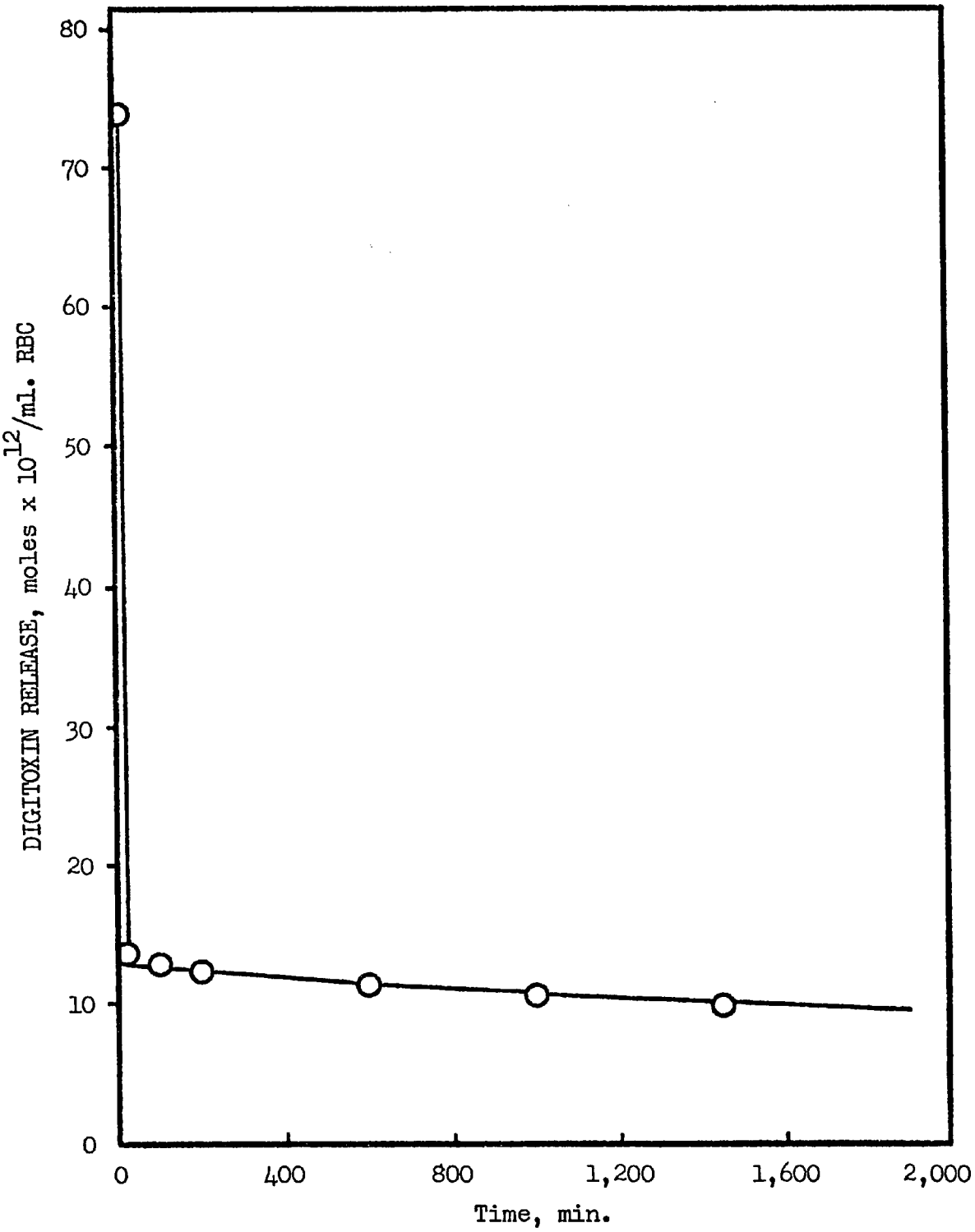


Figure 47. Model 6 plot of cellular digitoxin release data. The media contained 15% FBS. The cells were preincubated for 10 hrs. in media containing 15% FBS and digitoxin -^{3}H. The theoretical transport parameters k_f, k_r and Q, determined with equation (75), and the experimental data for this figure are given in Table XXIII.

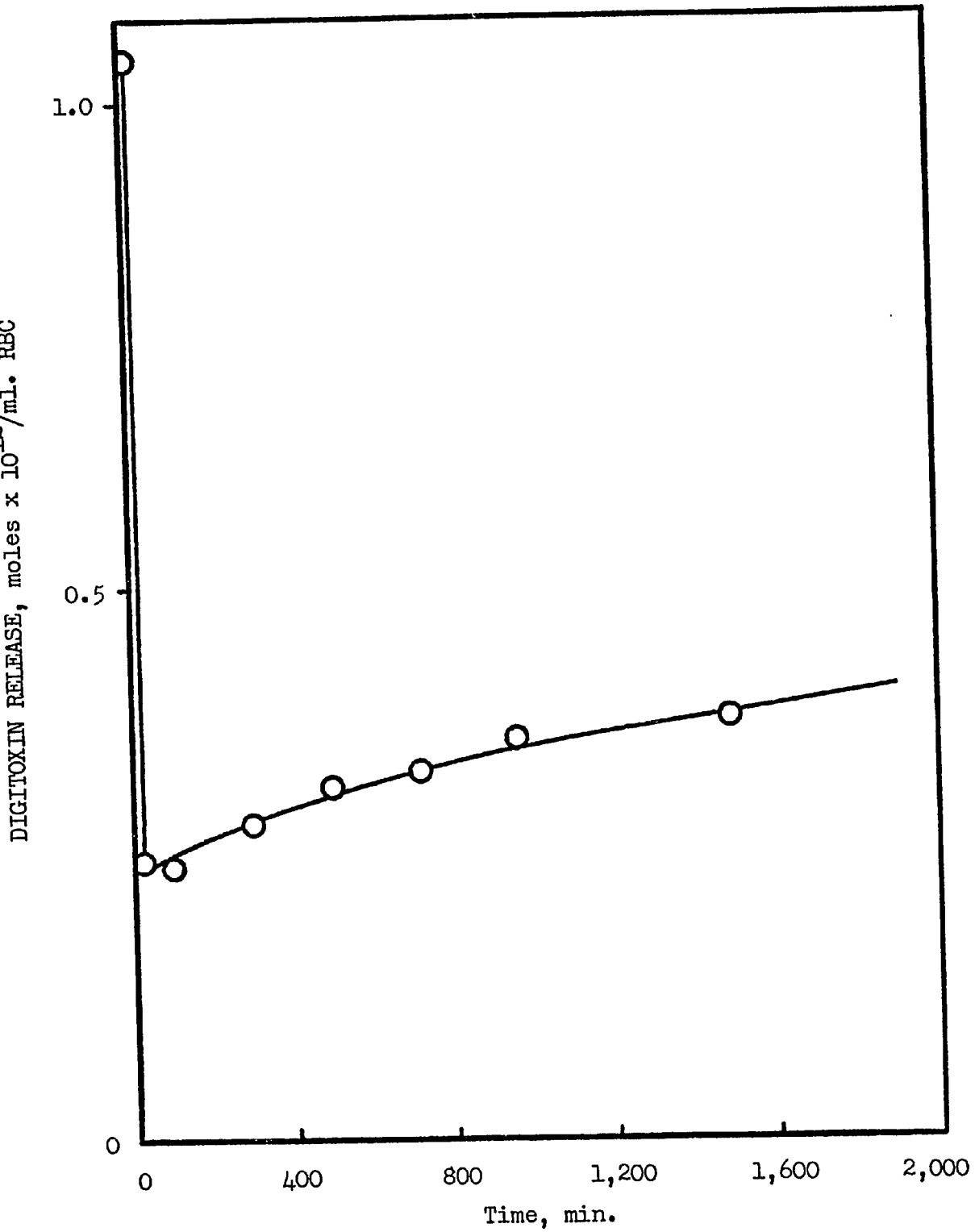


Figure 48. Model 6 plot of the cellular digitoxin release data. The medium contained 15% FBS and the temperature was 30 °C. The cells were preincubated in media containing 15% FBS and a low concentration of digitoxin -^{3}H for 2 hrs. The theoretical transport parameters k_f, k_r and Q, evaluated with equation (75), and the experimental data are given in Table XXIII.

Table XXIII. Summary of transport parameters evaluated with Model 6, equation (75), and the experimental data for digitoxin release experiments at 30 °C. The suspension media contained 15% FBS.

Figure	Symbol	T ($\frac{\text{moles/ml.}}{\text{suspension}}$)	H ($\frac{\text{ml.RBC/ml.}}{\text{suspension}}$)	K	Q (moles/RBC)	k_f (cm./sec.)	k_r (moles/cm.^{2} sec.)
45	O	5.76×10^{-12}	0.052	2.27	9.28×10^{-22}	4.32×10^{-9}	2.61×10^{-21}
46	O	2.17×10^{-21}	0.052	2.27	9.28×10^{-22}	4.32×10^{-9}	2.61×10^{-21}
47	O	2.15×10^{-12}	0.059	2.27	9.77×10^{-22}	4.32×10^{-9}	3.19×10^{-21}
48	O	8.47×10^{-14}	0.050	2.27	8.70×10^{-22}	4.32×10^{-9}	3.48×10^{-21}
Mean:					9.26×10^{-22}	4.32×10^{-9}	2.97×10^{-21}

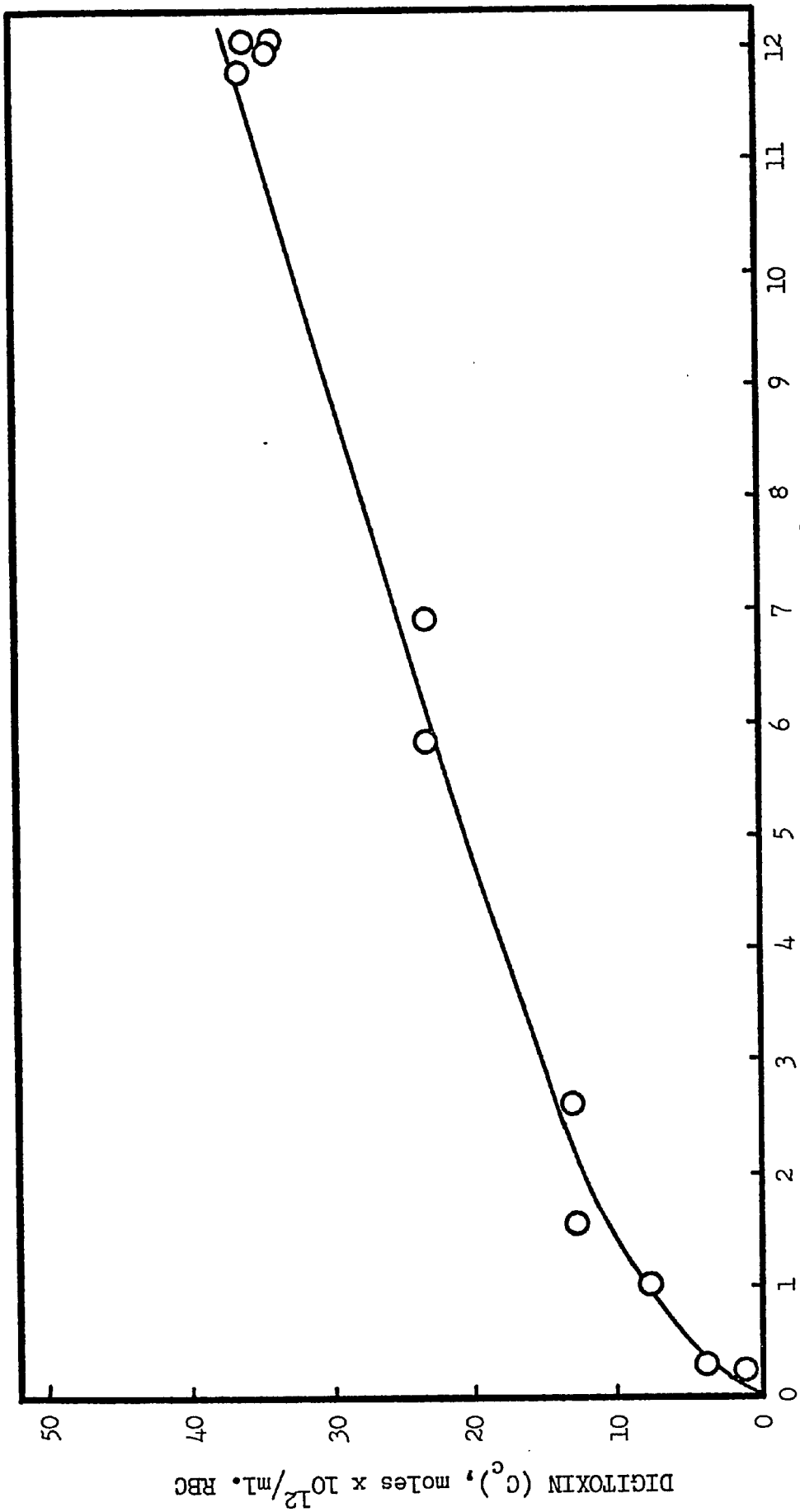


Figure 49. Equilibrium data of the total cell - associated digitoxin as a function of the unbound digitoxin concentration in the media containing 15% FBS. The temperature was 30 °C. The theoretical curve was computed with equation (79) using the following mean parameters determined from uptake and release experiments: $k_f = 4.32 \times 10^{-9}$ cm./sec., $k_r = 2.97 \times 10^{-21}$ moles/cm.^{2} sec., $Q = 8.99 \times 10^{-22}$ moles/RBC and $K = 2.27$.

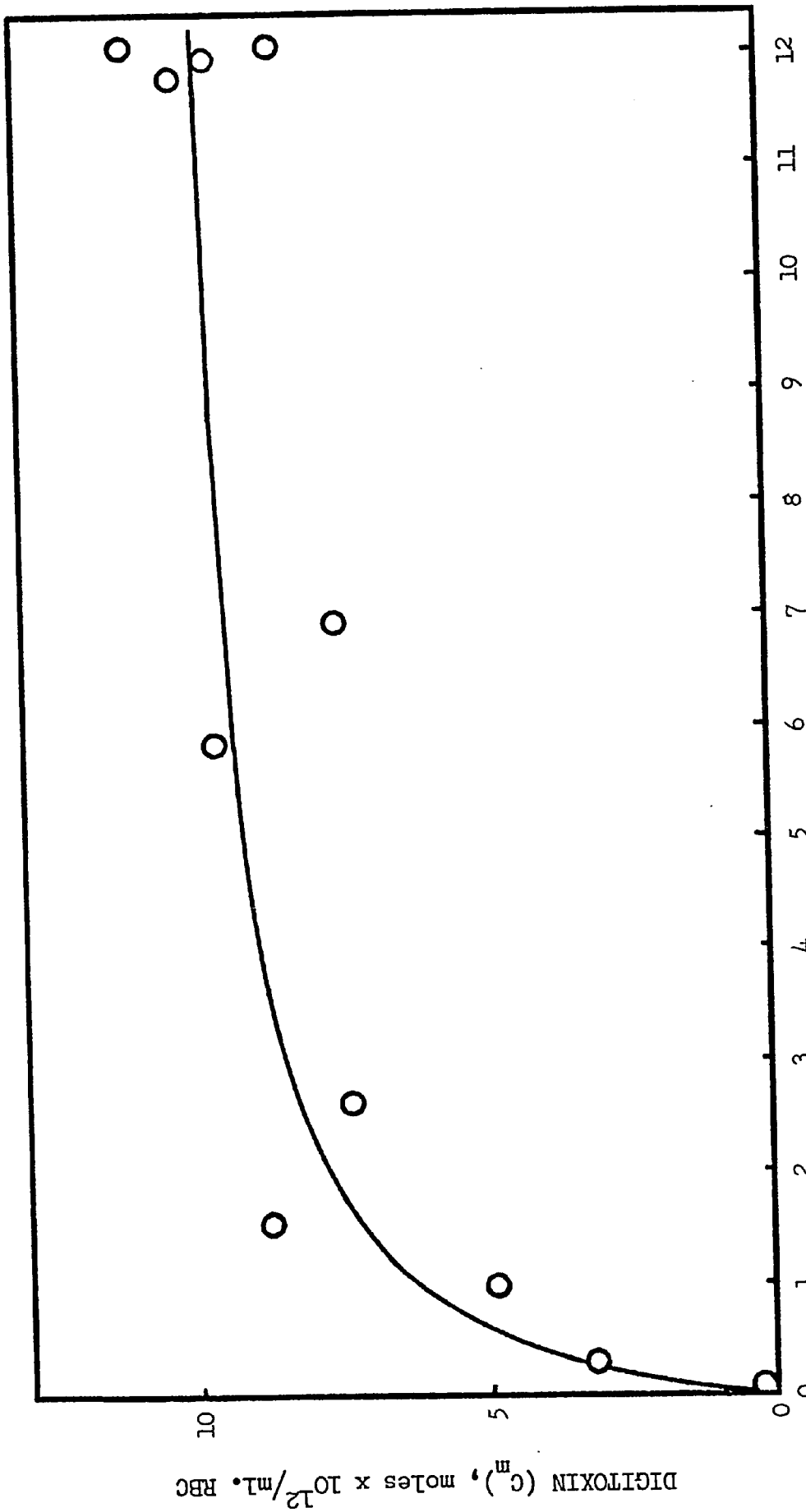


Figure 50. Equilibrium data of the cellular digitoxin bound to Langmuir sites as a function of the unbound digitoxin concentration in the media containing 15% FBS. The temperature was 30 °C. The theoretical curve was computed with equation (67) using the following mean parameters determined from uptake and release experiments: $k_f = 4.32 \times 10^{-9}$ cm./sec., $k_r = 2.97 \times 10^{-21}$ moles/cm.^{2} sec. and $Q = 8.99 \times 10^{-22}$ moles/RBC.

Table XXIV. Summary of the mean values of the transport parameters and their standard deviations determined from the digitoxin uptake and release experiments at 30 °C for the systems containing 0, 5 and 15% FBS using Model 6, equation (75).

% FBS	Q (moles/RBC)	S.D.* (moles/RBC)	k_f (cm./sec.)	S.D.* (cm./sec.)	k_r (moles/cm.^{2} sec.)	S.D.* (moles/cm.^{2} sec.)
0	1.21×10^{-21}	0.10×10^{-21}	1.93×10^{-8}	0.15×10^{-8}	3.92×10^{-21}	0.21×10^{-21}
5	1.07×10^{-21}	0.07×10^{-21}	1.34×10^{-8}	0.14×10^{-8}	3.58×10^{-21}	0.17×10^{-21}
15	8.99×10^{-22}	0.07×10^{-22}	4.32×10^{-9}	0.24×10^{-9}	2.97×10^{-21}	0.44×10^{-21}

* Standard deviation for the data listed in Tables XVIII through XXIII.

in Table XXI. The values of k_f and k_r for these systems containing 5% FBS and determined from the uptake and release data were 1.34×10^{-8} cm./sec. and 3.58×10^{-21} moles/cm.^{2} sec., respectively.

The dissociation constant for the digitoxin - erythrocyte complex in the presence of 5% FBS was evaluated as 2.7×10^{-13} moles/ml.RBC. The maximum number of molecular digitoxin binding sites per cell in the presence of 5% FBS was calculated from the average value of Q as 647 ± 42.

Figure 41 shows the equilibrium data of the total cell - associated digitoxin concentration as a function of the unbound digitoxin concentration in the media containing 5% FBS. The theoretical plot was computed with equation (79) using the mean values of k_f, k_r, Q and K that were determined from the uptake and release data. Figure 42 shows the equilibrium data of the cellular digitoxin bound to Langmuir sites as a function of the unbound digitoxin concentration in the media containing 5% FBS. The theoretical plot in this figure was computed with equation (67) using the average values of k_f, k_r and Q that were evaluated for the transport systems containing 5% FBS.

Figures 43 and 44 show Model 6 plots for the digitoxin uptake data. The media in these uptake studies contained 15% FBS and different concentrations of digitoxin. The transport parameters that were evaluated with Model 6 for the data shown in these figures and the experimental data are given in Table XXII. Figures 45 through 48 show Model 6 plots for the digitoxin release data. The transport parameters and experimental data for these plots are listed in Table XXIII. The media for these release studies contained 15% FBS. The cells for the release studies shown in Figures 45, 46 and 47 were preincubated in

media containing digitoxin -^{3}H long enough to reach complete cellular saturation. The release data shown in Figure 48 represent a most interesting case. The cells in this particular experiment were preincubated in media containing a low concentration of digitoxin for two hours. At the end of this incubation period, the Langmuir bound cellular digitoxin concentration was still far below the saturation value. The data indicate a rapid initial loss of drug from the cells followed by drug uptake by the cells. The theoretical Model 6 plot for the data in Figure 48, in fact, predicts the cellular uptake following the rapid initial loss of digitoxin from the cell interior. This example further supports the validity of Model 6.

The average values of k_f and k_r determined from the uptake and release data are 4.32×10^{-9} cm./sec. and 2.97×10^{-21} moles/cm.^{2} sec., respectively. The dissociation constant for the digitoxin - erythrocyte complex in the presence of 15% FBS was computed as 6.9×10^{-13} moles/ml.RBC. The maximum number of molecular digitoxin binding sites per cell in the presence of 15% FBS in the media was computed from the average value of Q as 531 ± 52. Figure 49 shows the equilibrium data of the total cell - associated digitoxin concentration as a function of the unbound digitoxin concentration in the medium containing 15% FBS. The theoretical curve in Figure 49 was computed with equation (79) using the average values of k_f, k_r, Q and K that were determined from the uptake and release data. Figure 50 shows the equilibrium data of the cellular digitoxin bound to Langmuir sites as a function of the unbound digitoxin concentration in the media containing 15% FBS. The theoretical plot of the Langmuir isotherm was computed with equation (67) using the mean values of

k_f, k_r and Q that were determined from the transport data.

Summary of Digitoxin Transport

The excellent correlation that was obtained between the theory of Model 6 and the experimental digitoxin transport data for the suspension systems containing 0, 5 and 15% FBS and a wide range of digitoxin concentrations clearly demonstrates that the model is compatible with the findings of this study. The mean values of the transport parameters that were evaluated for the different digitoxin transport systems are listed in Table XXIV.

The theoretical plots for all the digitoxin transport data were computed by adjusting the parameters k_f, k_r and Q until the best fit between the theory and the experimental data was obtained. The reader should recognize, however, that the deviations of the parameters, k_f, k_r and Q as shown in Table XXIV are quite small and for this reason, reasonably good theoretical fits to all the digitoxin transport data could also be obtained by utilizing a single set of the mean values of k_f, k_r and Q as determined for any particular fetal bovine concentration in the suspension media.

Analogous to the ouabain transport, a significant decrease in the magnitude of the adsorption and desorption rate constant was observed with increasing FBS levels in the external media. In order to resolve the question of whether the influence of the fetal bovine serum on the magnitudes of k_f and k_r was due to protein components or other components of the fetal bovine serum, the following studies were carried out with chemically well defined media. The uptake of digitoxin by erythrocytes from phosphate buffered saline containing 5, 10, 15 and 30% fetal bovine albumin was determined at

30 °C. The transport parameters evaluated with equation (75) for these studies are listed in Table XXV. The constancy of the values for k_f and Q determined for these systems containing different concentrations of pure fetal bovine albumin support the hypothesis proposed in connection with the ouabain transport data that the change in affinity of the erythrocytes for ouabain as well as digitoxin is the result of competitive interaction of electrolyte components with the erythrocyte - glycoside receptor sites.

The maximum number of molecular digitoxin binding sites per cell in the absence of FBS in the media is approximately 730 which is comparable to the number of ouabain binding sites. The decrease in the maximum number of digitoxin binding sites with increasing FBS concentrations can be attributed to the same effects as those discussed for the ouabain transport data.

Finally, the transport data demonstrate that the rapid cellular digitoxin uptake, after factoring out the serum binding effects, is linearly related to the unbound digitoxin concentration in the suspension media and therefore, the intrinsic partition coefficient is independent of the digitoxin concentration and the fetal bovine serum level in the suspension media.

Table XXV. Transport parameters evaluated with equation (75) for the uptake of digitoxin at 30 °C from phosphate buffered saline containing different concentrations of fetal bovine albumin.

Fetal Bovine Albumin* %	Q (moles/RBC)	k_f (cm./sec.)	k_r (moles/cm.^{2}sec.)
5	1.16×10^{-21}	2.10×10^{-8}	3.92×10^{-21}
10	1.09×10^{-21}	1.80×10^{-8}	3.92×10^{-21}
15	1.31×10^{-21}	1.80×10^{-8}	3.92×10^{-21}
30	1.19×10^{-21}	1.90×10^{-8}	3.92×10^{-21}
Mean:	1.19×10^{-21}	1.90×10^{-8}	3.92×10^{-21}

* Whole fetal bovine serum contains 3.28 gm. of albumin per 100 gm. of serum (12).

THE ROLE OF THE PHYSICAL MODEL APPROACH

In the present section, the course that this investigation followed and the role that the physical model approach played in elucidating the true transport mechanism for the ouabain - and digitoxin - erythrocyte systems will be summarized.

The transport of the cardiac glycosides ouabain, digoxin and digitoxin into Burkitt lymphoma cells was recently investigated in our laboratories by Turi (12). The author reported that the transport data of the glycosides into the cells could well be explained with the use of diffusion models.

In the present investigation, it was then assumed that the transport of ouabain into erythrocytes may well occur by the same mechanism. Uptake experiments were carried out using a relatively narrow range of ouabain concentrations in the suspension medium. The kinetic data was evaluated using the simple diffusion model (Model 1) and excellent agreement was found between the theory and the experimental data. Figure 51 shows a typical ouabain uptake experiment and the good fit that was obtained with Model 1. The transport parameters for this experiment are listed in Table XXVI. If the uptake of ouabain by the cells is truly the result of diffusion of the drug into the cell interior, then this process should be reversible and the permeability coefficient and partition coefficient for both the uptake and the release experiments should ideally be identical for both processes. Thus, to further test the validity of Model 1, release experiments were carried out. Figure 52 shows the data of a typical release study. Using the permeability and partition coefficient determined for the uptake experiment shown in Figure 51, the data in Figure 52 was analyzed with Model 1 and the theo-

retical curve plotted in Figure 52. There was obviously a large discrepancy between the experimental data and the predictions of the model and the question arose as to whether or not the drug had been degraded in the cell interior or whether the drug could have altered the membrane permeability itself. TLC analysis of the drug revealed that no bioconversion of the drug had taken place. To check the latter possibility, uptake experiments were carried out using lower concentrations of the ouabain in the suspension medium. The uptake data using these lower drug concentrations were evaluated with Model 1. No change was observed in the magnitude of the permeability coefficient, but the partition coefficients showed a marked increase with the lower drug concentration. A plot of all the equilibrium data for the cell - associated ouabain concentration versus the ouabain concentration in the medium revealed a nonlinear relationship. The plot, in fact, closely resembled a Langmuir isotherm. This nonlinear binding clearly demonstrated that Model 1, which requires a constant partition coefficient, could not be the proper model for the ouabain transport process.

Subsequently, Model 3 was derived which was to account for the nonlinear drug - erythrocyte interaction. This model assumes that the drug molecules diffuse into the cells and rapidly bind to Langmuir sites. The analysis of the transport data with this model required a knowledge of the overall Langmuir rate constant, k, and the value of the maximum amount of drug that can bind to the cell - associated Langmuir sites, Q. Figure 53 shows the plot that was to allow for the evaluation of the parameters k and Q with equation (51). The nonlinearity that was observed between $(C/C_c - C)$ and C clearly demonstrates that it was impossible to evaluate k and Q from the data shown in Figure 53.

Therefore, Model 3 in its original form could not be the proper model.

Using the assumption that $C_m >> C_f$, Model 3 was then modified. The parameters k and M for this modified Model 3 were evaluated from the plot (C/C_m) versus (C) shown in Figure 54 using equation (67). The overall Langmuir rate constant, k, was found to be 4.88×10^{11} ml.RBC/mole and the cellular saturation concentration was computed as 1.47×10^{-21} moles/RBC.

The theory of the modified version of Model 3 was then tested against the ouabain uptake data shown in Figure 51. The transport parameters that were used in the evaluation of this model are listed in Table XXVI. The theoretical plot of this model is shown in Figure 51. The theory of Model 3 follows the experimental data at early times but soon deviates and finally chokes off before reaching the maximum cell concentration. The model was then tested against the release data shown in Figure 52. The transport parameters for this analysis are listed in Table XXVI. As can be seen in Figure 52, the theoretical plot for the release poorly correlated with the experimental data. Thus, Model 3 in its original form as well as the modified form of this model failed to explain the ouabain transport data.

The argument was then made that if the ouabain molecules bound to Langmuir sites are in rapid equilibrium with the unbound ouabain molecules in the cell interior, as proposed in the two versions of Model 3, then the ouabain molecules bound to these Langmuir sites should readily exchange with nonradioactive ouabain molecules that had permeated into the cell interior. To resolve this question, cells were incubated in the presence of ouabain $-^3H$. Subsequently, the release of the tritiated ouabain from the cells was investigated in the presence of 1×10^{-5} M

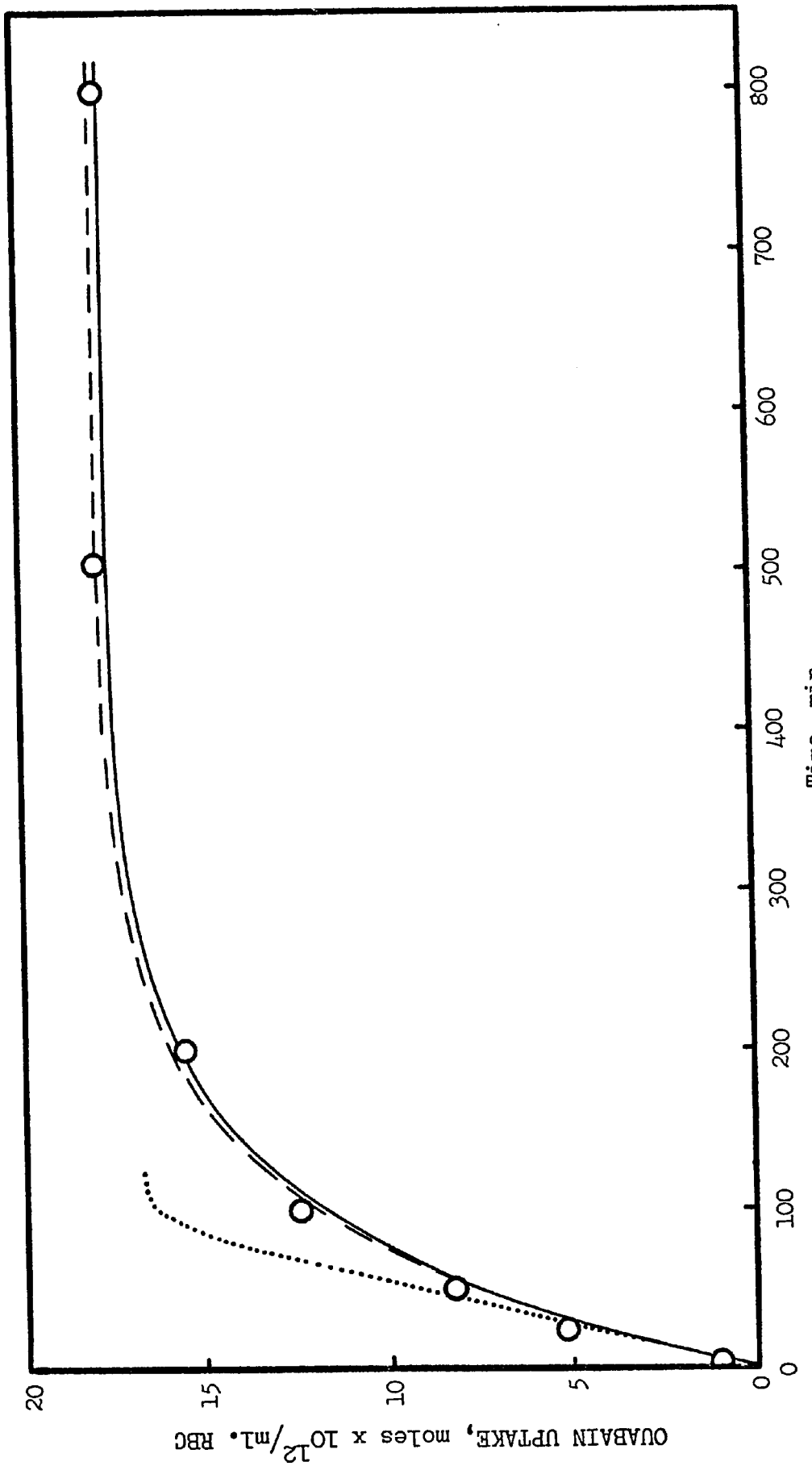


Figure 51. Cellular ouabain uptake data analyzed with Models 1, 3 and 4. The medium was phosphate buffered saline and the temperature was 30 °C. Key: solid line was obtained with Model 4, equation (64); dashed line was obtained with Model 1, equation (6); dotted line was obtained with Model 3, equation (54). The transport parameters used for the different theoretical plots are summarized in Table XXV.

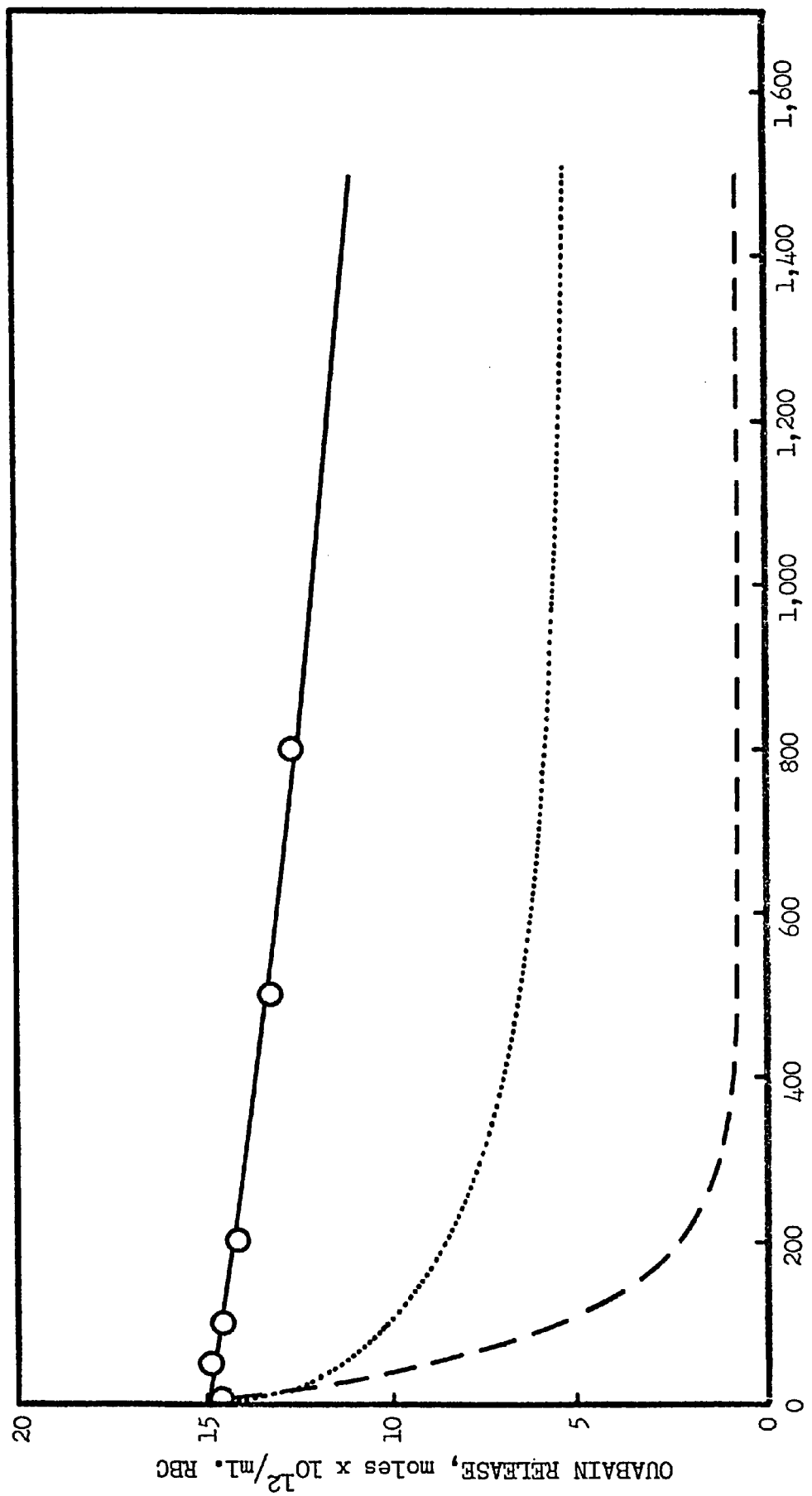


Figure 52. Cellular ouabain release data analyzed with Models 1, 3 and 4. The medium was phosphate buffered saline and the temperature was 30 °C. Key: the solid line was obtained with Model 4, equation (64); the dashed line was obtained with Model 1, equation (6); the dotted line was obtained with Model 3, equation (54). The transport parameters used for the different theoretical plots are given in Table XXV.

Table XXVI. Transport parameters for Models 1, 3 and 4 used to compute the theoretical plots which gave the best fit to the ouabain uptake data shown in Figure 51 and the ouabain release data shown in Figure 52.

	Model	Equation	P (cm/sec)	k_f (cm/sec)	k_r (mol/cm^{2}sec)	k (ml/mol)	Q (mol/RBC)	K (ml RBC/ml medium)	T (mol/ml suspension)	H (ml RBC/ml suspension)
Figure 51	1	6	5.8×10^{-9}					0.58	3.00×10^{-11}	0.054
	3	54	5.8×10^{-9}			4.88×10^{11}	1.55×10^{-21}		3.00×10^{-11}	0.054
	4	64		5.9×10^{-9}	3.39×10^{-21}		1.55×10^{-21}		3.00×10^{-11}	0.054
Figure 52	1	6	5.8×10^{-9}					0.58	1.22×10^{-12}	0.051
	3	54	5.8×10^{-9}			4.88×10^{11}	1.30×10^{-21}		1.22×10^{-12}	0.051
	4	64		5.8×10^{-9}	3.48×10^{-21}		1.30×10^{-21}		1.22×10^{-12}	0.051

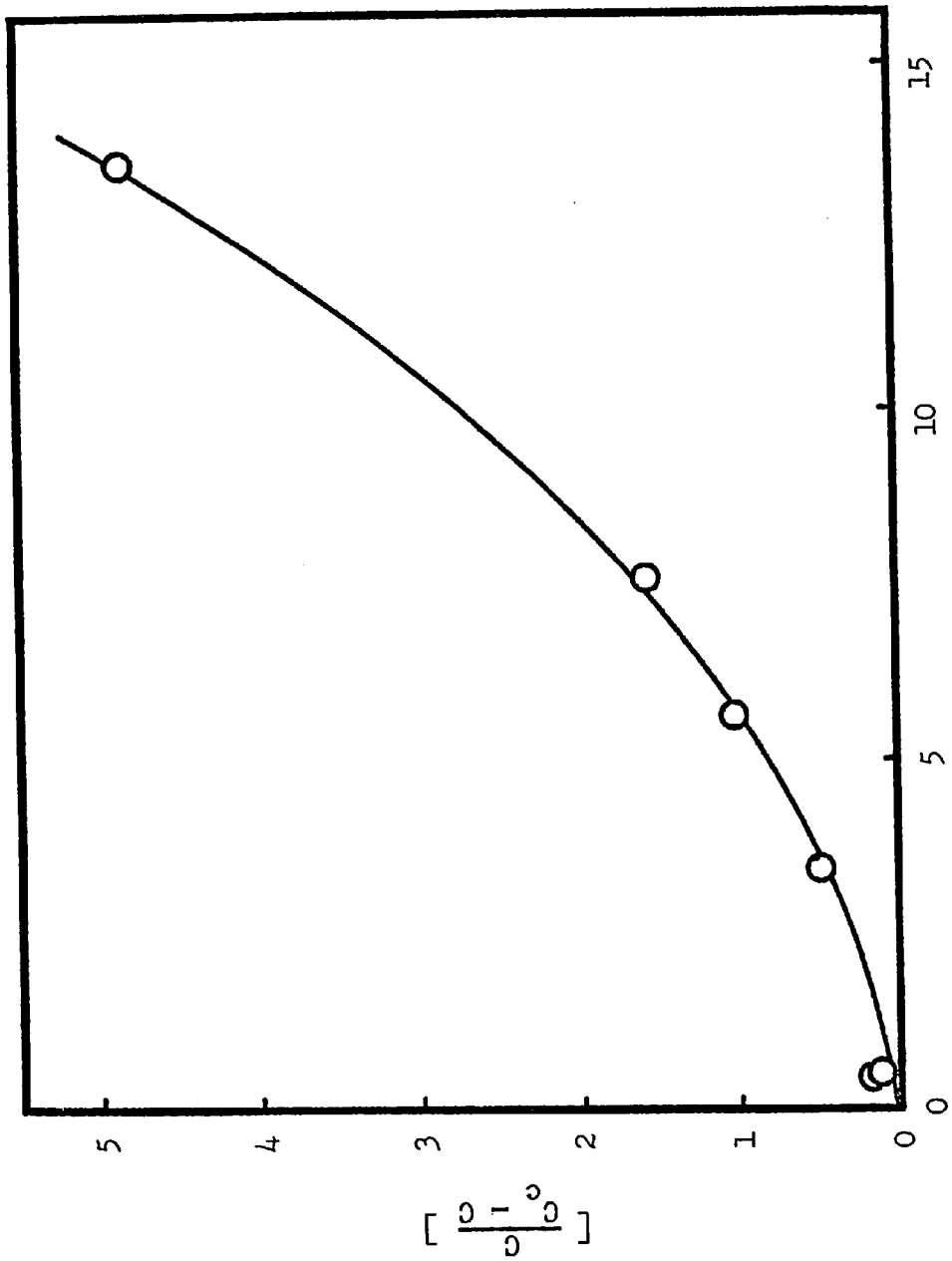


Figure 53. Plot of $(C/C_c - C)$ versus the ouabain concentration of the medium (C) for the equilibrium ouabain uptake data. The suspension medium contained 0% FBS and the temperature was 30 °C. The non-linear relationship between $(C/C_c - C)$ and (C) clearly demonstrates the unsuitability of Model 3 since it is impossible to evaluate the parameters Q and k from the above plot with equation (51).

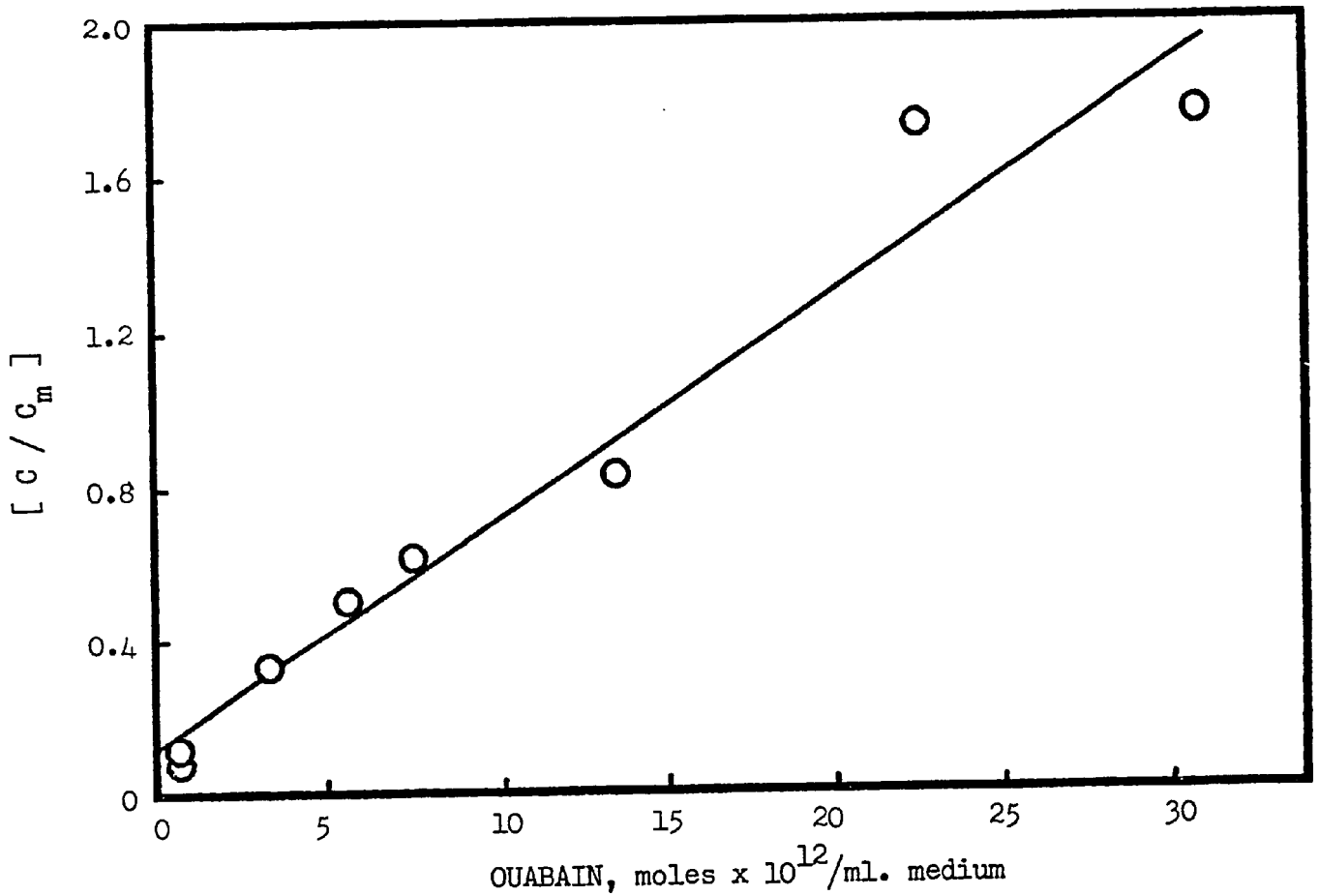


Figure 54. Plot of (C/C_m) versus the ouabain concentration in the medium (C) for the equilibrium ouabain uptake data. The suspension medium contained 0% FBS and the temperature was 30 °C. Linear regression analysis for the data gives a slope of 5.90×10^{10} and an intercept of 0.121 with a correlation coefficient of 0.979. By the use of equation (67), the cellular saturation value, Q, was computed from the slope as 1.47×10^{-21} moles/RBC and the ratio of the slope to the intercept gave the overall Langmuir rate constant, k, as 4.88×10^{11} ml./mole. The latter value was used to evaluate the modified form of Model 3.

and 1×10^{-3} M nonradioactive ouabain in the suspension media. The data of these experiments, shown in Figure 28, clearly indicate that the presence of nonradioactive ouabain in the media had essentially no effect on the rate of cellular drug release thereby further suggesting the inappropriateness of Model 3.

At this stage of the investigation, it became apparent that the uptake of ouabain by erythrocytes may not represent a diffusion process at all but rather that the drug, in fact, may merely adsorb to Langmuir sites that are associated with the plasma membrane. This conclusion led to the derivation of Model 4. Whereas Models 1 and 3 failed to satisfactorily explain the ouabain transport data shown in Figures 51 and 52, the theoretical plots of Model 4 correlated well with the transport data shown in these figures as well as all the transport studies discussed in the previous section. The transport parameters and experimental data for the Model 4 analysis of the data shown in Figures 51 and 52 are listed in Table XXV.

Model 4 possesses some characteristic features which are noteworthy to mention. In the analysis of uptake data it was found that the theoretical plots were quite sensitive to any changes in the magnitude of k_f and Q but rather insensitive to k_r. This point is illustrated in Figure 55. Large variations in the magnitude of k_r, while keeping the remaining transport parameters constant, produced relatively small deviations of the theory from the experimental uptake data as shown in Figure 55. The analysis of the release data with Model 4, on the other hand, revealed that the theory was sensitive to any changes in k_r and Q but rather insensitive in k_f. This point is illustrated in Figure 56 which shows typical ouabain release data and the best theoretical plot

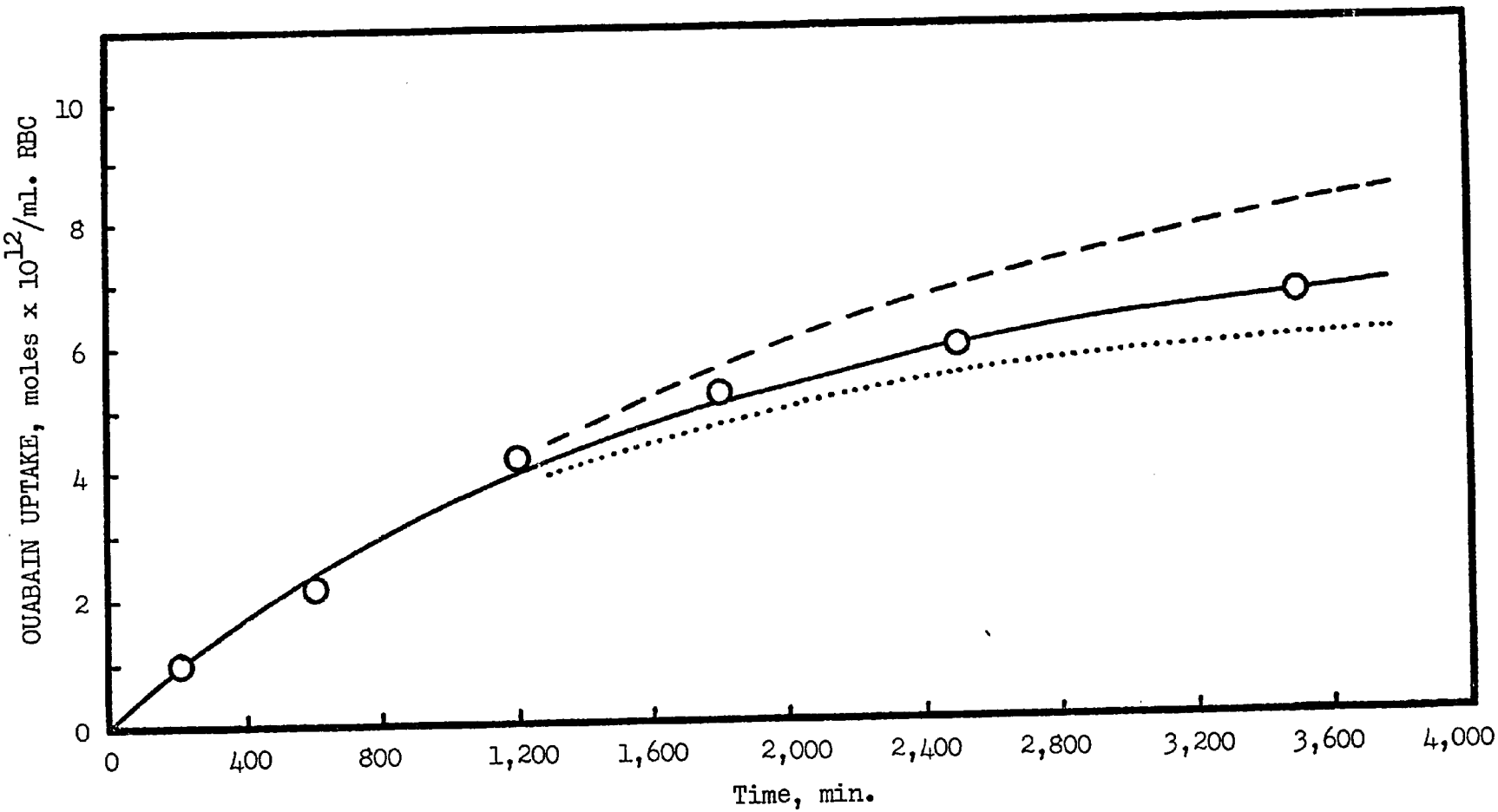


Figure 55. Model 4 plot of ouabain uptake data. The medium contained 5% FBS and the temperature was 30 °C. The plots demonstrate the low sensitivity of the theory to changes in the magnitude of the desorption rate constant, k_r, for uptake experiments. All transport parameters in these plots were held constant except for k_r. Key: solid line, giving the best fit to the experimental data, was obtained with $k_r = 2.99 \times 10^{-21}$; the dashed line was computed with $k_r = 8.92 \times 10^{-22}$; and the dotted line was calculated with $k_r = 4.46 \times 10^{-21}$ moles/cm.^{2} sec..

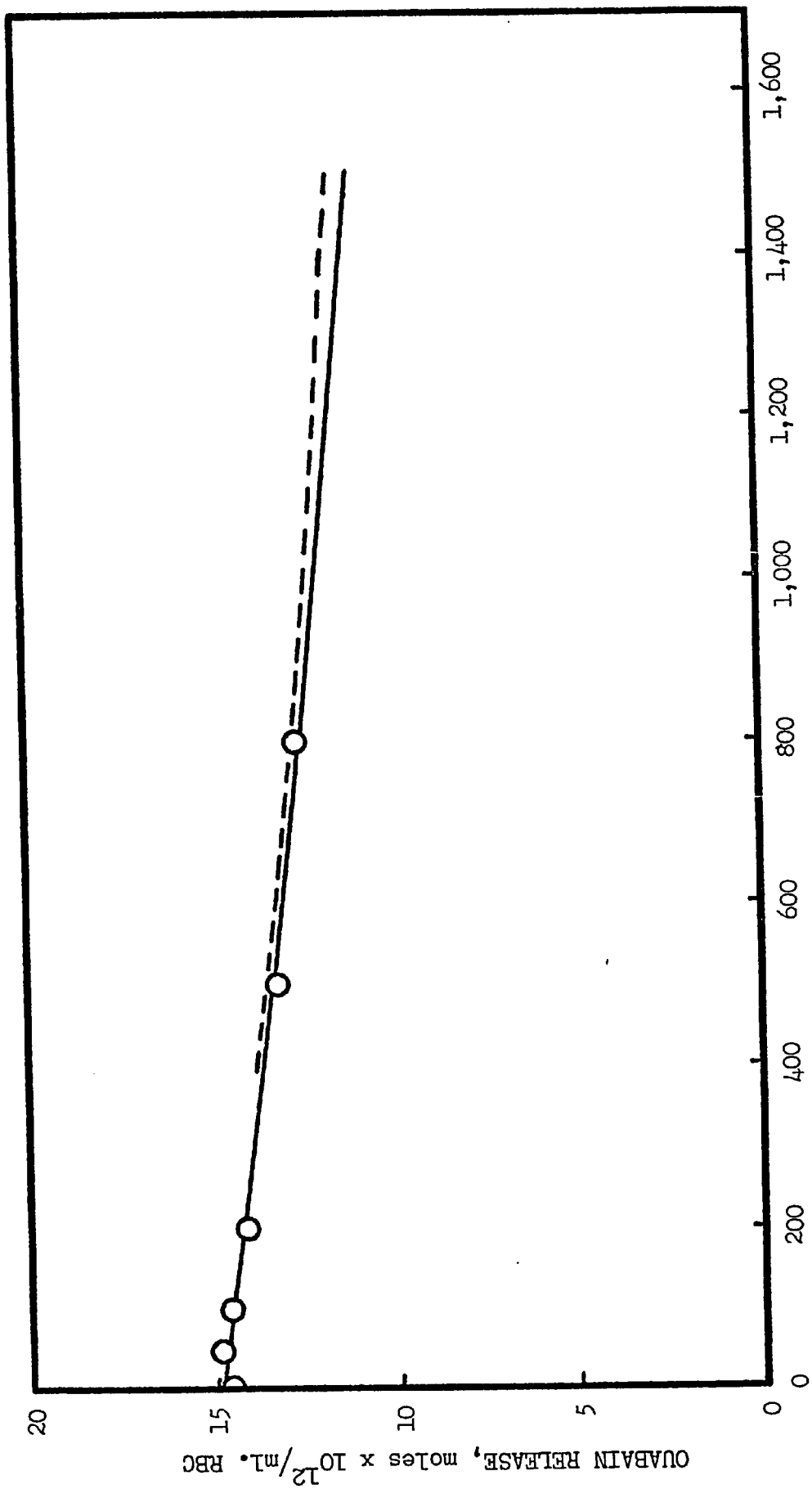


Figure 56. Model 4 plot of ouabain release data demonstrating the low sensitivity of the theory to changes in the magnitude of the adsorption rate constant, k_f, for release experiments. All transport parameters in the plots were identical except for k_f. Key: solid line, giving the closest association between experimental data and theory, was computed with $k_f = 5.8 \times 10^{-9}$; whereas the dashed line was obtained with $k_f = 1.2 \times 10^{-8}$ cm./sec.

of Model 4. Increasing the magnitude of k_f by more than 50%, while leaving the remaining transport parameters constant, produced very little deviation between the theoretical plot and the experimental data as shown in Figure 56.

The analysis of the data associated with the plateau of the Langmuir isotherms shown in Figures 19, 24 and 29 indicated that the deviation between the experimental points was approximately ± 15%.

Utilizing the observations discussed above, a decision was made to analyze the ouabain transport data using Model 4 in the following manner: For uptake experiments, the value of k_f was determined by best fitting the theory to the experimental data, using the average value of k_r determined from release experiments. For release experiments, the magnitude of k_r was evaluated by obtaining the best fit of the theory to the experimental data using the average value of k_f determined from uptake experiments. For uptake and release experiments, which clearly indicated that steady-state conditions had been reached, the cellular saturation value Q, directly computed from the particular equilibrium data, was used for the theoretical analysis; whereas for systems which had not yet reached equilibrium, the theoretical analysis was carried out using the average value of Q that was determined from the plateau of the Langmuir isotherms but allowing for a ± 15% variation of the magnitude of this parameter.

Preliminary uptake studies for digitoxin revealed that a certain fraction of drug was rapidly taken up by the cells. This rapid drug accumulation was followed by a slow cellular drug uptake. The same transport phenomenon was reported by Turi (12) for the uptake of digitoxin by Burkitt lymphoma cells. Turi proposed that the rapid digi-

toxin uptake was the result of binding of the drug to the cell membrane while the slow drug uptake component was shown to be the result of diffusion of digitoxin into the cell interior. His observations extrapolated to the erythrocyte system suggested that digitoxin may rapidly bind to the erythrocyte plasma membrane and that the slow cellular drug uptake could be attributed to diffusion of digitoxin into the cell interior.

Model 1 was subsequently modified to account for the presumed rapid membrane binding process as well as the digitoxin - serum binding effects. This new model, Model 2, was tested with the digitoxin transport data. Figure 57 shows experimental data that were observed for a particular digitoxin uptake experiment. The analysis of the data shown in Figure 57 with Model 2 gave excellent agreement between the theory and the experimental data. The transport parameters for this analysis are listed in Table XXVII. To further test the validity of Model 2, release experiments were carried out. Figure 58 shows the data for a typical release experiment. The release data were tested with Model 2 using the same transport parameters as those used for the uptake experiment shown in Figure 57. The transport parameters utilized for the analysis are given in Table XXVI. As shown in Figure 58, Model 2 failed to give any correlation with the release data. Uptake experiments which were subsequently carried out using a wide range of digitoxin concentrations indicated that the intrinsic partition coefficient was concentration dependent and that there was a nonlinear relationship between the cell - associated equilibrium drug concentration and the equilibrium concentration of the drug in the medium. Thus, although Model 2 was well able to predict the uptake data, it could not be the proper model since it failed to predict the release data and also because the partition coefficient was concentration dependent.

The above observation suggested that the slow digitoxin uptake may very well follow the same transport mechanism as that found for the ouabain transport, i.e., the slow cellular digitoxin uptake component could be the result of adsorption of the drug to plasma membrane - associated Langmuir binding sites. Model 4 was modified to account for the presumed instantaneous membrane binding of digitoxin and the serum binding effect of the drug. The digitoxin transport data were then evaluated with the newly derived Model 5 and excellent agreement was found between the theory of this model and the digitoxin transport data. Model 5 proposed that the plasma membrane possesses linear and nonlinear receptor sites for digitoxin. Although the proposed concept of the membrane possessing two distinct types of binding sites is plausible, it nevertheless raised the question of whether or not the instantaneous digitoxin uptake by the cells could not instead be attributed to rapid permeation of the drug into the cell interior. To resolve this question, the interaction between digitoxin and human hemoglobin as well as the interaction between digitoxin and human erythrocyte ghosts were quantitatively assessed. The information gathered from these experiments subtly suggested that the concept proposing the rapid digitoxin uptake to be the result of permeation was to be favored. For this reason, Model 5 was then replaced by Model 6 which treats the rapid digitoxin uptake component in terms of permeation of the drug into the cell interior. Mathematically and kinetically, however, Models 5 and 6 are indistinguishable.

Figure 57 shows the good fit that was obtained with Model 6 (or 5) for the digitoxin uptake data shown in this figure. The digitoxin release data shown in Figure 58 was evaluated with Model 6 and

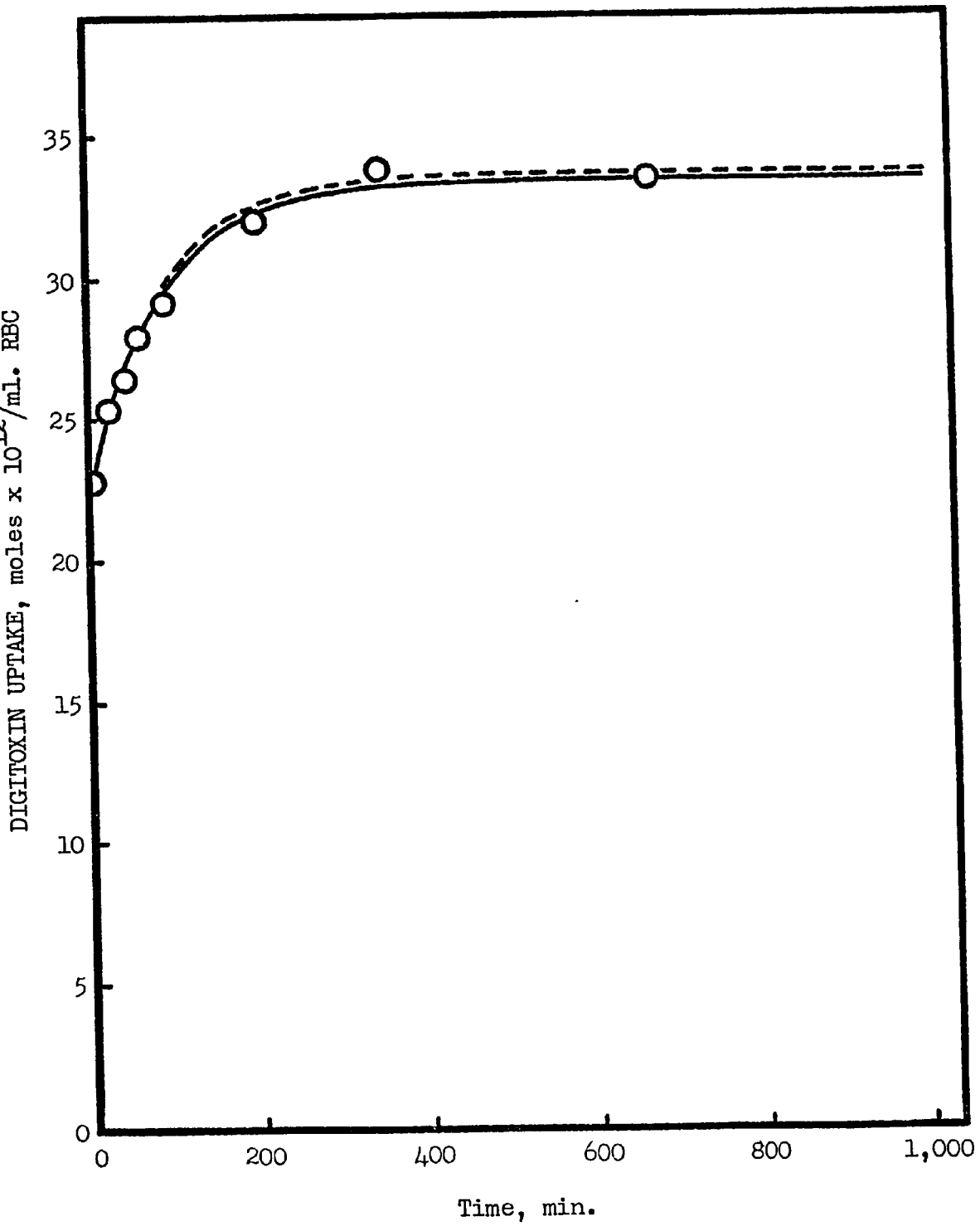


Figure 57. Cellular digitoxin uptake data analyzed with Models 2 and 6 (or 5). The medium was phosphate buffered saline and the temperature was 30 °C. Key: solid line was computed with Model 6, equation (75); dashed line was obtained with Model 2, equation (24). The transport parameters used for the theoretical curves are summarized in Table XXVI.

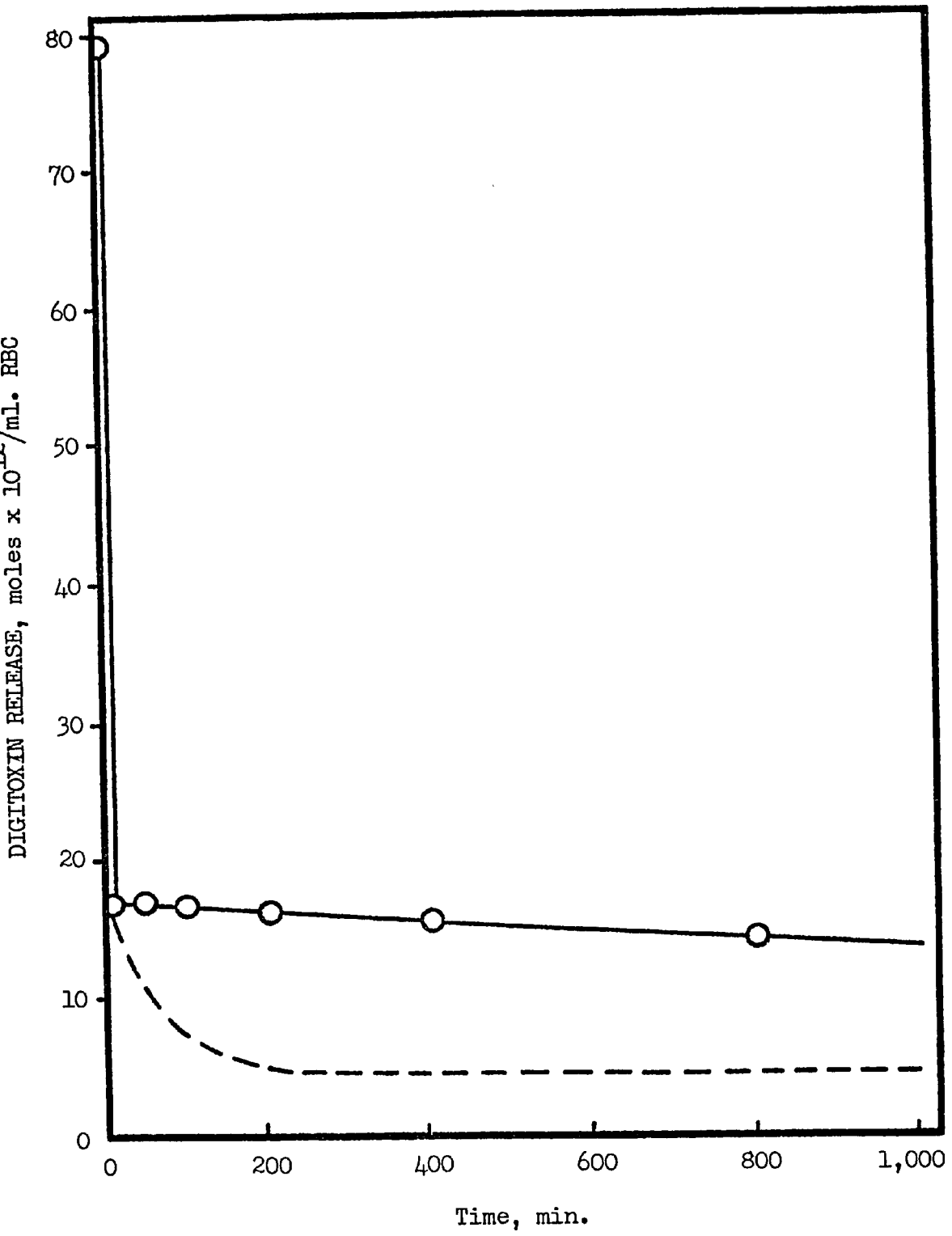


Figure 58. Cellular digitoxin release data analyzed with Models 2 and 6 (or 5). The medium was phosphate buffered saline and the temperature 30 °C. Key: the solid line was obtained with Model 6, equation (75); the dashed line was calculated with Model 2, equation (24). The transport parameters used for the two theoretical curves are given in Table XXVI.

Table XXVII. Transport parameters for Models 2 and 6 used to compute the theoretical plots for the digitoxin uptake data shown in Figure 55 and the digitoxin release data shown in Figure 56.

	Model	Equation	P (cm/sec)	k_f (cm/sec)	k_r ($mol/cm^2 sec$)	Q (mol/RBC)	K	K_{bm}	T ($\frac{mol/ml}{suspension}$)	H ($\frac{ml\ RBC/ml}{suspension}$)
Figure 55	2	24	1.7×10^{-8}				1.41	2.31	1.02×10^{-11}	0.057
	6	75		1.7×10^{-8}	3.92×10^{-21}	1.17×10^{-21}	2.31		1.02×10^{-11}	0.057
Figure 56	2	24	1.7×10^{-8}				1.41	2.27	1.29×10^{-12}	0.056
	6	75		1.7×10^{-8}	3.97×10^{-21}	1.37×10^{-21}	2.27		1.29×10^{-12}	0.056

as can be seen in this figure, as well as the data presented in the previous section, excellent agreement was found between the theory and the kinetic data. The transport parameters used for the theoretical Model 6 plot in Figures 57 and 58 are listed in Table XVI. The analysis of the digitoxin transport data with Model 6 was carried out analogously to the method used with Model 4; i.e., the mean value of k_r that was determined from the release experiments was utilized in the analysis of the uptake data and vice versa, the mean value of k_f that was determined from uptake experiments was used to analyze the release data.

The study presented here illustrates that the physical model approach to the quantitative and mechanistic analysis of drug transport in cell suspensions is a most powerful tool if used to its fullest potential. The excellent fit that was obtained with Models 1 and 2 for the uptake of ouabain and digitoxin, respectively, is a case in point. Only by further testing these models with uptake experiments using a wide range of drug concentrations as well as release experiments, did it become apparent that these models were mechanistically unsuitable.

It can therefore be concluded that the physical model approach to transport studies is unique in that it provides the investigator with a continuous frame of reference. As demonstrated in the present investigation, the physical model approach combined with the thorough examination of all aspects related to the drug transport phenomena eventually revealed the precise nature of the transport mechanisms as well as provided a quantitative assessment of all transport related parameters for the transport of ouabain and digitoxin into eryth-

rocytes.

Many questions regarding the transport and pharmacological activity of cardiac glycosides remain to be answered. From a physical chemistry point of view it would be of interest to examine the influence that various anions and cations in the suspension media may have on the transport process. Also, transport studies at different temperatures would allow for the estimation of the activation energies of the glycoside - erythrocyte interactions whereas uptake studies with erythrocytes whose plasma membranes have been carefully stripped of various components may eventually reveal the precise nature and location of the glycoside receptor sites.

Furthermore, it would be of great interest to investigate the biological and pharmacological implications of the glycoside - erythrocyte interactions in view of the findings of the present investigation. Gardner and Conlon (52) have already demonstrated that there is a direct relationship between the potassium influx in human erythrocytes and the extent of ouabain binding to the red cell membrane. The pharmacological activity and mode of action of glycosides on heart cells could be studied by relating the rate and amplitude of cellular contraction to the rate of cellular glycoside uptake as well as the total amount of drug that is bound to the cell surface. One study to elucidate the action of cardiac glycosides on the heart has been conducted by Okarma et al.(57). These authors examined the influence of digoxin, dihydrodigoxin and their covalently bound albumin conjugates on cultures of neonatal heart cells and found that these compounds elicited dose - related

increases in contraction amplitudes and contraction rates from the cells. Finally, the investigation of the structure - activity relationships of the various glycosides would represent a novel and pharmacologically most beneficial project. It is well known that the aglycon portion of the cardiac glycoside molecules contains the essential structures for the pharmacological activity. Although the sugar residue or residues of the glycosides possess no biological activity per se, they nevertheless significantly influence the magnitude of the pharmacological activity. Therefore, the substitution of different sugar moieties to the aglycones of naturally occuring glycosides could yield new, more powerful drugs for cardiac therapy.

The study and elucidation of the many unanswered physical, chemical and pharmacological phenomena concerning the transport and action of cardiac glycosides requires a multidisciplinary approach. The present investigation should provide a solid base line for many of the studies yet to follow.

REFERENCES

1. Miller, I.R. (1968). In Biological Interfaces: Flows and Exchanges, (Basic Science Symposia of the New York Heart Association), p. 145. Boston: Little & Brown.

2. Sessa, G. and Weissman, G. (1968). J. Lipid. Res., 9, 310.

3. Bikhazi, A.B. (1970). Thesis, The University of Michigan, Ann Arbor.

4. Ghanem, A.H., Higuchi, W.I. and Simonelli, A.P. (1970). J. Pharm. Sci., 59, 659.

5. Beckett, A.H. and Moffat, A.C. (1968). J. Pharm. Pharmacol., 20, 2395.

6. Kakemi, K., Sezaki, H., Muranishi, S. and Tsujimura, Y. (1969). Chem. Pharm. Bull., 17, 1641.

7. Mattocks, A.M. (1969). J. Pharm. Sci., 58, 595.

8. Scheuplein, R.J., Blank, I.H., Brauner, G.J. and MacFarland, D.J. (1969). J. Invest. Dermatol., 52, 63.

9. Wagner, J.G. (1968). Ann. Rev. Pharmacol., 8, 67.

10. Caldwell, P.C. (1971). In Membranes and Ion Transport., vol. 1, ed. E.E. Bittar, p. 433. New York: Wiley - Interscience.

11. Widdas, W.F. (1954). J. Physiol., 125, 163.

12. Turi, J.S. (1972). Thesis, The University of Michigan, Ann Arbor.

13. Le Fevre, P.G. (1961). Nature, London, 191, 970.

14. Bodansky, M. (1932). J. Cell. Comp. Physiol., 1, 429.

15. Green, J.W. (1949). ibid., 33, 247.

16. Holder, L.B. and Hayes, S.L. (1965). Mol. Pharmacol., 1, 266.

17. Ho, N.F.H., Turi, J.S., Shipman, Jr., C. and Higuchi, W.I. (1972). J. Theor. Biol., 34, 451.

18. Turi, J.S., Higuchi, W.I., Shipman, Jr., C. and Ho, N.H.F. (1972). J. Pharm. Sci., 61, 1618.

19. Turi, J.S., Higuchi, W.I., Ho, N.F.H. and Shipman, Jr., C. ibid., (in press).

20. Turi, J.S., Ho, N.F.H., Higuchi, W.I. and Shipman, Jr., C. ibid., (in press).

21. Roos, H. and Pfleger, K. (1972). Mol. Pharmacol., 8, 417.

22. Sha'afi, R.I., Rich, G.T., Sidel, V.W., Bossert, W. and Solomon, A.K. (1967). J. Gen. Physiol., 50, 1377.

23. Whittam, R. (1964). In Transport and Diffusion in Red Blood Cells, p. 1. London: Edward Arnold Publishers Ltd.

24. Ponder, E. (1944). In Medical Physics, ed. Glasser, p. 1203. Chicago: Year Book Publishers Inc.

25. Dodge, J.T., Mitchel, C. and Hanahan, D.J. (1963). Arch. Biochem. Biophys., 100, 119.

26. Zahler, P. and Weibel, E.R. (1970). Biochim. Biophys. Acta, 219, 320.

27. Robertson, J.D. (1972). Arch. Intern. Med., 129, 202.

28. Hawk, P.B., Oser, B.L. and Summerson, W.H. (1951). In Pratical Physiological Chemistry, 12th ed., p. 422. New York: The Blakiston Company.

29. Danielli, J.F. and Davson, H. (1935). J. Cellular Comp. Physiol., 5, 495.

30. Robertson, J.D.J. (1957). Biophys. Biochem. Cytol., 3, 1043.

31. Sjostrand, F.S. (1963). J. Ultrastruct. Res., 9, 561.

32. Green, D.E. and Perdue, J.F. (1966). Proc. Natl. Acad. Sci. U.S., 55, 1295.

33. Hendler, R.W. (1971). Physiol. Rev., 51, 66.

34. Phillips, G.B. and Roome, N.S. (1959). Proc. Soc. exp. Biol., 100, 489.

35. Dawson, R.M.C., Hensington, N. and Lindsay, D.B. (1960). Biochem. J., 77, 226.

36. Reed, C.F. (1960). J. lab. clin. Med., 56, 281.

37. Munn, J.I. and Crosby, W.H. (1961). Brit. J. Hematology, 7, 523.

38. James, A.T., Lovelock, J.E. and Webb, J.P. (1959). Biochem. J., 73, 106.

39. Stengel, T.L. (1974). J. Cell. Biol., 62, 1.

40. Abramson, H.A. and Moyer, L.S. (1936). J. Gen. Physiol., 19, 601.

41. Ponder, E. and Ponder, R.V. (1960). ibid., 43, 503.

42. Eylar, E.H., Madoff, M.A., Brody, O.V. and Oncley, J.L. (1962). J. Biol. Chem., 237, 1992.

43. Beckman, H. (1958). In Drugs: Their Nature, Action and Use., p. 77. Philadelphia: W.B. Saunders Company.

44. Farah, A. (1945). J. Pharmacol. Exp. Theor., 83, 143.

45. Spratt, J.L. and Okita, G.T. (1958). ibid., 124, 109.

46. Lukas, D.S. and Peterson, R.E. (1966). J. Clin. Invest., 45, 782.

47. Weissler, A.M., Snyder, J.R., Schoenfeld, C.D. and Cohen, S. (1966). Am. J. Cardiol., 17, 768.

48. Schatzmann, H.J. (1952). Helv. phy. acta, 11, 346.

49. Glynn, I.M. (1964). Pharmacol. Rev., 16, 381.

50. Hoffman, J.F. (1969). J. Gen. Physiol., 54, 343.

51. Smith, T.W., Wagner, Jr., H., Markis, J.E. and Young, M. (1972). J. Clin. Invest., 51, 1777.

52. Gardner, J.D. and Conlon, T.P. (1972). J. Gen. Physiol., 60, 609.

53. Gardner, J.D., Kiino, D.R., Swartz, T.J. and Butler, Jr., V.P. (1973). J. Clin. Invest., 52, 1820.

54. Boyce, W.E. and DiPrima, R.C. (1969). In Elementary Differential Equations and Boundary Value Problems., p. 353. New York: John Wiley & Sons, Inc.

55. Bray, G.A. (1960). Anal. Biochem., 1, 279.

56. Dittrich, H. (1963). Med. Klin., 58, 1882.

57. Okarma, T.B., Tramell, P. and Kalman, S.M. (1972). J. Pharmacol. Exp. Ther., 183, 559.